AD-A073 590 MCDONNELL DOUGLAS RESEARCH LABS ST LOUIS MO F/G 11/9
MAGNETIC RESONANCE STUDIES OF EPOXY RESINS AND POLYURETHANES.(U)
MAY 79 I M BROWN, A C LIND, T C SANDRECZKI N00019-78-C-0031
UNCLASSIFIED MDC-Q0673 NL

1 OF 2

AD A073590

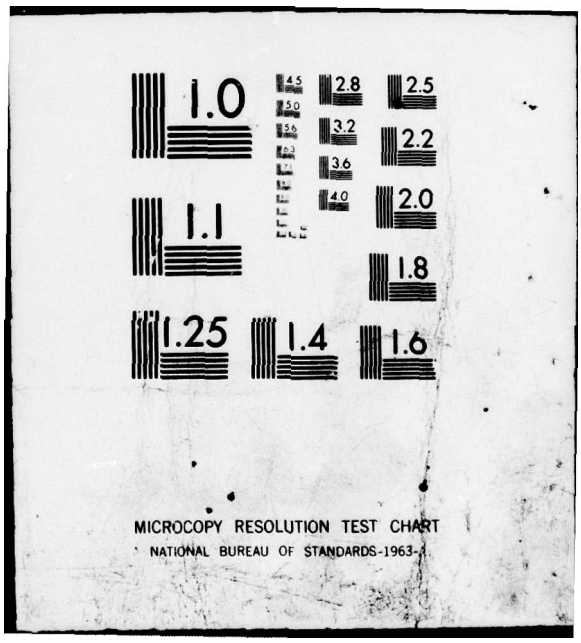
1.0
1.1
1.25
1.4
1.6
1.8
2.0
2.2
2.5
2.8
3.2
3.6
4.0
4.5
5.0
5.6
MICROCOPY RESOLUTION TEST CHART
NATIONAL BUREAU OF STANDARDS-1963-A

(10) LEVEL II

MCDONNELL DOUGLAS RESEARCH LABORATORIES

MCDONNELL DOUGLAS CORPORATION

UNCLASSIFIED

SECURITY CLASSIFICATION OF THIS PAGE (When Data Entered)

REPORT DOCUMENTATION PAGE

READ INSTRUCTIONS BEFORE COMPLETING FORM

1. REPORT NUMBER: MDC Q0673
2. GOVT ACCESSION NO.:
3. RECIPIENT'S CATALOG NUMBER:

4. TITLE (and Subtitle): MAGNETIC RESONANCE STUDIES OF EPOXY RESINS AND POLYURETHANES

5. TYPE OF REPORT & PERIOD COVERED: Final Report 3 Feb 78 — 3 May 79

6. PERFORMING ORG. REPORT NUMBER:

7. AUTHOR(s): I. M. Brown, A. C. Lind, T. C. Sandreczki

8. CONTRACT OR GRANT NUMBER(s): N00019-78-C-0031

9. PERFORMING ORGANIZATION NAME AND ADDRESS:
McDonnell Douglas Research Laboratories
McDonnell Douglas Corporation
St. Louis, Missouri 63166

10. PROGRAM ELEMENT, PROJECT, TASK AREA & WORK UNIT NUMBERS:

11. CONTROLLING OFFICE NAME AND ADDRESS:
Department of the Navy
Naval Air Systems Command
Washington, DC 20361

12. REPORT DATE: 3 May 1979

13. NUMBER OF PAGES: 111

14. MONITORING AGENCY NAME & ADDRESS (if different from Controlling Office): 110p.

15. SECURITY CLASS. (of this report): Unclassified

15a. DECLASSIFICATION/DOWNGRADING SCHEDULE:

16. DISTRIBUTION STATEMENT (of this Report)

Approved for public release; distribution unlimited.

17. DISTRIBUTION STATEMENT (of the abstract entered in Block 20, if different from Report)

18. SUPPLEMENTARY NOTES

19. KEY WORDS (Continue on reverse side if necessary and identify by block number)

Epoxy resins, Spin probes, Spin labels, Electron paramagnetic resonance, Nuclear magnetic resonance, Polyester polyurethanes, Local mode of segmental motion, Glass transition temperature, Water plasticizer, Hydrolysis, Quaternary salts, Relaxation times.

20. ABSTRACT (Continue on reverse side if necessary and identify by block number)

Electron paramagnetic resonance (EPR) and proton nuclear magnetic resonance (NMR) have been used to investigate the changes in molecular motions that result in samples of the epoxy resin bisphenol-A diglycidyl ether (DGEBA) cured with diethylene triamine (DETA) and in samples of several polyester polyurethanes subjected to humid environments. The cured epoxy resin is known to show a lowering of the glass transition temperature following water sorption, whereas the polyester polyurethanes undergo hydrolysis and catastrophically depolymerize from rubbery solids to viscous liquids. (continued)

DD FORM 1 JAN 73 1473

405315

UNCLASSIFIED

SECURITY CLASSIFICATION OF THIS PAGE (When Data Entered)

20. In the EPR experiments, spin-label and spin-probe techniques were employed where stable nitroxide free radicals were used to probe their static and dynamic environments in the polymers. The uncured DGEBA was spin-labeled at the oxirane group with nitroxide amines, and two different spin labels were positively identified, an end-label and a spin-labeled quaternary salt. The latter can undergo a Hofmann elimination to release a stable spin probe.

Following water sorption, the spin labels and spin probes in the cured DGEBA samples showed two effects. In samples with 1:1 stoichiometry, the nitrogen hyperfine coupling constant increases approximately 1.5% following a 3.8 wt% water sorption as a result of a change in the polarity of the polymer matrix. In samples with 1:3 stoichiometry containing more than 10 wt% water, both the spin labels and spin probes exhibited two superimposed spectra (a mobile phase and a rigid phase). The behavior of the nitroxides in the mobile phase obeyed the predictions of the Fujita-Doolittle equation. It was tentatively concluded that the nitroxides in the mobile phase were relaxed by local modes of main-chain segmental motions which are located in regions of low crosslink density. The rigid phase exhibited the polarity effect following the water sorption.

In the NMR experiments, pulsed techniques were used to measure the relative number of protons in mobile and rigid regions of dry and wet cured epoxy resins. The relaxation times of the protons in both regions were measured and used to determine the molecular motions. From these data the plasticizing effects of sorbed water and the glass transition temperatures were determined in DGEBA/DETA samples at stoichiometries of 1:0.5 to 1:3.

The polyester polyurethanes were end-labeled at an ester group and at an isocyanate group. The temperature dependence of the motional correlation times for a spin probe in polyester polyurethane showed an Arrhenius behavior, and the values between 293 K and 400 K were given by $\tau_c(s) = 1.3 \times 10^{-18} \exp(50.2 \text{ kJ mole}^{-1}/RT)$ in the unreverted state and $\tau_c(s) = 4.5 \times 10^{-19} \exp(48.8 \text{ kJ mole}^{-1}/RT)$ in the reverted state. The activation energy was independent of reversion whereas the inverse frequency factor was dependent on reversion; both are consistent with published viscosity data. The correlation time for the nitroxide in the end-labeled ester group showed a similar Arrhenius behavior before and after reversion; between 293 K and 370 K the values were $\tau_c(s) = 8.3 \times 10^{-17} \exp(42.7 \text{ kJ mole}^{-1}/RT)$ before reversion and $\tau_c(s) = 4.8 \times 10^{-17} \exp(42.3 \text{ kJ mole}^{-1}/RT)$ after reversion. The spectra for the end-labeled isocyanate group indicated anisotropic motion. In both the unreverted and reverted states, two superimposed spectra were observed. These spectra were identified with the unreacted nitroxide probe and the end-labeled isocyanate group.

Proton NMR experiments provided quantitative measurements of the number of protons in rigid domains and/or crystalline regions of polyurethanes. The spin-spin relaxation time was observed to increase significantly after polyester polyurethane samples were exposed to 100% relative humidity at 363 K for only 1 h. After a 30 h exposure the NMR spectra revealed both carboxyl and alcoholic hydrogen resulting from the reversion process. As reversion progressed further, spectral changes occurred which showed that the ester bond undergoes hydrolysis; the spectral changes also could be used to determine the extent of reversion.

PREFACE

This report is an account of the work performed by the McDonnell Douglas Research Laboratories on the Magnetic Resonance Studies of Epoxy Resins and Polyurethanes for the Naval Air Systems Command, Contract No. N00019-78-C-0031, from 3 February 1978 to 3 May 1979. The work was performed in the Chemical Physics Department, managed by Dr. D. P. Ames. The principal investigators were Dr. I. M. Brown and Dr. A. C. Lind; Dr. T. C. Sandreczki was a co-investigator. The project monitor was Mr. C. F. Bersch, Naval Air Systems Command, Washington, DC.

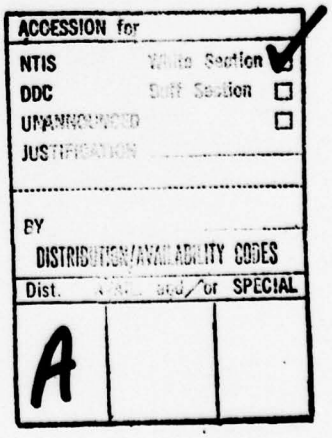

TABLE OF CONTENTS

LIST OF ILLUSTRATIONS

LIST OF ILLUSTRATIONS (Continued)

LIST OF ILLUSTRATIONS (Continued)

LIST OF ILLUSTRATIONS (Continued)

LIST OF ILLUSTRATIONS (Continued)

LIST OF TABLES

1. INTRODUCTION

With the increasing employment of organic polymers in structural and electrical components of military aircraft, an understanding of the mechanisms that produce degradative changes and limit the lifetime of these materials is of paramount importance. In this study we have applied the techniques of magnetic resonance spectroscopy, both electron paramagnetic resonance (EPR) and nuclear magnetic resonance (NMR), to two problems that occur in the long-term behavior of epoxy resins and polyurethane materials. First, sorbed water lowers the glass transition temperature of cured epoxy resins and decreases their high-temperature mechanical properties.[1,2] Second, polyester polyurethane can catastrophically depolymerize, thereby reverting from a rubbery solid to a viscous liquid following exposure to hot ($\sim$ 360 K) humid environments.[3]

Both problems intimately involve molecular motions in the polymer. For the epoxy resin, the motions are the main-chain segmental motions associated with the glass transition; for the polyurethanes, the motions are associated with changes in the microviscosity resulting from depolymerization. Magnetic resonance techniques are powerful and specific for investigating these problems since spectral lineshapes and relaxation times are sensitive to molecular motions.[4]

The EPR experiments used the spin-label[5] and spin-probe[6] methods wherein stable nitroxide free radicals are employed to probe their static and dynamic environments in the polymers. In the spin-probe method, the nitroxide is incorporated as a solid solution in the polymer; in the spin-label method, the nitroxide is covalently bound at a known site in the polymer. The EPR spectra of these nitroxide radicals are sensitive to their rotational correlation times, τ_c, over a wide range of values ($\tau_c = 10^{-6}$ to 10^{-11}s). In the slow-motion region ($\tau_c = 10^{-6}$ to 10^{-8}s), the spectrum has an asymmetric shape characteristic of randomly oriented free radicals with an electron spin S = 1/2 and a nuclear spin I = 1. The spectral lines are inhomogeneously broadened because of anisotropic hyperfine and g-tensor interactions and unresolved proton hyperfine splittings. Moreover, in the fast-motion region ($\tau_c = 10^{-9}$ to 10^{-11}s), the spectrum has a narrow three-line shape and is usually homogeneously broadened.

With the present theory of EPR lineshapes, it is possible to evaluate motional correlation times from $\tau_c = 10^{-7}$ to 10^{-11}s using computer simulation of the observed lineshapes.[7] However, sometimes it is more convenient to evaluate τ_c in the slow-motion region using an analytical method developed by Freed[8], whereas in the fast-motion region the theory of Kivelson[9] is normally used. The theory is sufficiently precise[10] to obtain details of motional processes such as the anisotropy in the rotational diffusion rates from the exact way the spectrum develops with increasing motion.

Hydrogen NMR techniques have been employed to study the molecular motion and chemical composition of solid polymers. Measurements of the spin-lattice and spin-spin relaxation times as a function of temperature reveal molecular motion occurring with a correlation time τ_c from 10^{-4} to 10^{-9}s.[11] The spin-spin relaxation time increases abruptly at the onset of extensive molecular motion associated with the glass transition, and the rate of increase provides a qualitative measure of the crosslink density.

Multiple-pulse hydrogen NMR techniques[12] provide chemical-shift information in some solid polymers. Thus, chemical composition can be determined, molecular motion can be identified, and chemical changes can be monitored.

2. EPOXY RESINS

2.1 Epoxy Sample Preparation

The epoxy system studied was the diglycidyl ether of bisphenol-A (DGEBA) cured with diethylene triamine (DETA). The molecular structures are shown in Figure 1. The commercial resin used was DER 332 obtained from Dow Chemical Company.

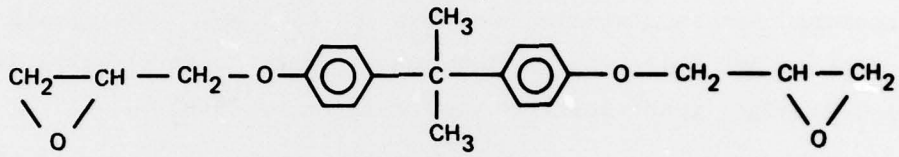

(DGEBA)

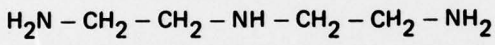

(DETA)

GP79-0258-50

Figure 1 Structures of DGEBA and DETA.

EPR Samples - The DGEBA was heated (∿ 333 K) prior to use to melt any crystals which had formed. In the spin-labeling experiment, the samples containing uncured DGEBA and the nitroxide radicals were usually kept at 358 K to speed up the reactions. The EPR spectra were monitored at suitable intervals either at 293 K or 315 K until the formation of the desired label, e.g., end label or quaternary salt, was indicated. Curing of the spin-labeled samples was accomplished by adding the necessary amount of the curing agent, DETA, to these samples at 293 K. The resulting mixture was thoroughly stirred, heated slightly (∿ 320 K), and degassed in a vacuum oven until all air bubbling ceased. The mixture was then poured into flexible silicone molds[13] (G.E. type RTV 664/B silicone mold compound was found to be ideal for this use). After 24 h curing at 294 K, cylindrical samples 3.2 mm in diameter were released from the molds.

NMR Samples - NMR samples were made from a stoichiometric mixture of 100 g DGEBA and 11.86 g DETA. Nonstoichiometric samples were also made by mixing

100 g DGEBA with R x 11.86 g of DETA; these samples were denoted as 1:R stoichiometric samples. The DGEBA was heated in a vacuum oven at 333 K for 30 min to melt any crystals which might be present. The DGEBA and DETA were thoroughly mixed, put in a vacuum oven for 5 min to remove trapped air, and poured into silicone rubber molds to produce 3.2 mm diam cylindrical samples. The epoxy samples were cured at 294 K for 24 h, removed from the molds, and cut into approximately 8 mm lengths (≈ 80 mg weight). The resulting samples were bubble-free, colorless, and optically transparent.

The usual procedure for introducing water into the cured epoxy samples consisted of soaking them in distilled water at 368 to 373 K. The sample weight was obtained prior to and following the NMR measurements to assure that the sample did not lose significant moisture during the measurements.

2.2 Spin Labeling Reactions in the Uncured Epoxy

The nitroxide amines used were 4-amino-2,2,6,6-tetramethylpiperidine-1-oxyl (TAMIN)[14], 4-methylamino-2,2,6,6-tetramethylpiperidine-1-oxyl (METAMIN), and 4-trimethylammonium-2,2,6,6-tetramethylpiperidine-1-oxyl iodide (TRIMETAMIN iodide).[15] Complementary experiments involving the spin probes di-t-butyl nitroxide (DBNO)[14], 4-hydroxy-2,2,6,6-tetramethylpiperidine-1-oxyl (TANOL)[14], and 2,2,6,6-tetramethylpiperidine-1-oxyl (TEMPO)[15] also were performed. The structures of these nitroxide labels and probes are shown in Figure 2.

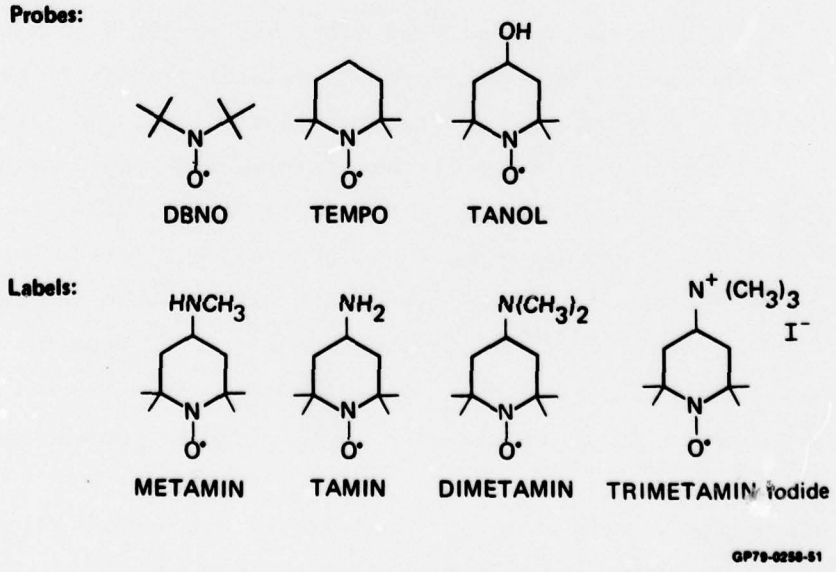

Figure 2 Nitroxide spin labels and spin probes used in epoxy studies.

First the results of the spin-labeling experiments obtained when METAMIN reacted with uncured DGEBA at 353 K are discussed. Immediately after mixing METAMIN with uncured DGEBA resin, the spectrum of the unreacted spin probe METAMIN was observed at 293 K (designated spectrum 1 in Figure 3). As the reaction proceeded at 353 K, the spectrum of a more rigid species developed (spectrum 2 in Figure 3) and increased in intensity as the intensity of spectrum 1 decreased. This process is illustrated in Figure 3 which shows spectra recorded at 3 min, 15 min, and 20 h after initiation of the reaction. On further heating of the DGEBA samples containing METAMIN at 353 K ($\geq$ 20 h), a third spectrum (spectrum 3) more rigid than spectrum 2 was observed; it could be distinguished from spectrum 2 only above 310 K, as illustrated in Figures 4 and 5. The spectra in Figure 4 were obtained from METAMIN and DGEBA after 6 h of reaction and were recorded at 293 and 318 K. On the other hand, the spectra in Figure 5 were obtained after 72 h of reaction. The spectra taken at 293 K in Figures 4 and 5 show only small differences; for example, there is an additional unresolved peak on the centerline in Figure 5. However, as also shown in Figures 4 and 5, the corresponding spectra at 318 K differ greatly. After heating at 353 K for $\sim$ 70 h, yet another spectrum (spectrum 4 in Figure 5) consisting of three narrow lines was observed at 318 K. This spectrum is clearly resolved at 318 K as shown in Figure 5 but only indicated at 293 K in Figure 5. Observations at some temperatures following certain sample heating times showed the simultaneous presence of three spectra, viz., spectrum 2, spectrum 3, and spectrum 4. A typical example is the spectrum shown in Figure 5 recorded at 318 K.

Spectrum 1 is assigned to the spin probe METAMIN, spectrum 2 to the DGEBA monomer end-labeled with METAMIN (Figure 6a), spectrum 3 to the spin-labeled quaternary salt (Figure 6b), and spectrum 4 to the spin probe TEMPENE (Figure 6d). The latter forms as the result of a Hofmann elimination reaction[16] involving a molecular rearrangement following bond scission in the quaternary salt. Its formation is evidence that spectrum 3 can be assigned to the spin-labeled quaternary salt.

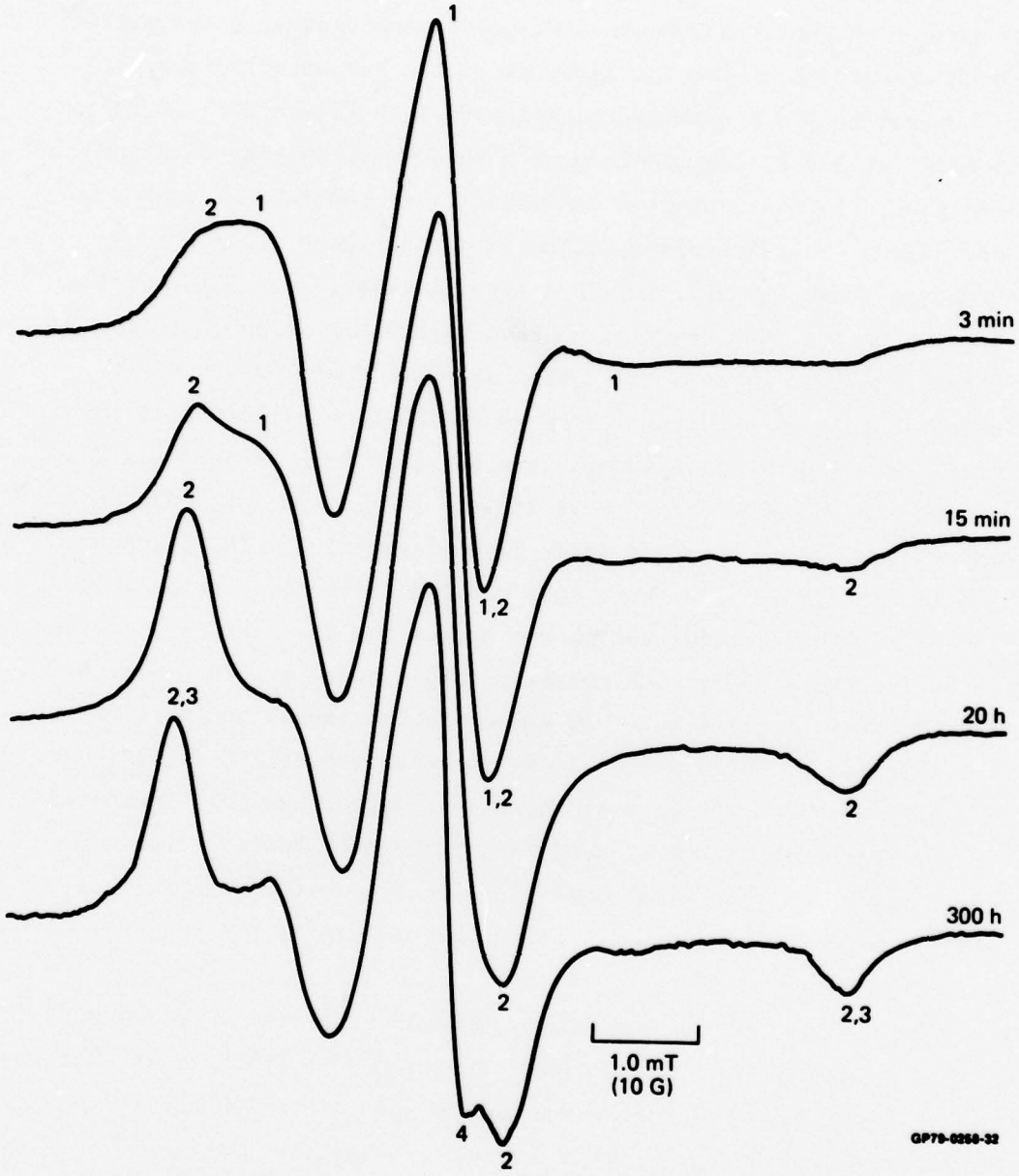

Figure 3 Spectra observed at times 3 min, 15 min, 20 h, and 300 h into the reaction of METAMIN with uncured DGEBA. Spectrum 1 denotes the spectrum of the unreacted METAMIN spin probe. Spectrum 2 denotes the spectrum of DGEBA end-labeled with METAMIN. Spectrum 3 denotes the spectrum of the spin-labeled quaternary salt. Spectrum 4 denotes the spectrum of the TEMPENE spin probe.

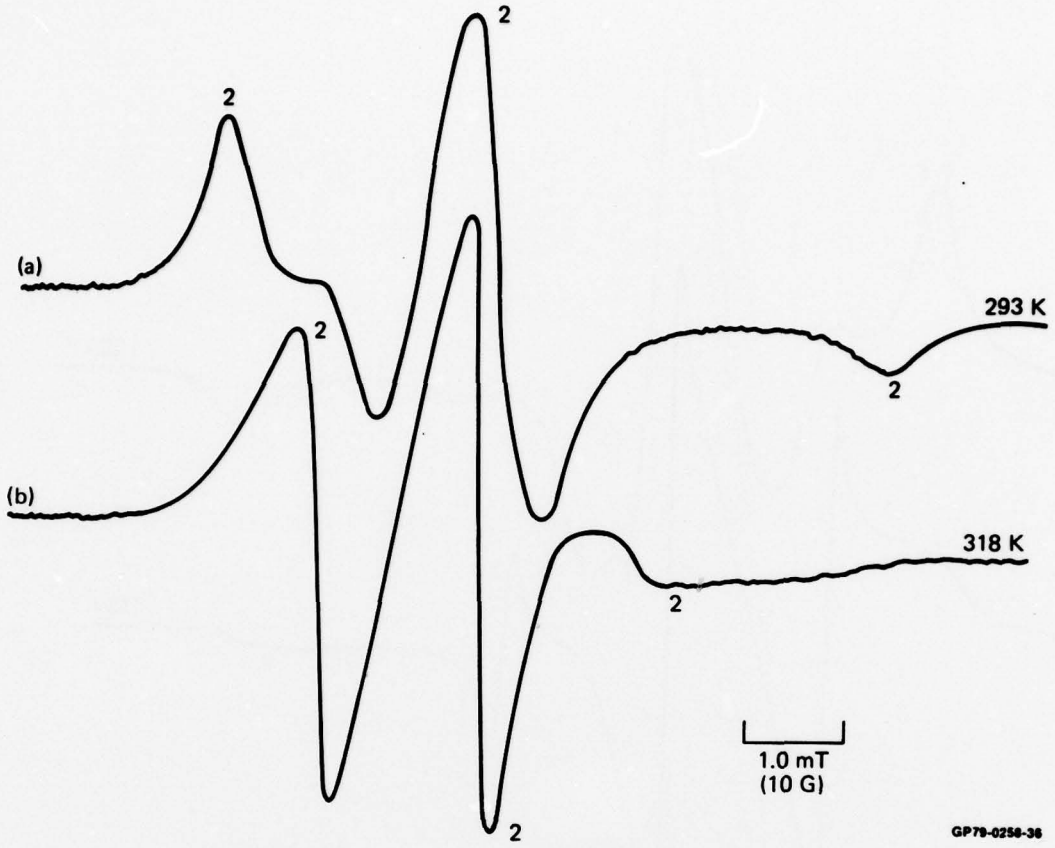

Figure 4 The spectra observed at 293 K and 318 K after 6 h into the reaction of METAMIN with uncured DGEBA. Spectrum 2 denotes the spectrum of DGEBA end-labeled with METAMIN.

Figure 5 The spectra observed at 293 K and 318 K after 72 h into the reaction of METAMIN with uncured DGEBA. Spectrum 2 denotes the spectrum of DGEBA end-labeled with METAMIN. Spectrum 3 denotes the spectrum of the spin-labeled quaternary salt. Spectrum 4 denotes the spectrum of the TEMPENE spin probe.

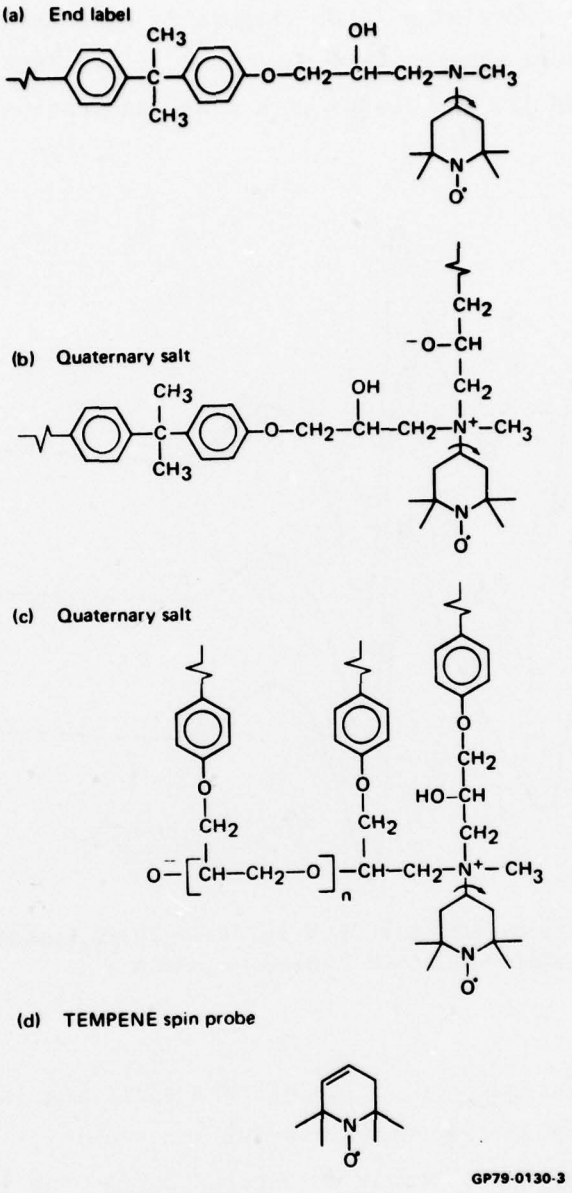

Figure 6 Structures of nitroxide species resulting from the reaction of DGEBA with METAMIN: (a) the *end*-labeled DGEBA, (b) and (c) the quaternary salts, and (d) the TEMPENE spin probe.

Samples of DGEBA containing TANOL (Figure 2) were heated at 353 K for several hours, and their spectra were monitored at set intervals. As shown in Figure 7, the spectrum did not change with time, indicating that TANOL does not react with DGEBA.

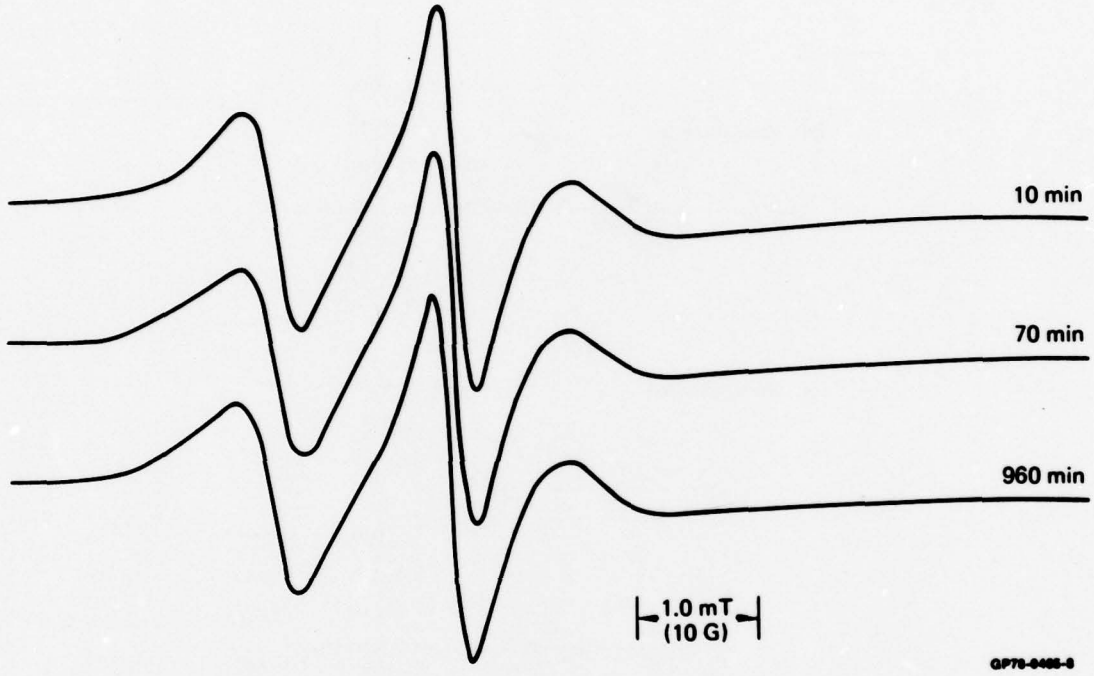

Figure 7 The spectra observed at 293 K after 10 min, 70 min, and 960 min from initial mixing of TANOL with uncured DGEBA.

The temperature dependences of the extrema splitting (the separation between the major peaks in the derivative EPR spectrum) for spectrum 2, spectrum 3, spectrum 4, and a sample of uncured DGEBA containing the spin probe TANOL were measured and are plotted in Figure 8. The onset of the motional narrowing, as is indicated by the spectral collapse, occurs at increasingly higher temperatures for the TEMPENE spin probe, the METAMIN spin probe, the end-labeled monomer, and the spin-labeled quaternary salt, respectively. This feature indicates the increasing order of the motional correlation times for these observed species. Furthermore, the large difference in extrema splittings resulting from the difference in the correlation times allows spectral discrimination between the end-labeled monomer and the spin-labeled quaternary salt above 310 K.

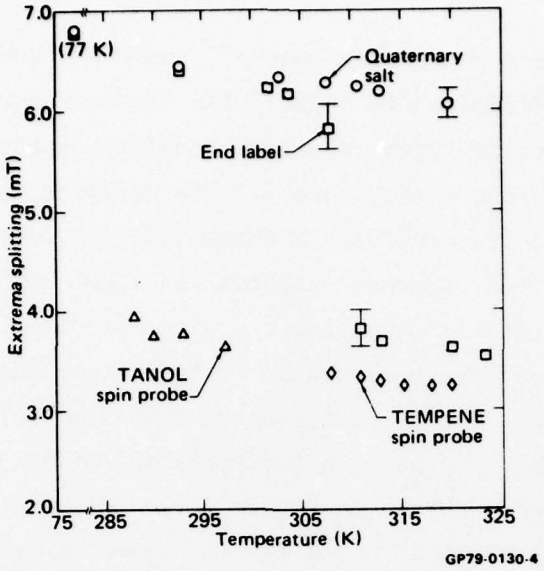

Figure 8 Temperature dependence of extrema splittings for the end label and quaternary salt of METAMIN, and also the spin probes TANOL and TEMPENE.

Quaternary salts of the type shown in Figure 6c should also form with METAMIN. However, only one EPR spectrum could be identified with the spin-labeled quaternary salts. This result implies that if the different quaternary salts (i.e., with n > 1 in Figure 6c) were present, they all had similar motional correlation times.

The data for TANOL and spectrum 4 in Figure 8 suggest that the species associated with spectrum 4 is a spin probe with a motional correlation time comparable with that of TANOL. However, the nitrogen isotropic hyperfine coupling constants are measurably different.

TEMPENE was synthesized from TRIMETAMIN iodide (Figure 2) to verify that the three sharp lines appearing in the EPR spectra of DGEBA reacted with METAMIN could be conclusively assigned to TEMPENE. The TRIMETAMIN iodide was reacted with sodium isopropoxide to yield the TRIMETAMIN isopropoxide salt. This salt was thermally converted to TEMPENE by heating at 410 K in an evacuated container. The TEMPENE was recovered by vacuum sublimation onto a cold finger. The synthesized TEMPENE was dissolved in DGEBA, and the EPR spectrum was obtained at 318 K. The observed spectrum showed nitrogen hyperfine coupling constants and linewidths identical to those obtained in the reaction of METAMIN with DGEBA, viz., spectrum 4 in Figure 5.

TEMPENE obtained from a commercial source[15] which had been synthesized in yet another manner[17] was dissolved in DGEBA. Its EPR spectrum taken at 318 K also exhibited an isotropic nitrogen hyperfine coupling constant and linewidths identical to those of spectrum 4 in Figure 5. The starting material for this TEMPENE was TANOL which was reacted with methanesulfonyl chloride in a dry pyridine-ether solution. The recovered product was TANOL methanesulfonate which on reacting with alcoholic potassium hydroxide produced TEMPENE.

Analogous spectra have been observed in DGEBA reacted with TAMIN at 353 K (Figure 9), but the spectral interpretations are complicated by the nitroxide label acting as a bridging group between two DGEBA molecules (Figure 10). For example, the series of spectra shown in Figure 9 was observed at 293 K following reaction of DGEBA with TAMIN at 353 K for the times indicated. Spectrum 1

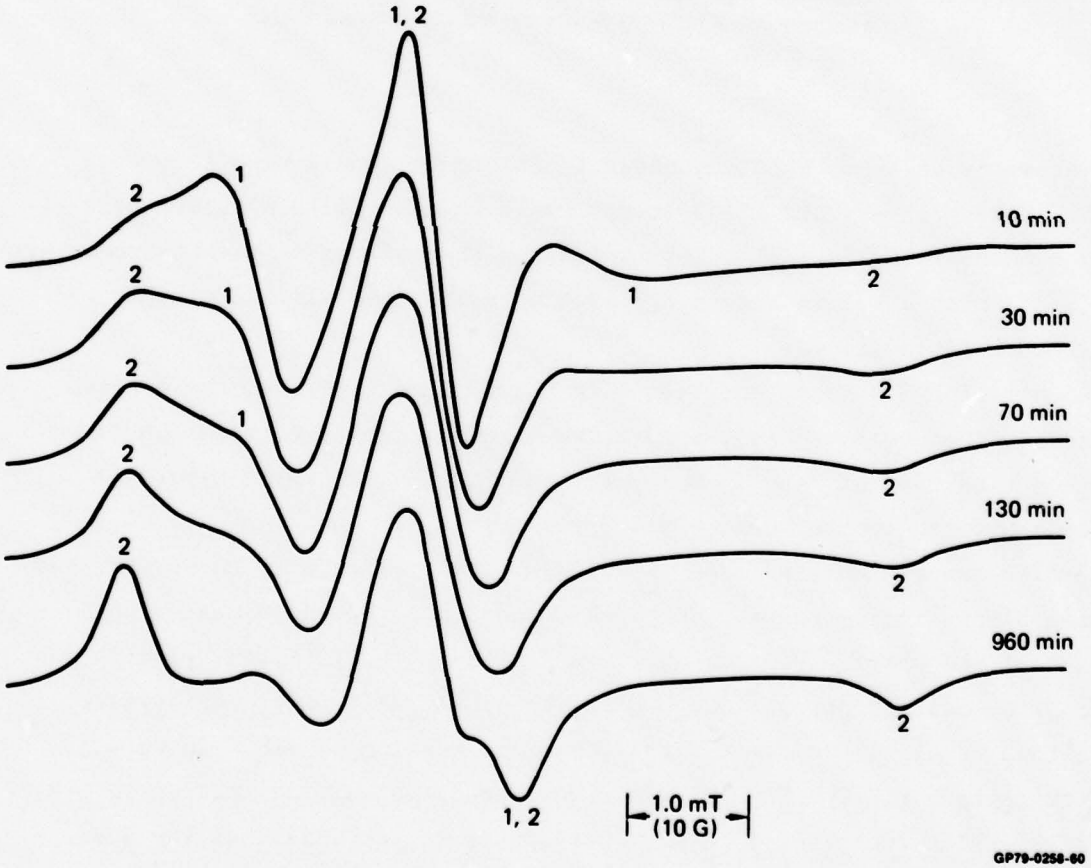

Figure 9 The EPR spectra observed at 293 K following heating at 358 K for the times shown as TAMIN reacts with DGEBA to form spin-labeled DGEBA. Spectrum 1 denotes the spectrum of the unreacted TAMIN spin probe. Spectrum 2 denotes the spectrum of DGEBA end-labeled with TAMIN.

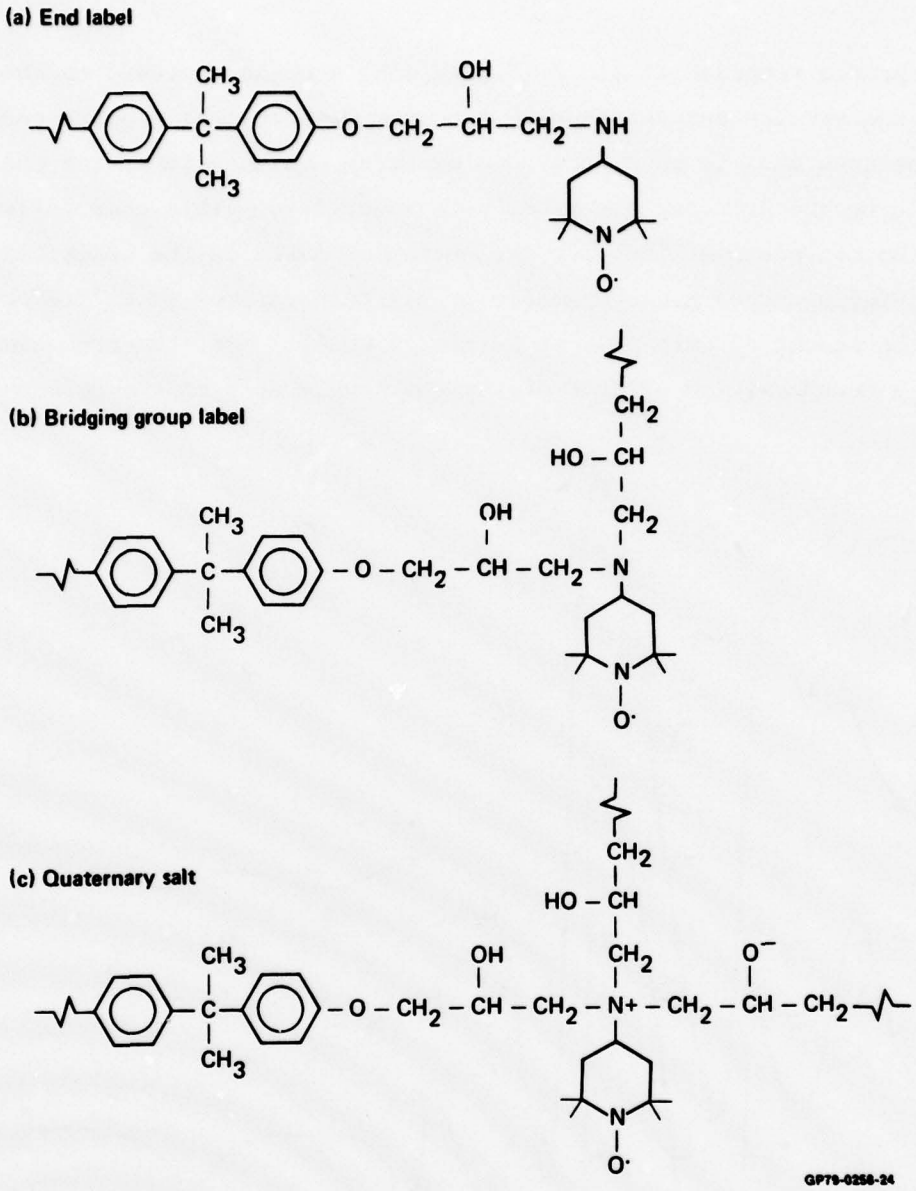

Figure 10 Structures of nitroxide species resulting from the reaction of DGEBA with TAMIN: (a) the end-labeled DGEBA, (b) the bridging group and (c) the quaternary salt.

is associated with the unreacted TAMIN spin probe, whereas spectrum 2 is the DGEBA monomer end-labeled with TAMIN. As shown in Figure 9, the intensity of the latter increases with time at the expense of the former. After reacting for 13 h at 353 K, the spectra shown in Figure 11 were recorded at 315 K. Spectrum 3 is associated with a more rigid species than the end-labeled DGEBA monomer. This species is either the bridging group (Figure 10b) or the quaternary salt (Figure 10c). Furthermore, after reacting for 136 h at 353 K,

the observed spectra recorded at 318 K (Figure 11b) show an increase in concentration of the species associated with spectrum 3 as well as the presence of TEMPENE (spectrum 4). To date, only one spectrum assigned to either the quaternary salt or the bridging group has been identified. This observation implies that the correlation times for the nitroxide label on the quaternary salt and the bridging group are comparable at all temperatures from 77 K to 360 K and/or the amount of salt present is always small. Yet, the presence of TEMPENE as a decomposition product of the quaternary salt in the Hofmann

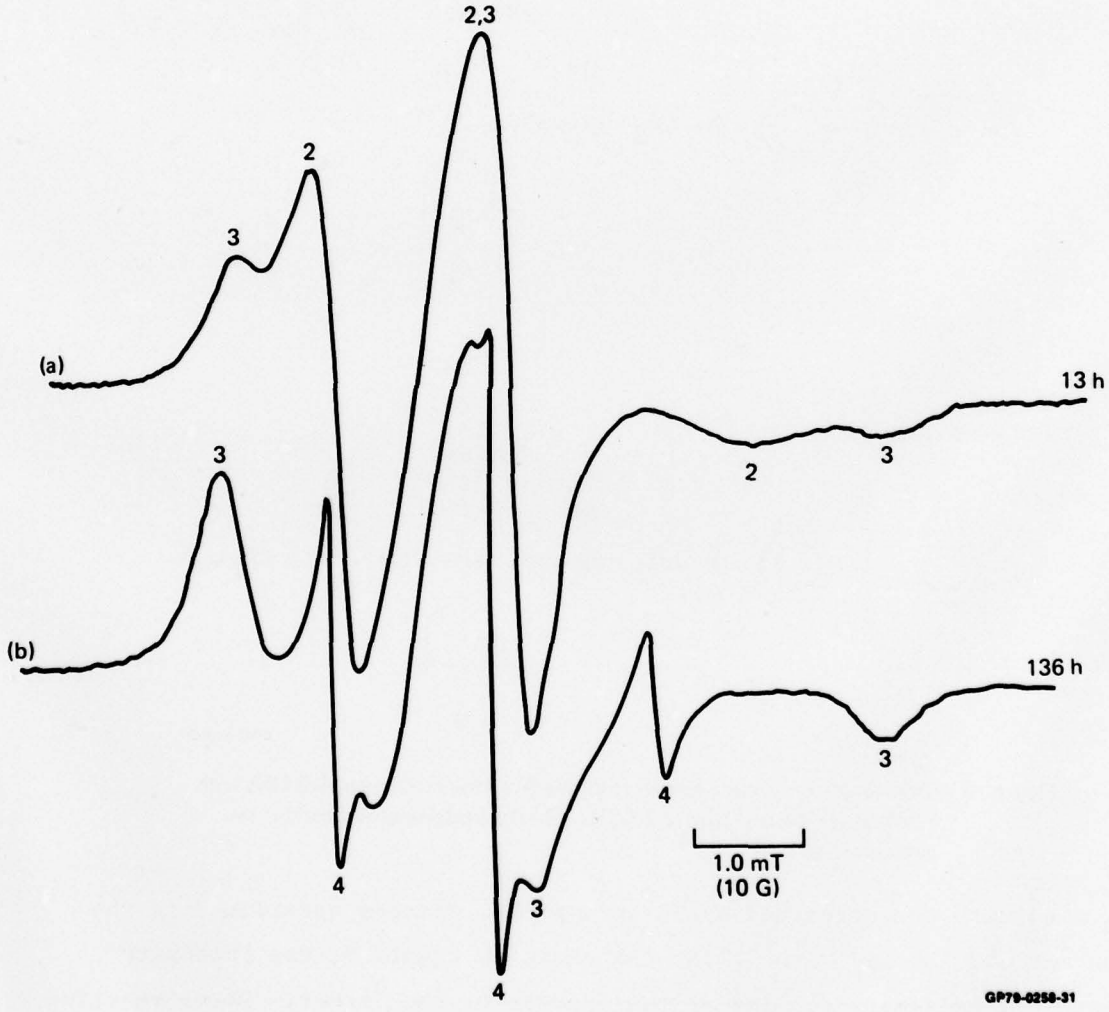

Figure 11 **The spectra observed at 318 K after 13 h and 136 h into the reaction of TAMIN with uncured DGEBA. Spectrum 2 denotes the spectrum of DGEBA end-labeled with TAMIN. Spectrum 3 denotes the spectrum of the bridging-group quaternary-salt. Spectrum 4 denotes the spectrum of the TEMPENE spin probe.**

elimination reaction[16] is a positive indication that the salt formed. Henceforth, the spin-label species associated with spectrum 3 will be referred to as the bridging-group/quaternary-salt.

The temperature dependence of the extrema splitting for the spin-labeled bridging-group/quaternary-salt in uncured DGEBA was measured and is shown in Figure 12 along with the extrema splitting for the spin probe TANOL in uncured DGEBA. The data show that the onset of the motional narrowing occurred at a lower temperature for TANOL than for the spin label; hence the probe is more mobile than the spin label.

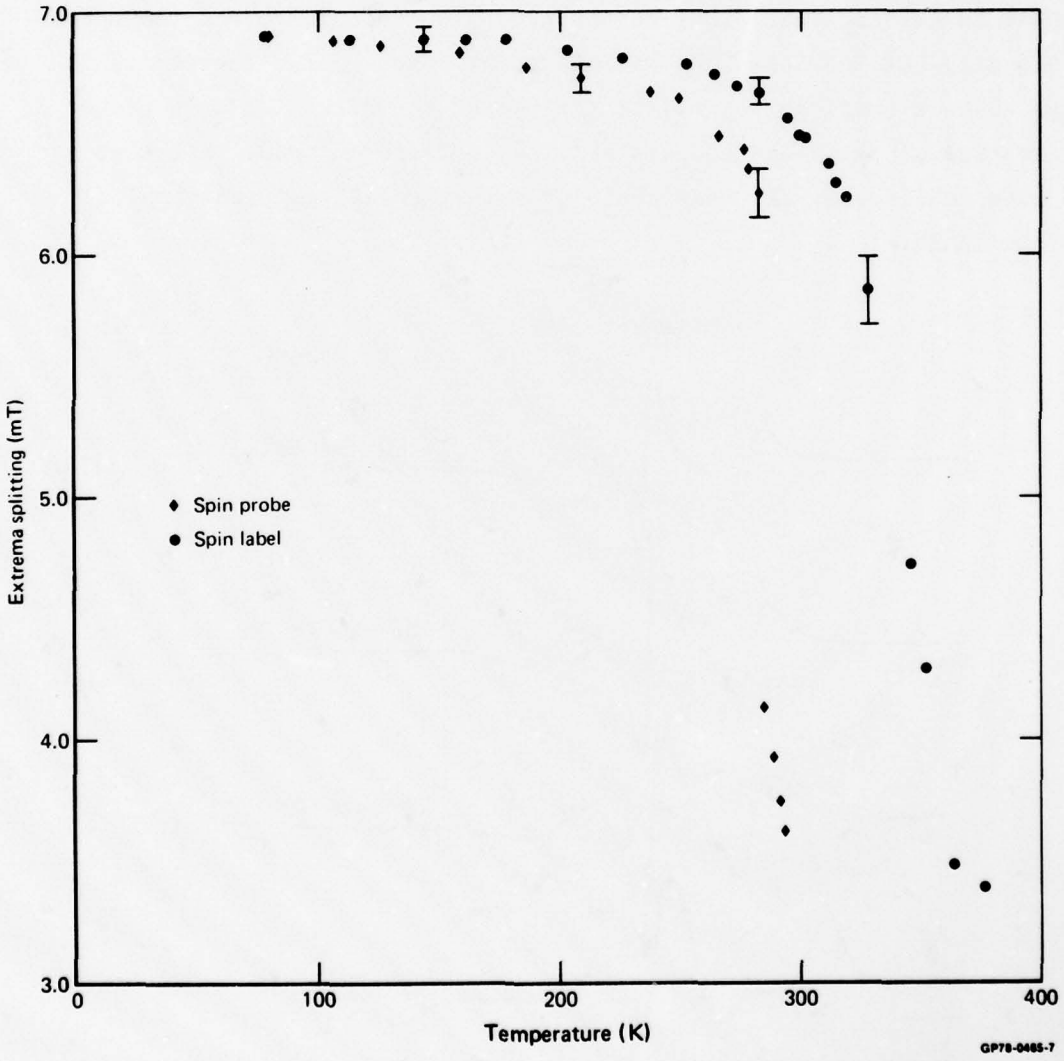

Figure 12 The temperature dependence of the extrema splitting for the spin-labeled bridging-group/quaternary-salt of DGEBA and TAMIN and also the spin probe TANOL in DGEBA.

In the results for the samples of uncured DGEBA containing DIMETAMIN (Figure 2) only three spectra have been observed. These are associated with the DIMETAMIN spin probe, the corresponding spin-labeled quaternary salt, and the spin probe TEMPENE. These results confirm the assignments given to the spectra observed from METAMIN and TAMIN in DGEBA.

The EPR spectra of uncured DGEBA containing the spin probes DBNO, TEMPO, TANOL, and the spin-labeled quaternary salt of TAMIN are shown in Figure 13. The lineshapes and linewidths for these spectra indicate a decreasing mobility of the nitroxides in the order DBNO, TEMPO, TANOL, and the quaternary salt of METAMIN. DBNO is the smallest probe in the group, whereas TEMPO and TANOL are of comparable size but TANOL has the ability to hydrogen bond. Therefore, it is concluded that the motional correlation times of the nitroxide spin probes depend on the size of the probe and its ability to hydrogen bond. All these probes are more mobile than the end-labels or spin-labeled quaternary salts of METAMIN and TAMIN.

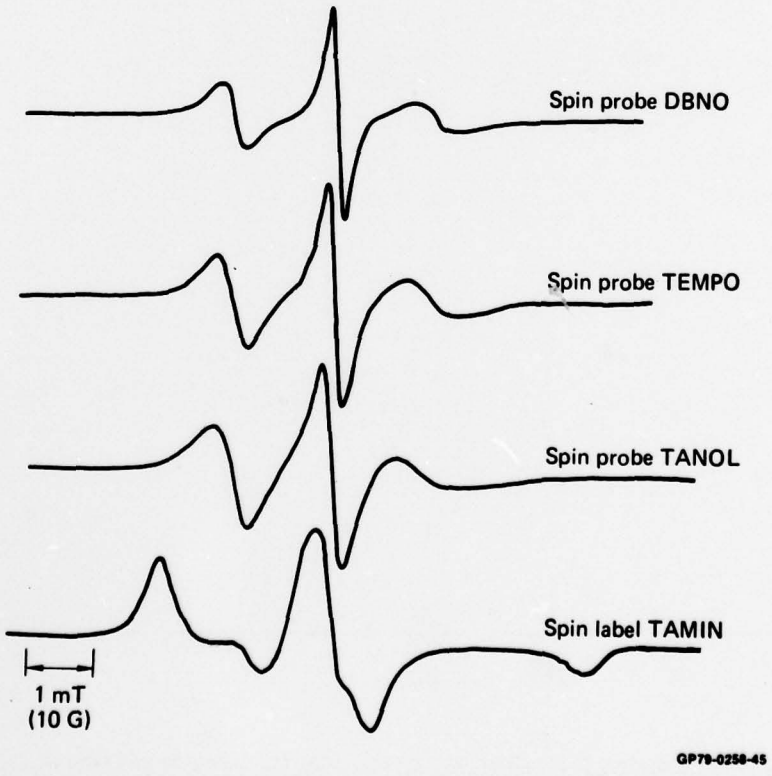

Figure 13 EPR spectra of the spin probes DBNO, TEMPO, TANOL and the spin-label TAMIN in uncured DGEBA.

TRIMETAMIN iodide (Figure 2) was also investigated in uncured DGEBA. The solubility of this salt in DGEBA is low; hence the spectra taken after 5 min and 5 h heating at 353 K (Figures 14a,14b) exhibited lineshapes characteristic of line broadening through Heisenberg spin exchange[18] effects which probably arise because of clustering of the nitroxide probes. After 20 h at 353 K, the observed spectrum (Figure 14c) was typical of randomly oriented dispersed immobile nitroxides and is attributed to the TRIMETAMIN cation spin probe.

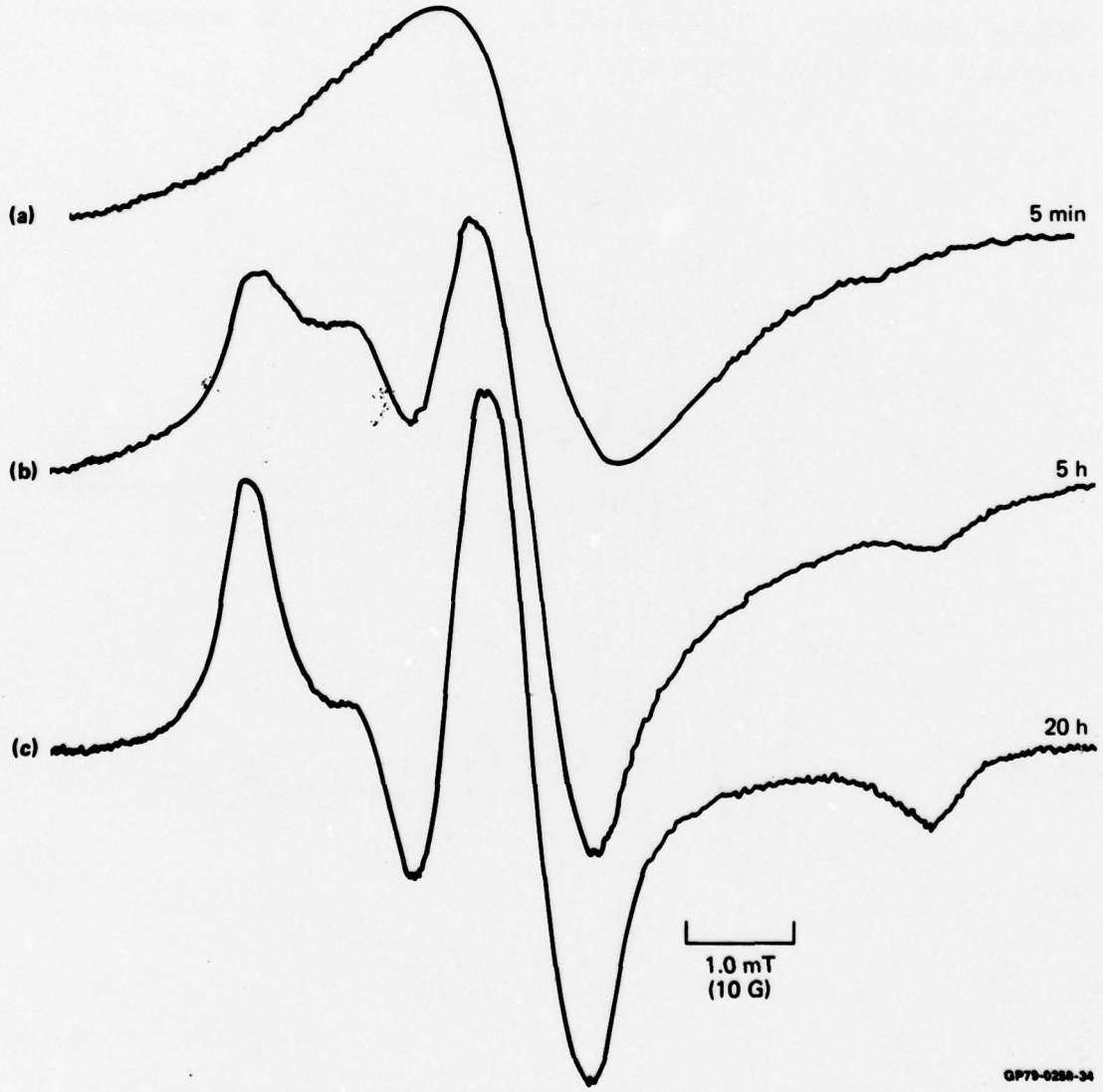

Figure 14 Spectra observed at 293 K after heating a mixture of TRIMETAMIN iodide in uncured DETA at 353 K for (a) 5 min, (b) 5 h and (c) 20 h.

This species is less mobile than the TAMIN, METAMIN, DBNO, TEMPO, or TANOL spin probes since it is present in DGEBA as part of an ion-pair or as a heavily solvated free cation and acts as a large spin probe. After 100 h reaction at 353 K, the spectra of samples of uncured DGEBA containing TRIMETAMIN iodide show the presence of three nitroxide species (Figure 15). These species are identified with the TRIMETAMIN iodide spin probe, the quaternary salt of DIMETAMIN, and TEMPENE. Hence, at ∿ 350 K the TRIMETAMIN cation must decompose by eliminating a methyl group to form DIMETAMIN. The DIMETAMIN is too reactive to be observed and rapidly forms the corresponding quaternary salt and subsequently TEMPENE.

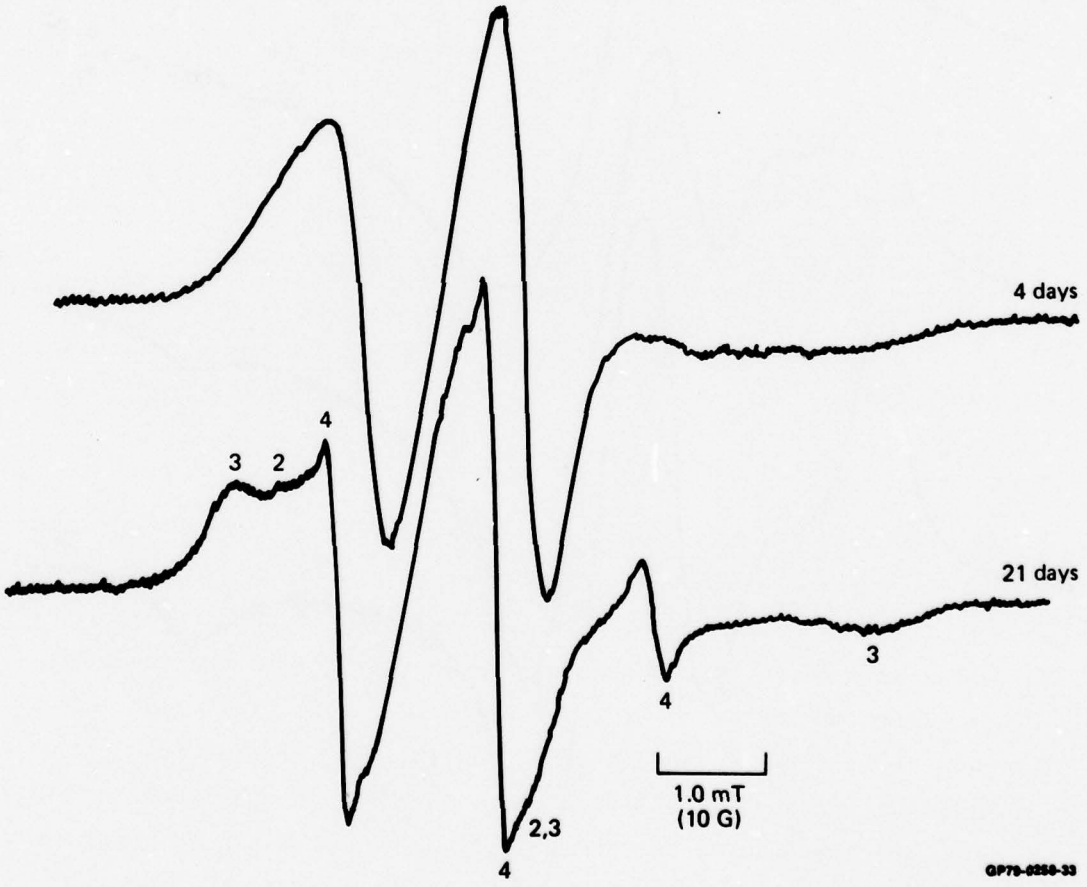

Figure 15 The spectra observed at 318 K after 4 days and 21 days into the reaction of TRIMETAMIN iodide with uncured DGEBA. Spectrum 2 denotes the spectrum of the TRIMETAMIN cation probe. Spectrum 3 denotes the spectrum of DGEBA end-labeled with DIMETAMIN. Spectrum 4 denotes the spectrum of the TEMPENE spin probe.

In summary, all EPR experiments with TAMIN, METAMIN, DIMETAMIN, and TRIMETAMIN iodide in uncured DGEBA indicate the formation of two types of spin-labels, an end-label, a spin-labeled quaternary salt, and the spin probe TEMPENE. Moreover, the identification of the spin probe TEMPENE is positive indication that its precursor, a quaternary salt, has formed. Since the quaternary salt can be an initiator in the self-polymerization reaction in DGEBA, its presence indicates that self-polymerization occurs.

2.3 Infrared Measurements in the Uncured Epoxy Containing TAMIN

The reaction of TAMIN with uncured DGEBA was monitored with infrared spectroscopy to obtain additional or new information supporting the conclusions of the EPR results. In particular, proof was sought that TAMIN could bind to one, two, or more DGEBA molecules.

Both the DGEBA and TAMIN were dried over P_2O_5 at 335 K and 298 K, respectively, using a glass pistol. These materials were then mixed under a dry-nitrogen atmosphere and monitored with an infrared spectrometer (Perkin Elmer model 457). Standard-solution cells with potassium-bromide windows and a 0.1-mm path length were used. Typical spectra are shown in Figure 16. The absorption bands at 3.03 μm and 2.97 μm, identified with TAMIN NH stretching vibrations, decreased in intensity with time, and a strong absorption band, presumably attributable to alcoholic OH stretching vibrations, appeared at 2.93 μm. This new absorption band is consistent with the reaction of an amine with an epoxy whereby OH groups are produced as a result of opening the epoxide ring.

A plot of the intensity of the 2.97 μm peak as a function of time is shown in Figure 17. The time dependence of the peak at 14.7 μm in Figure 17, attributable to NH bending vibrations, also is included. Both plots indicate that DGEBA reacts with TAMIN at a rate that is consistent with the reaction rates indicated from the EPR results; the reaction was essentially complete in $\sim$ 8 h. However, in contrast to the detailed conclusions inferred from the EPR results where it was possible to positively identify an end label, a quaternary salt, and the spin probe TEMPENE, it was not possible to conclude from the infrared spectra the number of DGEBA molecules bonded to TAMIN.

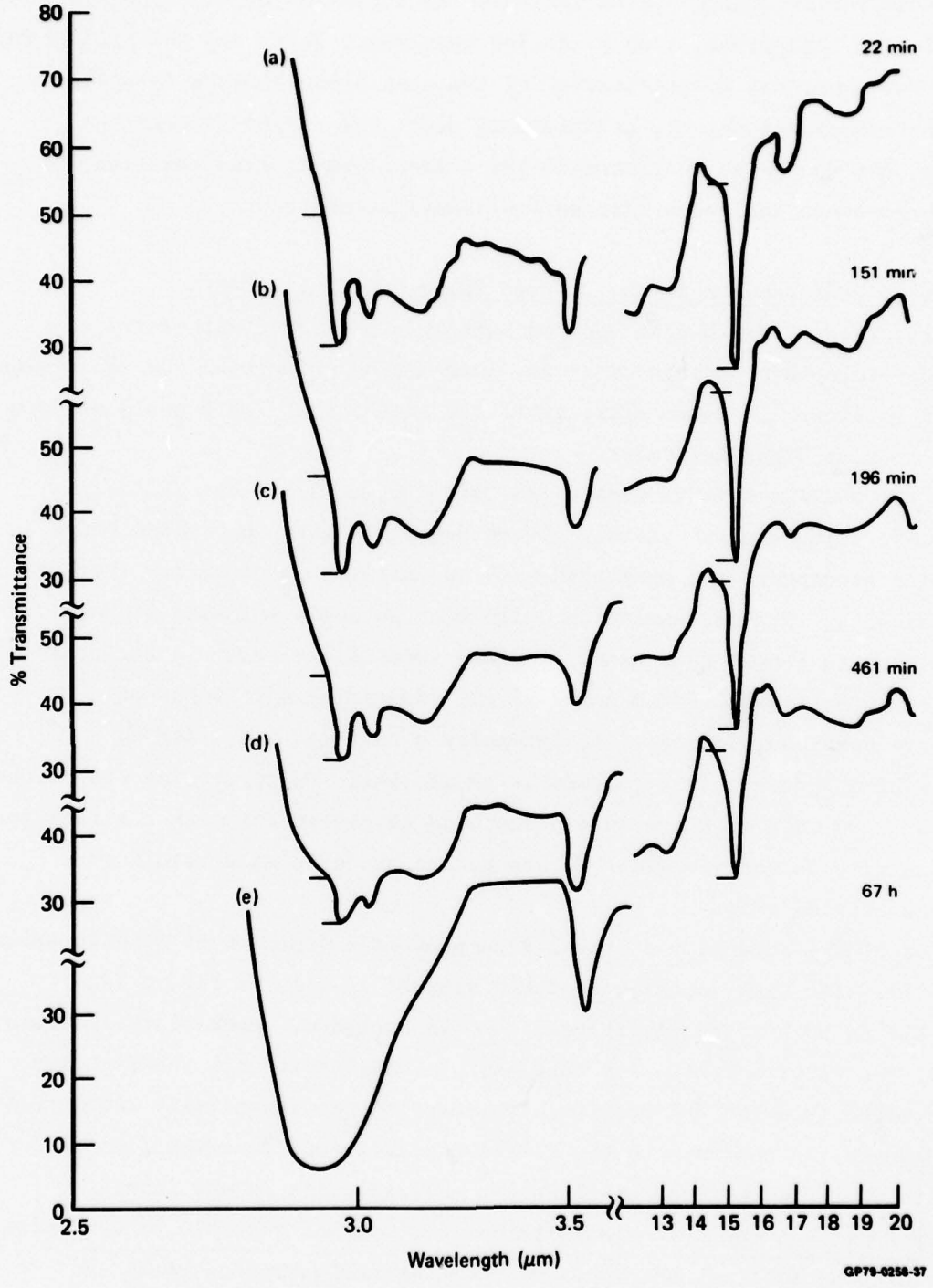

Figure 16 IR spectra observed at 293 K after (a) 22 min, (b) 151 min, (c) 196 min, (d) 461 min, and (e) 67 h following initial mixing of TAMIN with uncured DGEBA.

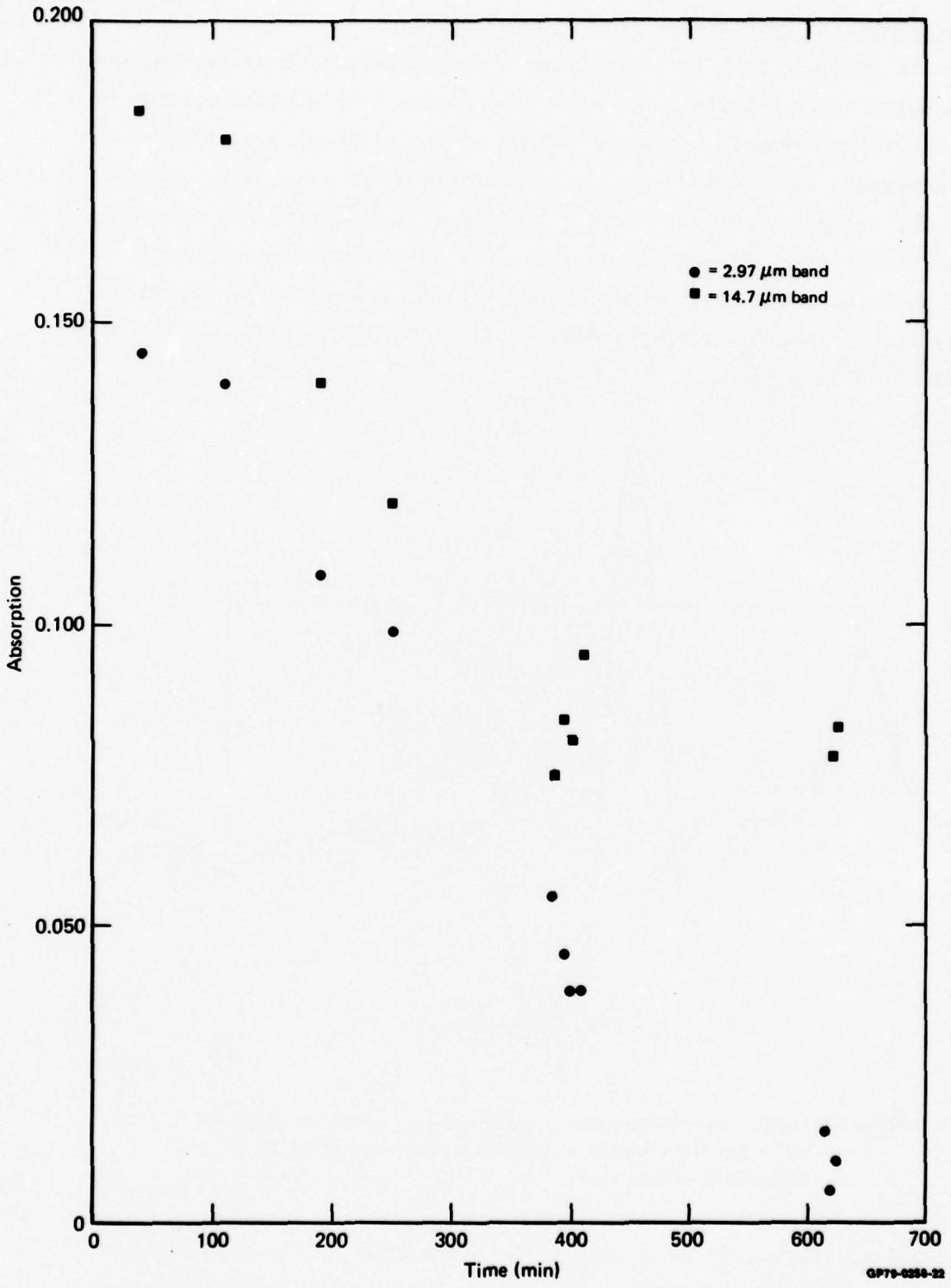

Figure 17 Plot of time dependence of the intensities of the 2.97 μm and 14.7 μm IR bands as TAMIN reacts with DGEBA.

2.4 Spin Labels and Spin Probes in Dry, Cured Epoxy

There is evidence that the lineshapes observed from spin probes and spin labels in DGEBA epoxy samples cured with DETA result from a superposition of spectra, each with slightly different values of the nitrogen hyperfine tensor (A), the g-tensor, and possibly the motional correlation time, τ_c. The distribution in the A-tensor, g-tensor, and τ_c values which leads to the spectral variations result from site-to-site differences in the polymer which the nitroxide probe or label experiences. The half-width and extrema splitting parameters Δ_ℓ, Δ_u, and Δ_o, respectively, used to characterize the lineshapes are defined in Figure 18.

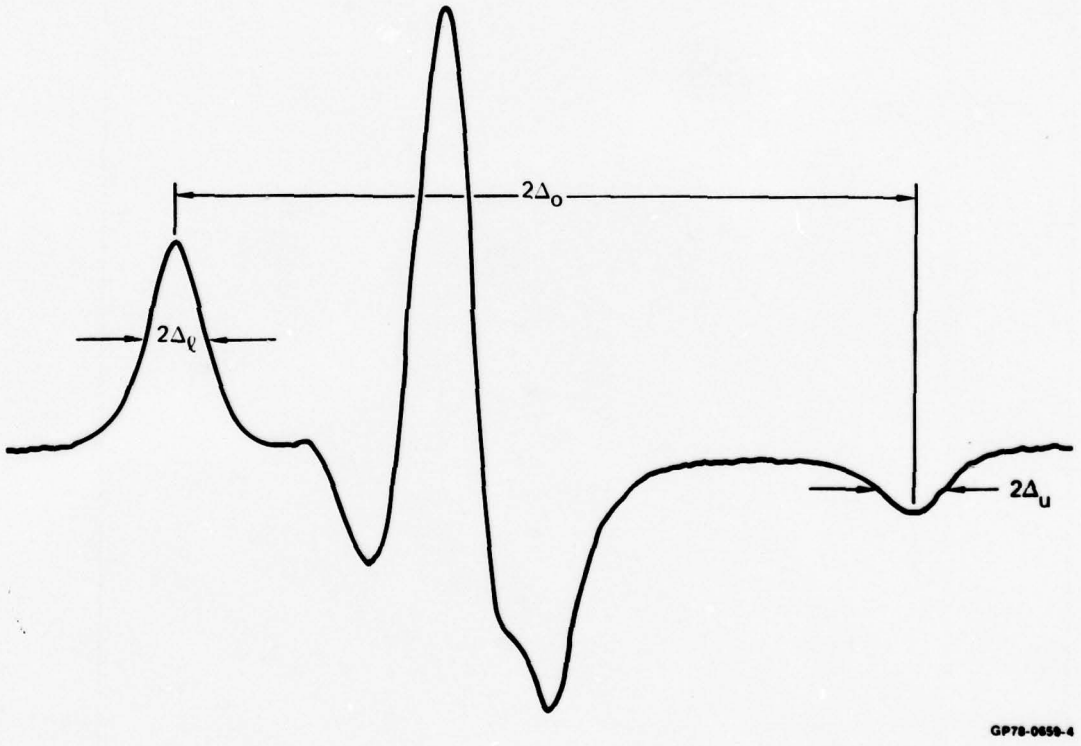

Figure 18 Definition of EPR lineshape parameters: Δ_ℓ, Δ_u are the half-width at half-height of the low-field and high-field peaks, respectively; $2\Delta_o$ is the *extrema* splitting.

In general, the values of Δ_ℓ and Δ_u for nitroxide spin probes and spin labels in solid polymers are larger than the values for nitroxide spin probes in low molecular weight glasses. Although contributions to Δ_ℓ and Δ_u from dipolar broadenings result from protons in the surrounding environment, the

increase in widths is caused mainly by an increase in the distributions of A_{zz}, the z-component of the A-tensor.

The temperature dependences of Δ_ℓ and Δ_u for TANOL in DGEBA cured with DETA were measured. The results in Figure 19 show that above 77 K, Δ_ℓ and Δ_u decrease with increasing temperature, reaching a minimum at $\sim$ 300 K, and then increase with increasing temperature. This behavior indicates that

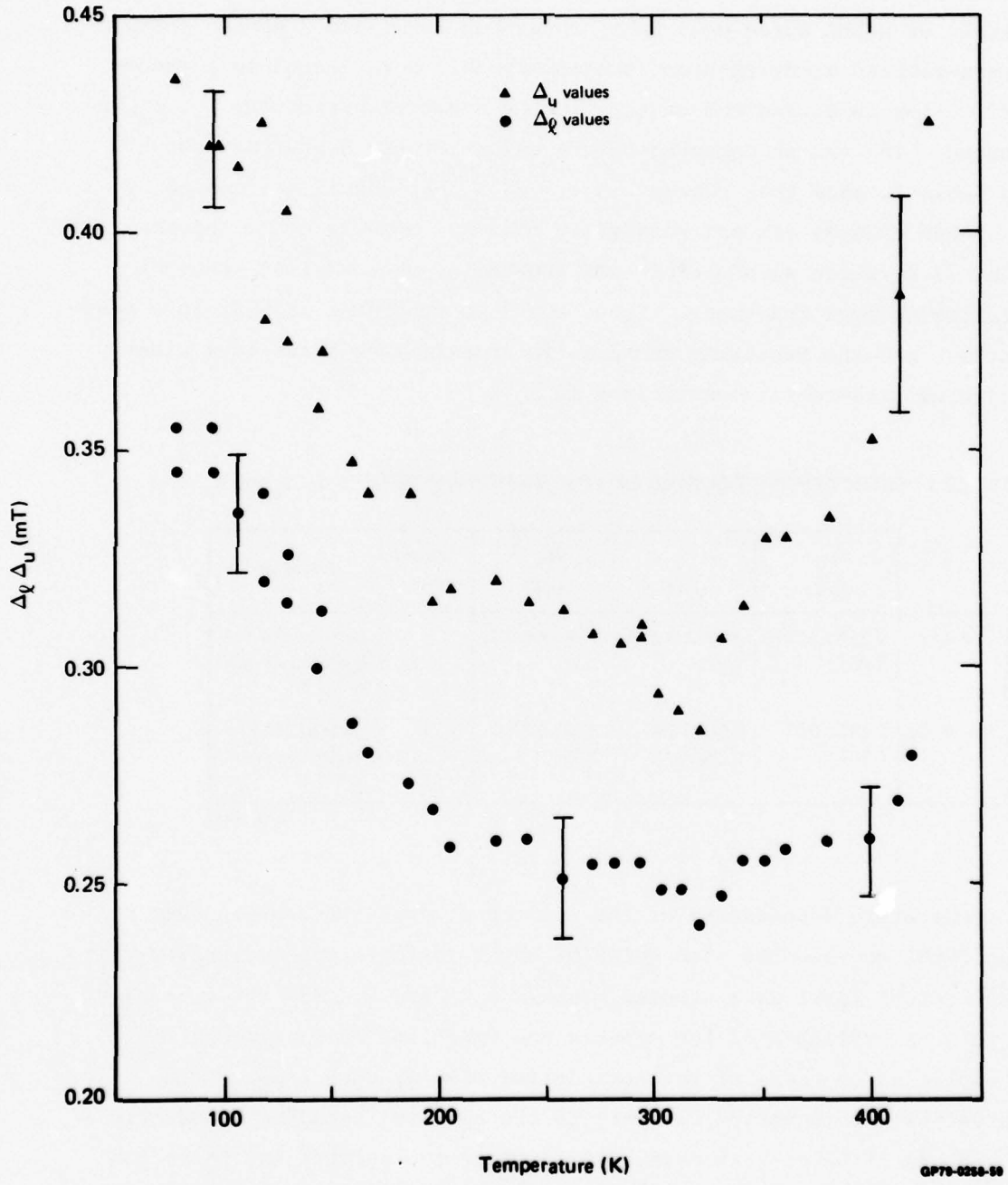

Figure 19 Temperature dependence of extrema widths Δ_ℓ and Δ_u of TANOL in DGEBA cured with DETA (1:1 stoichiometry).

below $\sim$ 300 K the motions are sufficiently fast ($\tau_c \leq 10^{-6}$s) to average out the site-to-site variations in A_{zz} but too slow to effect any reduction in Δ_o. Above 300 K the increase in Δ_ℓ and Δ_u predicted from the model for slow motion dominates, thereby leading to the observed increase of the line widths with increasing temperature.

A sample of DGEBA cured with DETA containing TANOL and a sample containing the spin-labeled bridging-group/quaternary-salt were heated in a vacuum oven at 373 K for 48 h, and the changes in the spectral parameters Δ_ℓ, Δ_u, and Δ_o were noted. The values measured before and after the heat treatment, listed in Table 1, show that changes in Δ_ℓ and Δ_u but not Δ_o are caused by heating. These changes are not related to motional effects since spectra recorded at 77 K, where such motions are frozen-in, show similar spectral changes following heat treatment. Thus, the heat treatment results in a post-cure reaction, and the resulting increase in crosslinking leads to a wider distribution of site-to-site variations in A_{zz}.

TABLE 1 EFFECT OF POST-CURING ON LINESHAPE PARAMETERS Δ_ℓ, Δ_u and Δ_o.

	Δ_ℓ (mT)	Δ_u (mT)	Δ_o (mT)	%weight change	Procedure
Spin label	0.247 ± 0.0075	0.314 ± 0.0075	3.345 ± 0.012	0	Cured at 293 K
	0.267	0.334	3.345	− 0.61	Heated in vacuum at 373 K
Spin probe	0.281 ± 0.01	0.368 ± 0.01	3.300 ± 0.012	0	Cured at 293 K
	0.301	0.394	3.305	− 0.74	Heated in vacuum at 373 K

GP79-0258-19

The temperature dependences of the spectra of dry, cured DGEBA samples containing DGEBA end-labeled with METAMIN, the bridging-group/quaternary-salt and the spin-probe TANOL were studied from 77 K to 400 K. All three samples showed a motional collapse of the spectra and exhibited lineshapes which could be explained in terms of one correlation time at each temperature. This observation was in marked contrast to the spectral behavior on addition of large amounts of water (see Section 2.5) where two spectra and hence two correlation times were observed. Figure 20 is typical of the changes in lineshape observed with increasing temperature.

Figure 20 Spectra observed at 77 K, 293 K, 428 K and 478 K for DGEBA cured with DETA (1:1 stoichiometry) containing DGEBA end-labeled with METAMIN.

The temperature dependences of the extrema splitting for the spin probe TANOL and the spin-labeled bridging-group/quaternary-salt in the cured DGEBA samples are shown in Figure 21. The data indicate that the spin probe is more mobile than the spin label. At 293 K the difference in mobility is detectable in the lineshapes shown in Figure 22 as well as in the extrema splitting. Also shown in Figure 21 is the range of T_g values (T_g = 378 ± 14 K) obtained for these DGEBA samples using differential scanning calorimetry[19] as well as

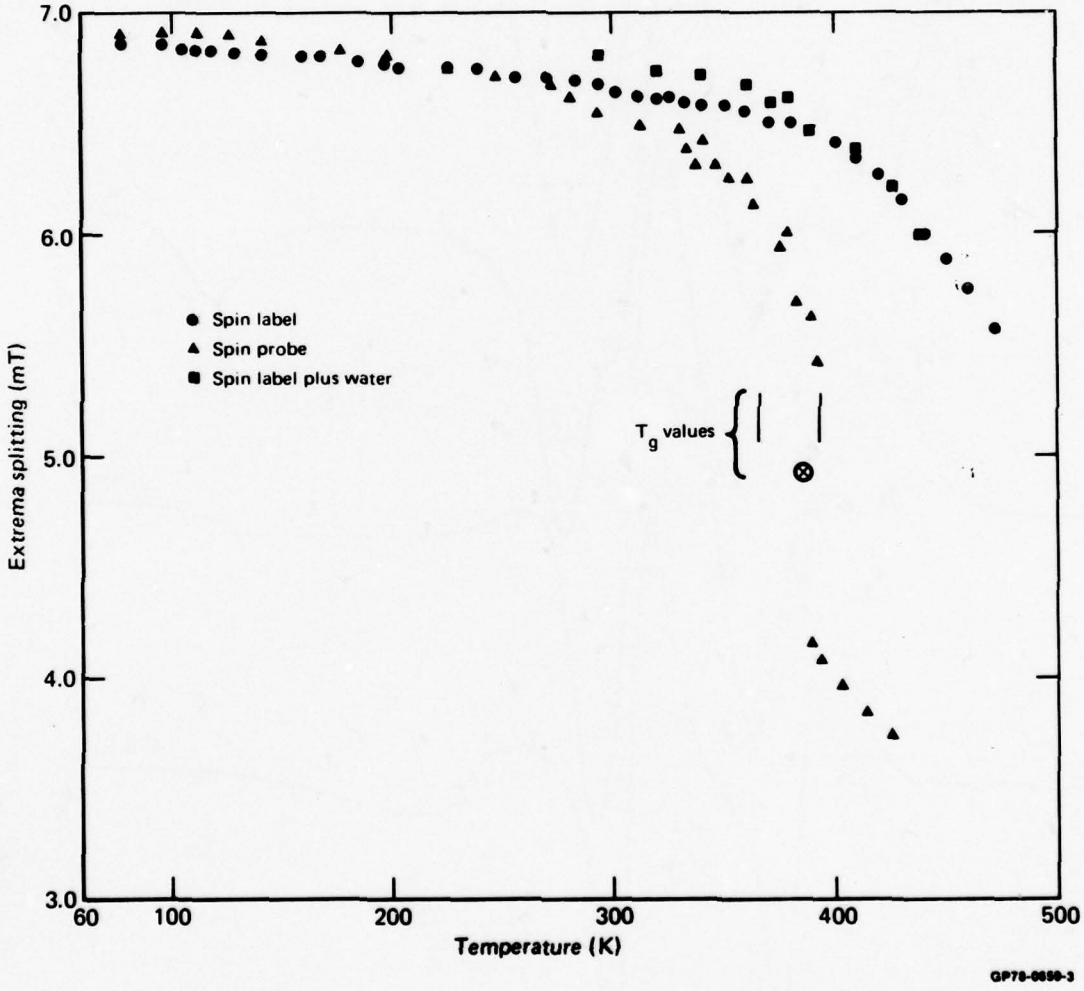

Figure 21 Temperature dependence of the extrema splitting ($2\Delta_o$) for the spin-label bridging-group/quarternary-salt of TAMIN and the TANOL spin probe in DGEBA cured with DETA (1:1 stoichiometry). Also shown are data for the TAMIN sample containing 3.3 wt % water. Vertical bars indicate range of T_g values obtained using DSC and ⊗ indicates the literature value for T_g.

the T_g value quoted in the literature[20]. Thus, T_{5m}, the temperature at which the extrema splitting for TANOL equals 5.0 mT (50 G) because of motional narrowing, correlates with the T_g value. This agreement would imply that the TANOL spin probe could be used to measure T_g in other epoxy systems. This correlation between T_{5m} for spin probes and T_g values has been found by others in different polymers.[21]

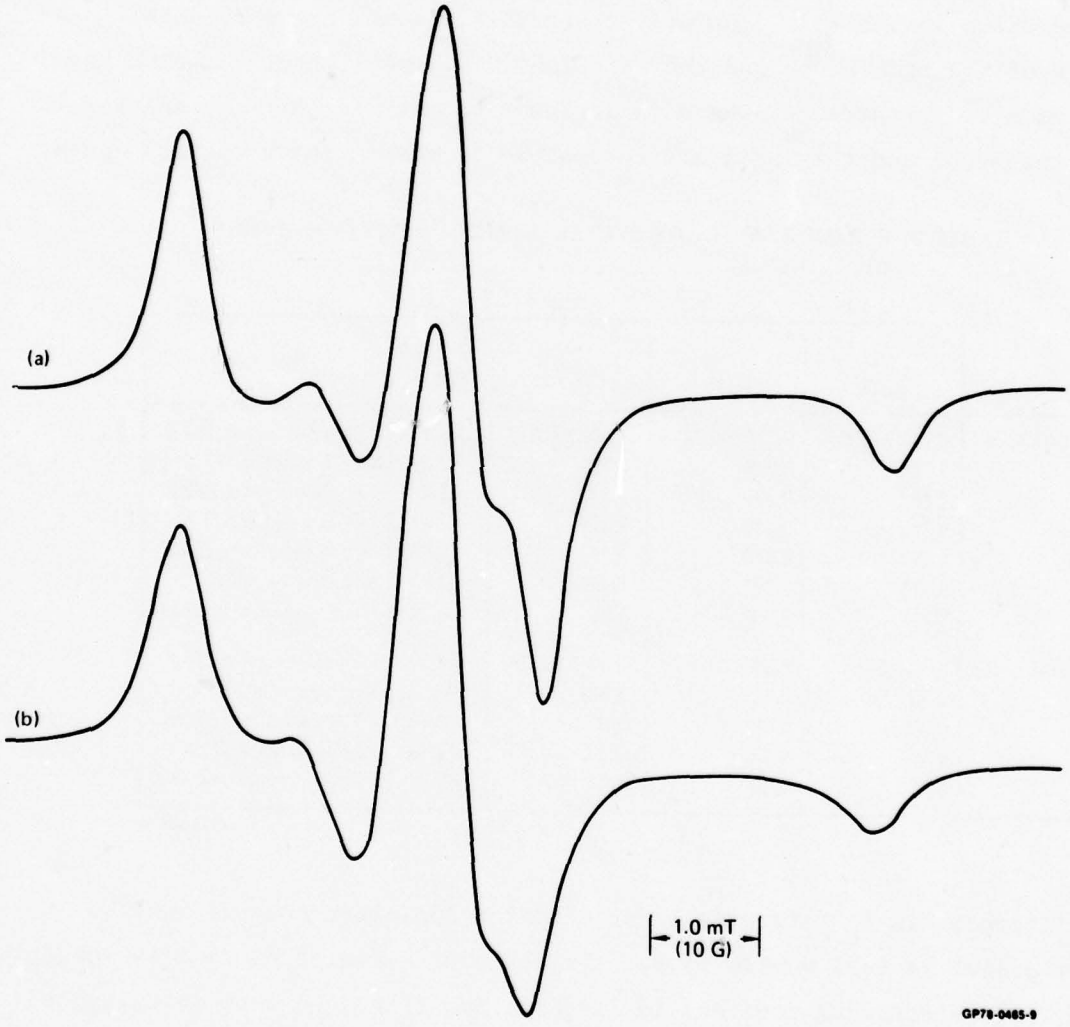

Figure 22 The EPR spectra observed at 293 K from (a) the TAMIN spin-label bridging-group/quaternary-salt in DGEBA cured with DETA and (b) the spin-probe TANOL in DGEBA cured with DETA.

2.5 Spin Labels and Spin Probes in Wet, Cured Epoxy

Samples of DGEBA cured with DETA (1:1 stoichiometry) containing TANOL and samples containing the spin-labeled bridging-group/quaternary-salt were investigated in absence of water, in the presence of various amounts of sorbed water, and after several wet-dry cycles. The water was introduced by immersing the samples in water at 373 K for several hours. The drying procedure involved placing the wet sample in a vacuum oven at 373 K for several hours.

The values of Δ_ℓ, Δ_u, Δ_o and the sample weight following several wet-dry cycles are shown in Table 2. The only observable change in the spectral parameters of the spin probe and the spin label following water sorption was a change in Δ_o. Furthermore, the data in Table 2 indicate that the change in Δ_o in the probe and the label are reversible on completing a wet, dry cycle.

TABLE 2 EFFECT OF WET-DRY CYCLES ON LINESHAPE PARAMETERS Δ_ℓ, Δ_u AND Δ_o.

	Δ_ℓ (mT)	Δ_u (mT)	Δ_o (mT)	%weight change	Procedure
Spin label	0.267 ± 0.0075	0.335 ± 0.0075	3.345 ± 0.012	0	70 h in vacuum at 373 K
	0.275	0.340	3.399	+ 2.35	12 h in water at 373 K
	0.267	0.335	3.34	+ 0.4	48 h in vacuum at 373 K
	0.280	0.340	3.399	+ 3.44	24 h in water at 373 K
	0.275	0.340	3.34	+ 0.34	48 h in vacuum at 373 K
	0.275	0.335	3.41	+ 3.8	60 h in water at 373 K
	0.267	0.335	3.34	+ 0.29	144 h in vacuum at 373 K
Spin probe	0.30 ± 0.01	0.39 ± 0.01	3.30 ± 0.015	0	72 h in vacuum at 373 K
	0.30	0.39	3.33	+ 2.15	9 h in water at 373 K
	0.30	0.39	3.318	+ 0.26	24 h in vacuum at 373 K
	0.30	0.39	3.339	+ 3.77	26 h in water at 373 K
	0.30	0.39	3.31	+ 0.08	144 h in vacuum at 373 K

GP79-0258-18

The increase in Δ_o following water sorption indicates that either the label (or probe) is less mobile (i.e., the motional correlation time is longer), or the hyperfine coupling constant is larger. The Δ_o values were investigated for wet and dry samples at 77 K where all motion can be assumed to be frozen-in. Figure 23 shows the spectrum from a dry, cured DGEBA sample that contains an end-label of METAMIN and has had no postcuring. Also shown is the spectrum of DGEBA end-labeled with METAMIN containing 3.6 wt% water after having been heated in water at 373 K for $\sim$ 4 days. The extrema splitting for the wet

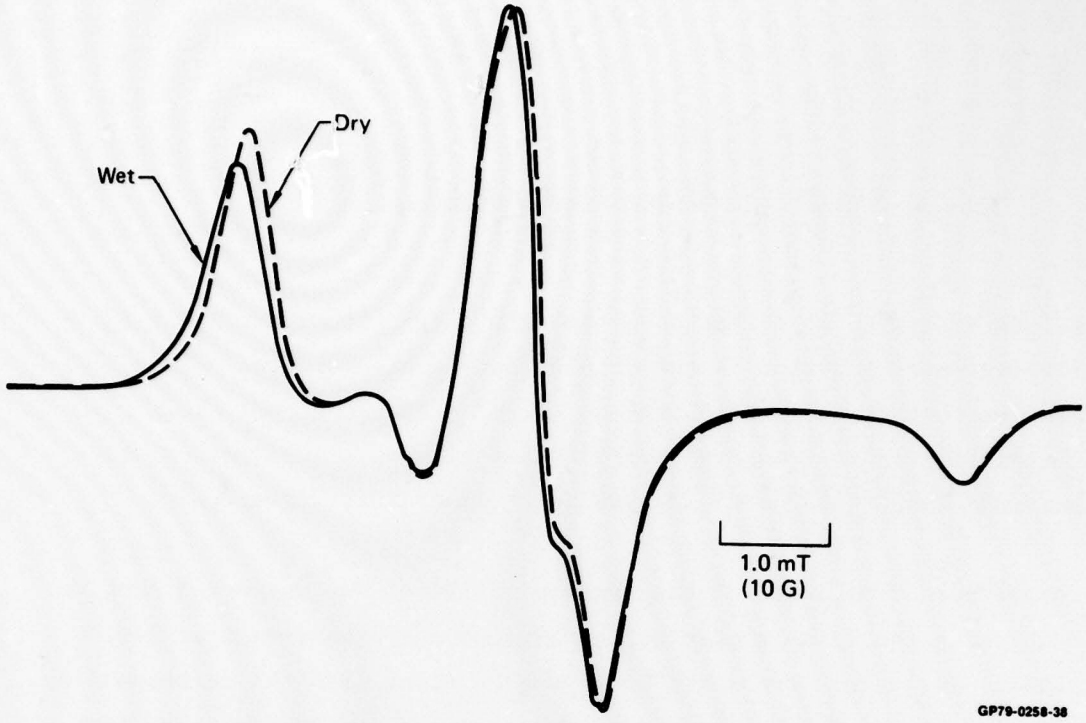

Figure 23 Spectra observed at 77 K from DGEBA end-labeled with METAMIN in DGEBA cured with DETA, dry and containing 3.3 wt % water.

sample (7.05 ± 0.05 mT) is detectably larger than that for the dry sample (6.9 ± 0.05 mT). This result indicates that the increase in Δ_o in wet samples is caused by the increase in the hyperfine coupling constant A_{zz}. An explanation can be given in terms of the canonical valence bond structures shown in Figure 24. In any given polymer medium, the actual electronic structure of the nitroxide is an admixture of these canonical structures where the relative mixing coefficients depend on the polarity of the polymer matrix.[22] If the polarity is increased, for example by a uniform distribution of sorbed water throughout the matrix, the ionic nature will be emphasized (i.e., the mixing coefficient of structure (b) in Figure 24 will increase). This effect will lead to an increase in the electron spin density on the nitrogen 2 p_z atomic orbital, thereby increasing the nitrogen hyperfine coupling constant.

In Figure 24 the low-field peak is less intense in the wet sample than in the dry sample. The postcuring effect described in Section 2.4 is responsible for this feature. The postcuring is caused by heating the sample in water at 373 K.

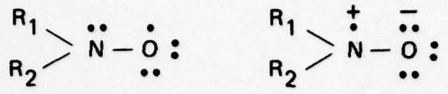

(a) (b)

GP79-0258-53

Figure 24 Canonical valence bond structures for nitroxide radicals.

It is interesting to note that no detectable change in either Δ_ℓ or Δ_u occurs following water sorption if the samples have been postcured. This result indicates that there is no change in the distribution of A_{zz} values following water sorption. Thus, the sorbed water affects all nitroxide molecules by the same amount and hence changes the polymer matrix properties uniformly.

The temperature dependence of the extrema splitting for wet, cured samples of DGEBA containing the spin-labeled bridging-group/quaternary-salt of TAMIN was determined. The values are shown in Figure 21 along with the corresponding values for dry samples. The values for the wet samples are greater than (or equal to within the experimental error) the values for the dry samples so that no distinctive increase in the nitroxide mobility is indicated following sorption of 3.3 wt% water. It is important to realize that the sample was losing water as the measurements were made at temperatures above 293 K. Thus, after making the measurement at 425 K, the sample had only a 1.8 wt% water content; however, the extrema splitting was still detectably greater than in the dry samples.

Attempts were made to study both spin labels and spin probes in cured samples containing more than 3.5 wt% water by using an autoclave with a chamber temperature above 400 K to provide a high-pressure steam environment. Although higher water contents were obtained ($\sim$ 4 wt%), the nitroxides, both labels and probes, decomposed.

A more acceptable method for incorporating larger quantities of water was devised by preparing samples with a DGEBA/DETA stoichiometry of 1:3, i.e., excess DETA. These samples were immersed in water at 293 K for several days whereupon they sorbed as much as 70 wt% water. Large amounts of water were sorbed by these samples because the excess DETA provides water-compatible regions possibly because of hydrogen bonding between DETA and the water.

The spectra of the probes and labels in the 1:1 dry samples were similar to the corresponding nitroxide in the 1:3 dry samples. Following water sorption, the 1:3 samples showed a marked decrease in hardness. The spectra for the spin probes DBNO, TEMPO, and TANOL, both dry and with amounts of sorbed water, are shown in Figures 25, 26, and 27. After the addition of the water, all three spin probes exhibit the presence of two spectra: a narrow three-line spectrum (fast phase) superimposed on a broader spectrum from a more rigid species (slow phase). The narrow-line spectrum shows substantial line narrowing compared with that in the dry sample, whereas the broad spectrum shows little change following water sorption.

Spectra of a DGEBA sample cured with DETA (1:3 stoichiometry) containing the spin probe TEMPO were investigated as a function of sorbed water content. The samples were treated by first soaking the sample in water at 293 K for several days, drying for certain intervals, weighing, and then recording the EPR spectrum. The observed spectra are shown in Figure 28.

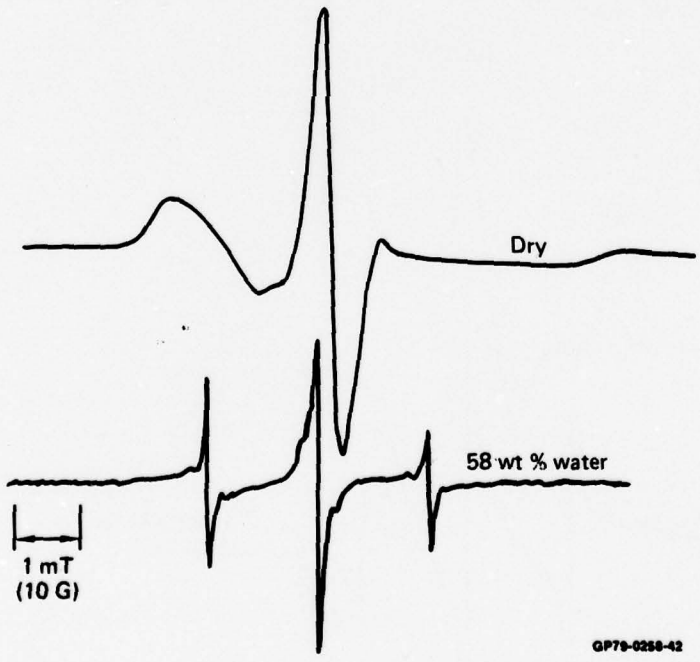

Figure 25 *Spectra observed at 293 K from DBNO in DGEBA cured with DETA (1:3 stoichiometry), dry and with 58% weight increase from sorbed water.*

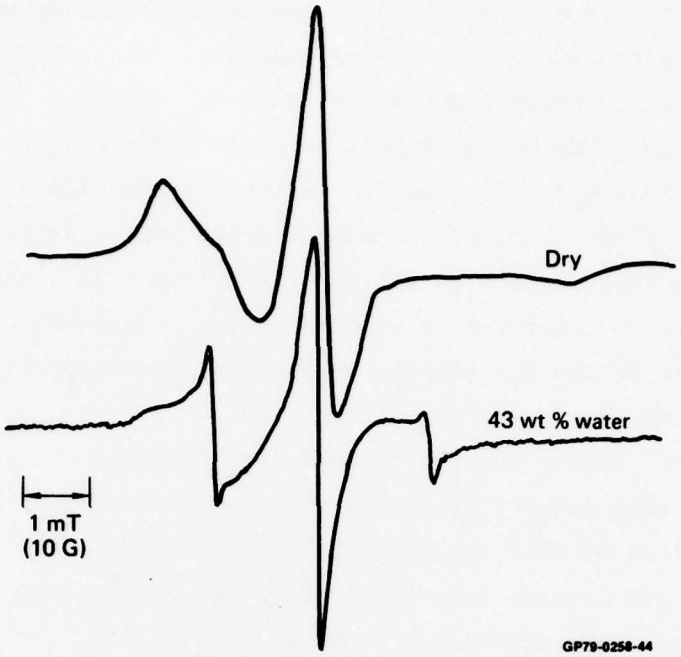

Figure 26 Spectra observed at 293 K from TEMPO in DGEBA cured with DETA (1:3 stoichiometry), dry and with 43% weight increase from sorbed water.

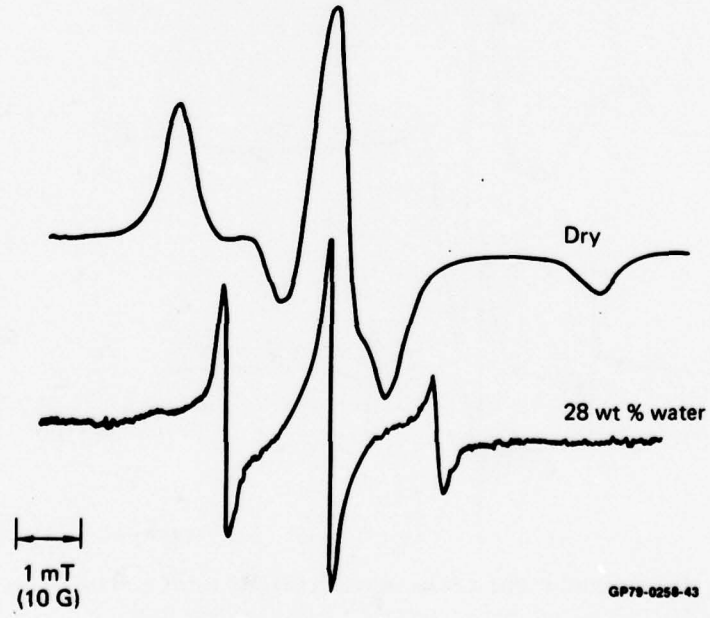

Figure 27 Spectra observed at 293 K from TANOL in DGEBA cured with DETA (1:3 stoichiometry), dry and with 28% weight increase from sorbed water.

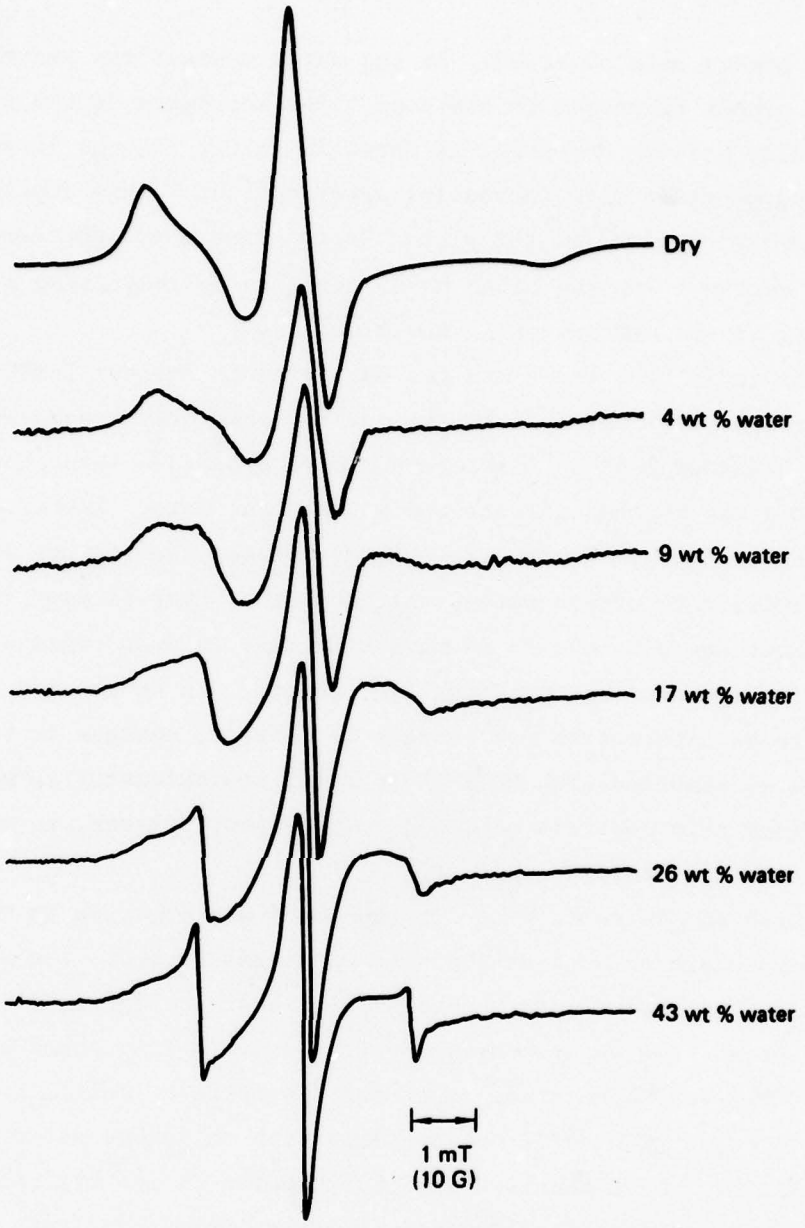

Figure 28 Spectra observed at 293 K from TANOL in DGEBA cured with DETA (1:3 stoichiometry) containing different amounts of sorbed water.

For samples with less than 9 wt% water, the extrema splittings are measurably larger ($\sim$ 1.5%) than the values in the dry samples. The reason for this increase is clearly the change in the polarity (dielectric constant) of the matrix caused by the sorbed water as has been described above for the samples with 1:1 stoichiometry. Above 9 wt%, two superimposed spectra (a slow

phase and a fast phase) were observed. As the water content was increased above 9 wt%, the number of probes in the fast phase increases at the expense of those in the slow phase. Moreover, as shown in Figure 28, the linewidths for the fast phase decrease with increasing water content. This implies that the motional correlation time for the probes in the fast phase decreases with increasing water content. On the other hand, there is no indication of increased mobility of the nitroxides in the slow phase.

These results imply that there are two environments for the TEMPO spin probes in the wet epoxy polymer. These two environments are associated with either (a) water being present in clusters and also dispersed throughout the polymer [the spin probe is then partitioned between the water clusters (the fast phase) and the wet polymer (the slow phase)] or (b) two regions with different sensitivities to sorbed water. Although the water is distributed uniformly throughout the polymer, it is more effective in some regions in causing main-chain segmental motions (the fast phase). In an attempt to answer which of these alternative conclusions is correct, changes in the spectrum of DGEBA end-labeled with METAMIN in a 1:3 stoichiometry sample were investigated. Since this label is attached to the epoxy polymer, it cannot penetrate into the water clusters present.

The cured DGEBA sample containing the end-label was immersed in water at 293 K for 3 days where as much as 45.5 wt% water was sorbed. The EPR spectra recorded for different water contents are shown in Figure 29. Above $\sim$ 10 wt% water content, two superimposed spectra (i.e., a fast phase and a slow phase) were observed. The presence of the two spectra implies two environments for the spin label with different sensitivities to sorbed water.

Veksli and Miller[23] have observed a similar series of spectra from spin-labeled polymethylmethacrylate plasticized with chloroform and dimethylformamide. At intermediate solvent compositions (14 to 25 wt%), two superimposed spectra, a slow phase and a fast phase, were observed. The amount of fast phase and the motional correlation time for the fast phase depend on the solvent volume fraction. It was shown that the dependence of the correlation time for the fast phase on the solvent volume fraction obeyed the Fujita-Doolittle equation[24] which can be written as

$$1/\ln a_c = f_2 + (f_2/\beta)/v_1 \qquad (1)$$

if the reference state is taken as the polymer, where f_2 is the fractional free volume, β is a parameter which for concentrated solutions is approximately the fractional free volume of the solvent, and a_c is the ratio of the diffusion coefficients at concentration v_1 to that in the reference state. If it is assumed that the monomeric translational diffusion coefficient behaves similarly to the rotational diffusion coefficient of the spin label, one obtains

$$a_c = \frac{\tau_{cR}}{\tau_c} = \frac{D_r}{D_{rR}} = \frac{D_t}{D_{tR}} = \frac{\xi_{oR}}{\xi_o}, \qquad (2)$$

where D_t, D_r are the monomeric translational diffusion coefficient and rotational diffusion coefficient of the label respectively, ξ_o is the monomeric friction coefficient[24], and τ_c is the motional correlation time of the label. The subscript R refers to the corresponding value in the reference state. Veskli and Miller[23] have explained the fast phase in terms of relaxation by a solvent-dependent local mode of segmental motion. This motion is confined to one or two dyads in the main chain and is possibly different for the different stereochemical isomeric sequences.

During these epoxy studies we have not rigorously verified that Equation (1) is obeyed because of a lack of hardware to perform spectral subtraction, a necessary procedure to obtain accurate values of the motional correlation times in the fast phase. However, the observed decrease of linewidth with increasing water content illustrated in Figures 28 and 29 is the behavior predicted by the Fujita-Doolittle equation [Equation (1)]. Therefore it is concluded that the nitroxides associated with the fast phases appearing in Figures 28 and 29 are relaxed by a local mode of segmental motion that is water sensitive. It is tentatively suggested that these local modes are excited in regions of low crosslink density.

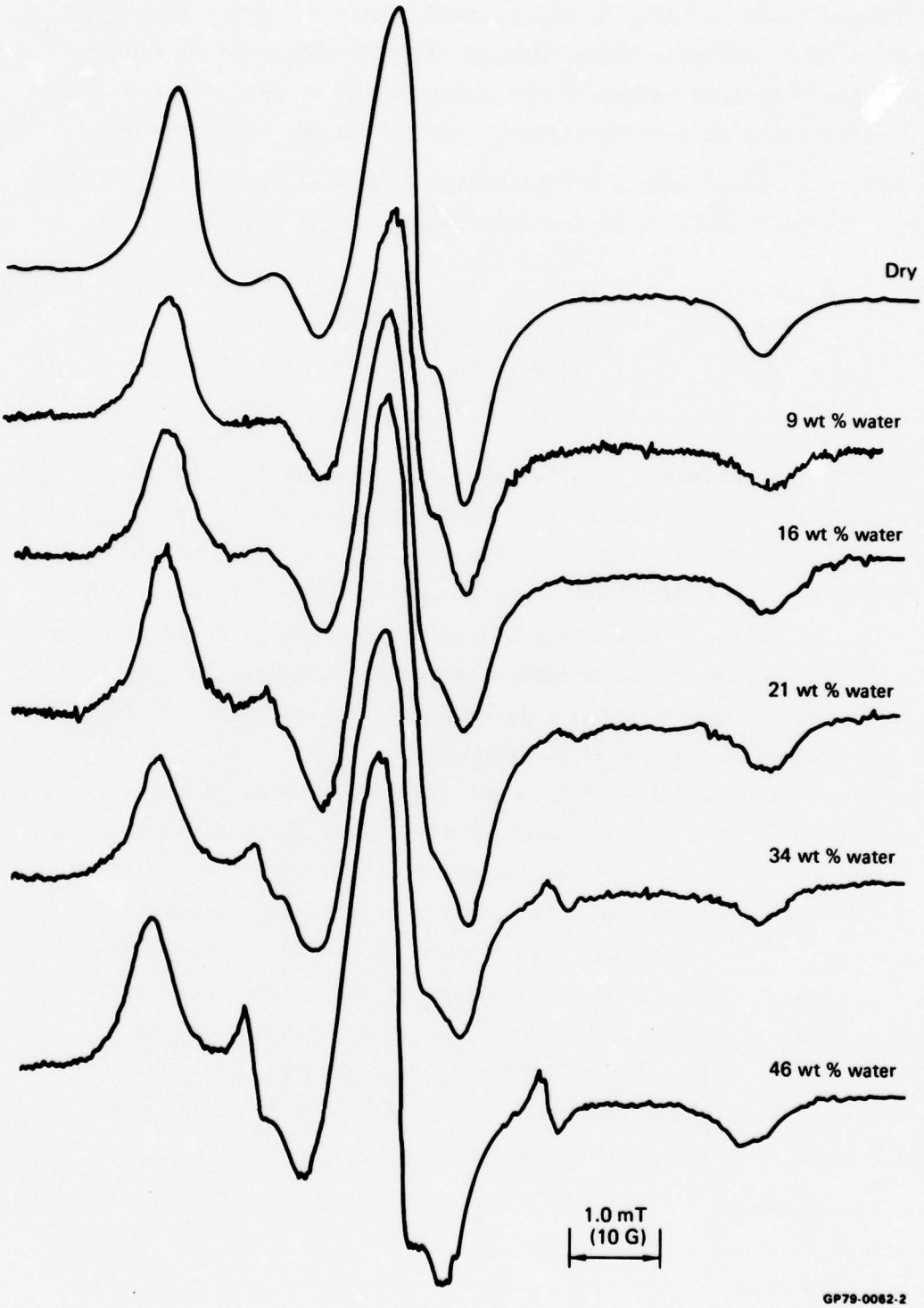

Figure 29 Spectra observed at 293 K from DGEBA end-labeled with METAMIN in DGEBA cured with DETA (1:3 stoichiometry) containing different amounts of sorbed water.

2.6 Characteristics of Epoxy Resin NMR Signals

The small spin-spin relaxation time T_2 of hydrogen nuclei in cured epoxy resins (< 20 ms) results in severe line broadening so that chemically nonequivalent hydrogens are not resolved in conventional NMR spectra. Multiple-pulse techniques can reduce the line broadening[25,26] if the multiple-pulse cycle time is short compared to the T_2 of the sample. Unfortunately it was not possible to reduce the multiple-pulse cycle time sufficiently to produce high-resolution hydrogen spectra of cured epoxy resins. Consequently, these hydrogen NMR studies rely upon analyses of the free-induction decay signal following a single 90° rf pulse, with or without preconditioning rf pulses. Fourier transforms of the free-induction decay signal were obtained in some cases to obtain the dipolar-broadened spectrum.

The free-induction decay signal of a cured DGEBA/DETA epoxy resin sample containing 2.8 wt% sorbed water is shown in Figure 30. This signal can be represented as a sum of Gaussian and Lorentzian signals, viz.,

$$S(t) = A_G \exp[-(t/T_{2G})^2] + A_L \exp(-t/T_{2L}). \qquad (3)$$

A PDP-8 computer, which is part of the NMR spectrometer system, was programmed to analyze these two components. The computer analysis of the free-induction decay signal in Figure 30 yielded a Gaussian component 90 000 $\exp[-(t/18\ \mu s)^2]$ and a Lorentzian component 4600 $\exp[-t/100\ \mu s]$.

In general, a Gaussian component results from hydrogen in molecules that are rigid, while a Lorentzian component results from hydrogen in molecules undergoing liquid-like motion. Thus, the Gaussian component is associated with the rigid epoxy and the Lorentzian component is associated with sorbed water, unreacted monomer, and/or plasticized cured resin. The amplitudes of the Gaussian, A_G, and Lorentzian, A_L, components are proportional to the number of hydrogens in the rigid and mobile portions of the sample, respectively. Thus quantitative measurements of the relative number of hydrogens in the rigid and mobile portions of the epoxy are possible.

While the Gaussian signal results from a rigid lattice, the Gaussian character of the signal is maintained if restricted molecular motion occurs. An increase in restricted motion as a result of an increase in temperature

and/or an increase in the plasticizing effects of sorbed water causes T_{2G} to increase. If the motion becomes unrestricted (i.e., liquid-like molecular tumbling over all orientations), the character of the signal changes to Lorentzian and A_G decreases while A_L increases. As the liquid-like motion increases, T_{2L} increases.

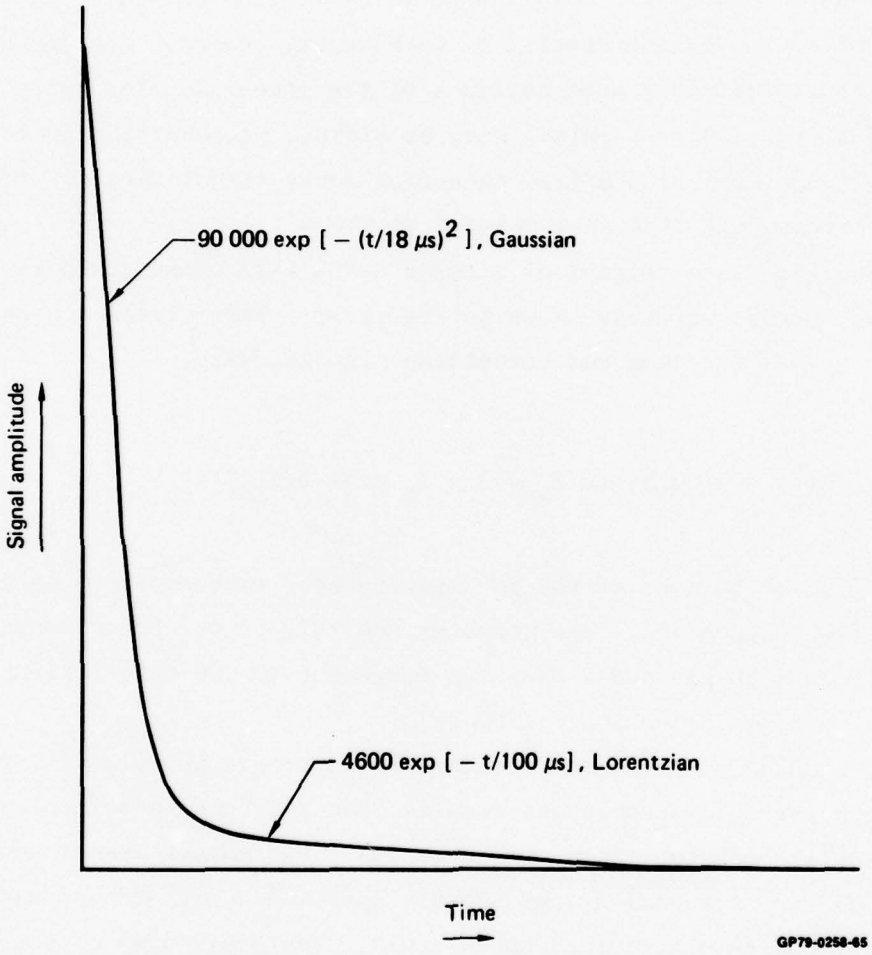

Figure 30 Free-induction decay signal from a cured epoxy sample containing 2.8 wt % sorbed water. The computer-fit Gaussian and Lorentzian components are identified.

The free-induction decay signal of an epoxy sample containing 3.26 wt% sorbed water is shown in Figure 31. The residual signal obtained by subtracting the computer-determined Gaussian and Lorentzian components from the free-induction decay is also shown. This residual signal is nearly zero in the latter part of the decay where the Lorentzian component dominates. This

result indicates that the computer-determined Lorentizian component is a good fit to the experimental data. In the early part of the decay, where the Gaussian component dominates, a small residual oscillatory signal of relative amplitude 0.03 shows that the Gaussian representation is not strictly correct, as would be true if all hydrogen-hydrogen internuclear vectors had random lengths and directions. The closely spaced pairs of hydrogen in the abundant methylene groups of the cured epoxy are the same distance apart and produce the small departure from a Gaussian signal.

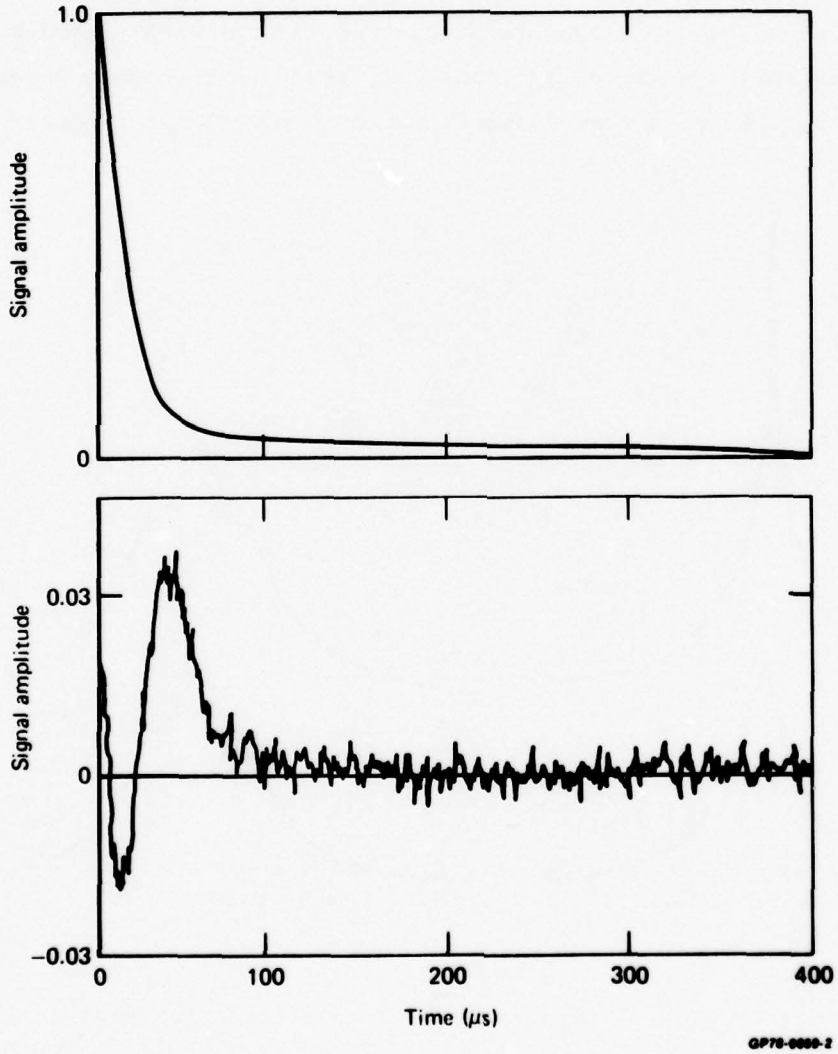

Figure 31 Room-temperature free-induction decay signal (a) for an epoxy resin sample containing 3.26 wt % water. In (b) the residual signal, after subtracting the Lorentzian signal, 0.057 exp (-t/176 μs), and the Gaussian signal, 0.943 exp $[-(t/17\ \mu s)^2]$, is shown.

This departure becomes more apparent at lower temperatures where the motion of the methylene groups is sufficiently reduced to produce the powder pattern of a Pake doublet[27]. These effects are seen in Figure 32 where the Fourier transform spectra of the off-resonance free-induction decays are presented. At 301 K the wet epoxy sample has a broad bell-shaped resonance, similar to a Gaussian resonance coincident with a narrow resonance from the sorbed water. The dry epoxy sample at 301 K lacks the large narrow resonance from the sorbed water, but it has a slightly pointed peak; this peak is a small Lorentzian component present in the dry epoxy sample. At 115 K little molecular motion occurs, and the spectra of the wet and dry epoxy samples have no Lorenztian component, are virtually identical, and have shoulders characteristic of a powder pattern of a Pake doublet; these shoulders are produced by

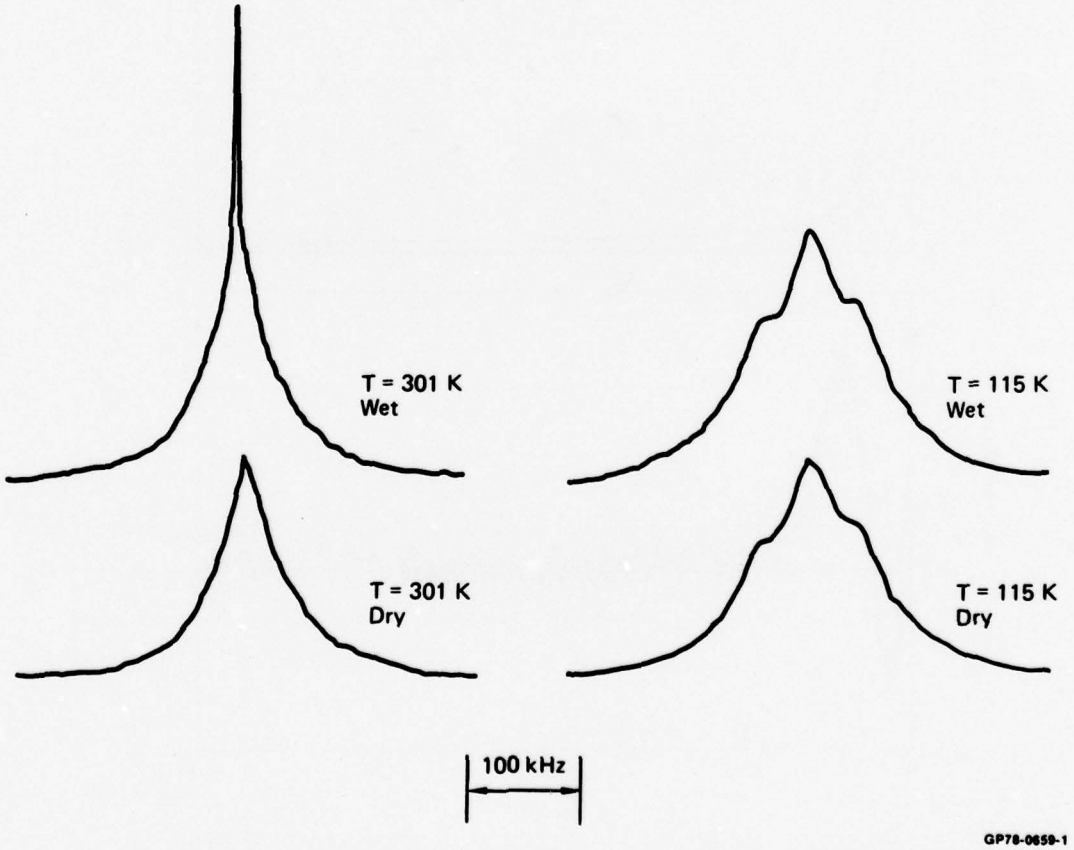

Figure 32 **Spectra of wet (3.26 wt %) and dry epoxy resin samples at two different temperatures. To enhance the details of the narrow water resonance and the Pake doublet, the magnitude spectra (square root of the sum of squares of real and imaginary spectra) rather than the real spectra are presented.**

the closely spaced pairs of methylene hydrogens. The central, somewhat broad peak, is produced by the remaining hydrogen in the epoxy sample.

While the low-temperature spectra in Figure 32 show a distinctly non-Gaussian shape, the deviation from Gaussian is not sufficient to affect the determination of the Gaussian amplitude by more than a few percent. Thus, the Gaussian assumption is suitable for quantitative measurements of the relative number of hydrogens in mobile and rigid portions of the epoxy.

2.7 Temperature Dependence of NMR Relaxation Times

The spin-lattice relaxation times T_1 of the Gaussian and Lorentzian components were obtained by computer analyzing the free-induction decay signals following a 180° - τ - 90° pulse sequence at resonance. The computer-determined amplitudes of the Gaussian and Lorentzian components as a function of τ were then plotted to determine the spin-lattice relaxation times for each of the two components. Figure 33 shows such a plot for a room-temperature measurement of a 1:1 DGEBA/DETA epoxy containing 2.8 wt% sorbed water. These data show that the hydrogen in the rigid epoxy is relaxing to the lattice slower than the hydrogen associated with the mobile portion of the epoxy. The fact that the two curves become parallel within 0.02 s indicates that the hydrogens in the rigid and mobile portions of the epoxy are strongly coupled; therefore, they are not located in isolated regions in the sample.

Since oxygen is paramagnetic, its presence in the epoxy introduces an additional relaxation process that could interfere with the observation of the relaxation processes intrinsic to the epoxy. However, the requirements that (1) the sample be in a 5 mm tube for the NMR studies, (2) the precise weight gain resulting from water sorption be determined, and (3) oxygen be totally excluded, were difficult to implement. To determine if it was necessary to exclude oxygen, the temperature dependence of T_1 was measured for two dry epoxy samples, one in air and the other in vacuum. These results are shown in Figure 34. While the sample in air does relax faster because of the presence of sorbed oxygen, the difference was not considered large enough to warrant the complicated procedures required to exclude oxygen. Hence, in our subsequent studies no effort was made to exclude oxygen.

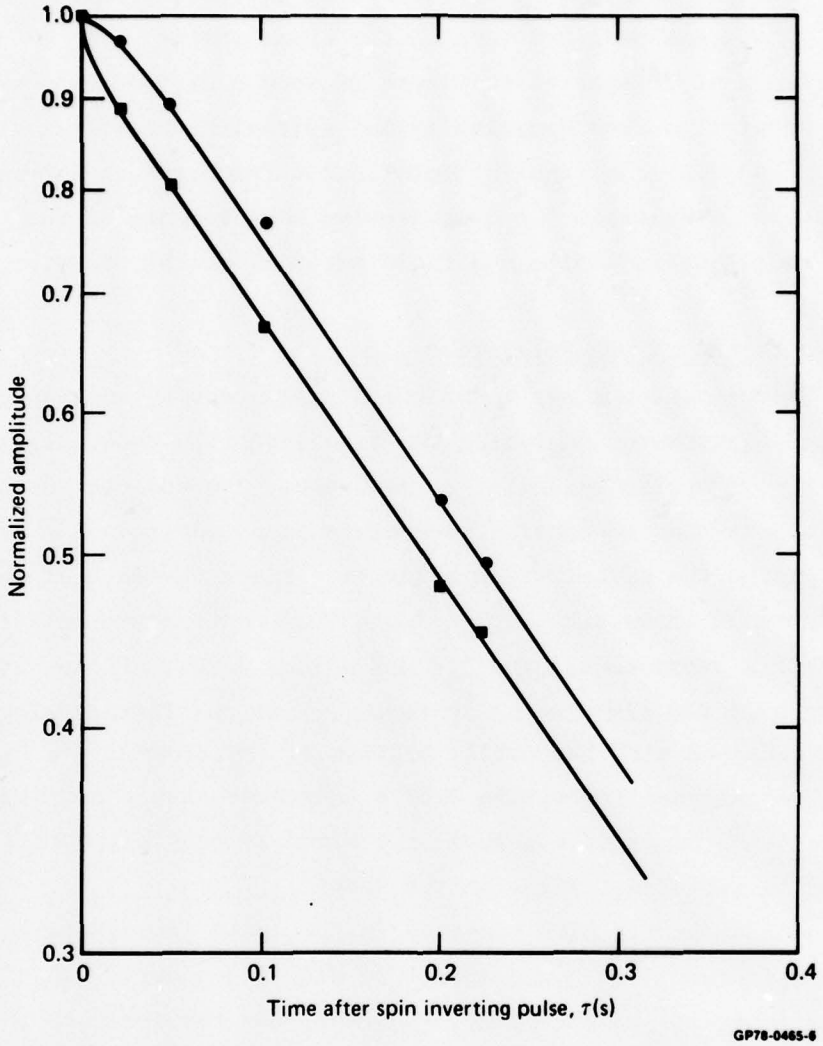

Figure 33 **Spin-lattice relaxation in a cured epoxy resin containing 2.8 wt % sorbed water. The circles identify the relaxation of the Gaussian decay, and the squares identify the relaxation of the Lorentizian decay.**

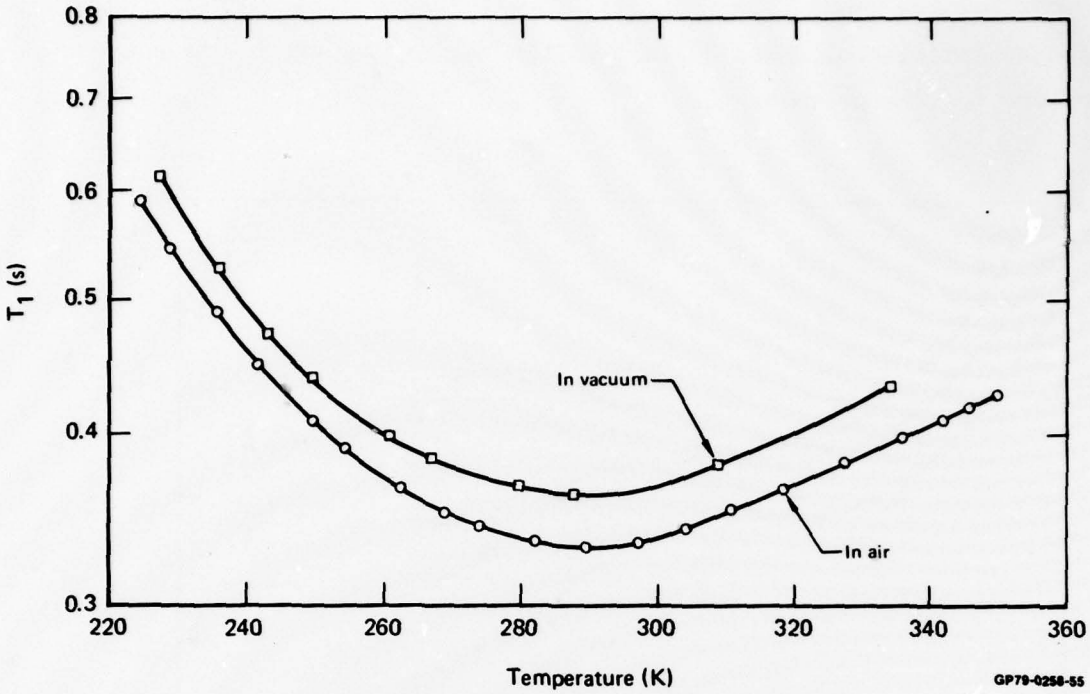

Figure 34 Spin-lattice relaxation times for 1:1 epoxy samples in air and in vacuum.

The effects of stoichiometry on the spin-lattice relaxation time T_1 are shown as a function of temperature in Figure 35. The T_1 data show the effects of two relaxation processes. The minimum in the T_1 data at 288 K is caused by methyl-group rotation in the DGEBA.[28] The minimum which occurs above the range of measured temperatures is caused by methylene hydrogen motion in the DETA. The manner in which T_1 changes as the stoichiometry is changed is quantitatively explained in the following paragraphs.

In tightly coupled spin systems where spin diffusion causes the spins to relax with a common relaxation time T_1,

$$T_1^{-1} = \sum_n f_n \, T_{1n}^{-1}, \tag{4}$$

where f_n is the fraction of spins whose relaxation time is T_{1n}[29]. If one group of spins dominates the spin-lattice relaxation process, then Equation (4) becomes

$$T_1 = T_{1d}/f_d \, , \tag{5}$$

where f_d is the fraction of spins dominating the relaxation and T_{1d} is the relaxation time for the process.

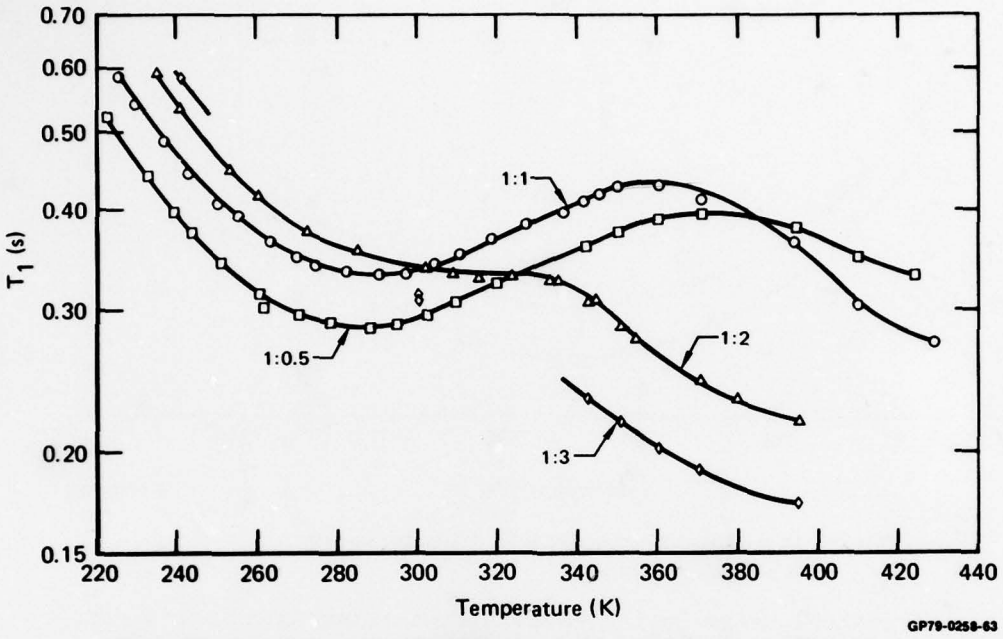

Figure 35 Spin-lattice relaxation times for samples of different stoichiometry.

To determine from experimental data if a single relaxation process is dominant at a particular temperature, Equation (5) is re-written as

$$T_{1d} = T_1 f_d . \qquad (6)$$

Since T_{1d} should be a constant, the product of the T_1 measured and the f_d calculated from the stoichiometry should remain constant as the stoichiometry is changed. These data are shown in Table 3 where the T_1 data at 240 K are tabulated. The product of T_1 and f_{CH_3} is constant to within 3% for stoichiometries from 1:0.5 to 1:3. This result shows that the methyl-group rotation in DGEBA is the dominant relaxation mechanism at 240 K.

In general a spin-lattice relaxation process has its greatest effect when the corrlation time for molecular motion τ_c is $\sim 0.1/f_o$, where f_o is the spectrometer frequency[4]. Thus, at 288 K, where T_1 goes through a minimum, the correlation time for methyl-group rotation in the DGEBA is $\sim 10^{-9}$ s.

TABLE 3 SPIN-LATTICE RELAXATION AT 240 K

Stoichiometry DGEBA: DETA	Calculated fraction of DGEBA methyl hydrogens, f_{CH_3}	Measured T_1 (s)	$f_{CH_3}T_1$ (s)
1:0.5	0.226	0.395	0.0893
1:1	0.206	0.452	0.0931
1:2	0.176	0.540	0.0950
1:3	0.153	0.588	0.0900

GP79-0258-58

At slightly higher temperatures, even at 288 K where the methyl-group rotation has its greatest effect, the 1:2 and 1:3 stoichiometry samples experience an additional relaxation process caused by the methylene-group rotation in DETA. At still higher temperatures, the T_1 data for the 1:0.5 and 1:1 samples also show the effects of the methylene-group rotation. The T_1 data at 395 K are analyzed in Table 4 to determine if the methylene hydrogen relaxation process dominates at this temperature. The product of T_1 and f_{CH_2} is constant to within 2% for the samples with stoichiometries of 1:1, 1:2, and 1:3 but is too small for the sample with a stoichiometry of 1:0.5. The reason for this discrepancy is that there are too few DETA methylene hydrogens in the 1:0.5 sample for them to dominate the relaxation process.

TABLE 4 SPIN-LATTICE RELAXATION AT 395 K

Stoichiometry	Calculated fraction of DETA methylene hydrogens, f_{CH_2}	Measured T_1 at 395 K (s)	$f_{CH_2}T_1$ (s)
1:0.5	0.0588	0.382	0.0225
1:1	0.108	0.368	0.0397
1:2	0.184	0.218	0.0401
1:3	0.238	0.174	0.0414

GP79-0258-57

The temperature dependence of the Gaussian spin-spin relaxation times, T_{2G}, are shown in Figure 36. At low temperatures the 1:1, 1:2, and 1:3 samples had nearly the same T_{2G}, which was slightly less than that for the 1:0.5 sample. At higher temperatures T_2G increased, indicating greater molecular motion. Extensive molecular motion occurred in the 1:3 and 1:2 samples at 310 K and 330 K respectively. At 370 K the spin-spin relaxation time for the 1:3 sample was totally Lorentzian with a T_{2L} of 243 μs, while for the 1:2 sample it was 22% Lorentzian with a T_{2L} of 92 μs and 78% Gaussian with a T_{2G} of 29 μs. At 395 K the 1:2 sample had a totally Lorentzian relaxation with a T_{2L} of 186 μs. This liquid-like motion is attributed to the low crosslink density present in samples with an excess of DETA.

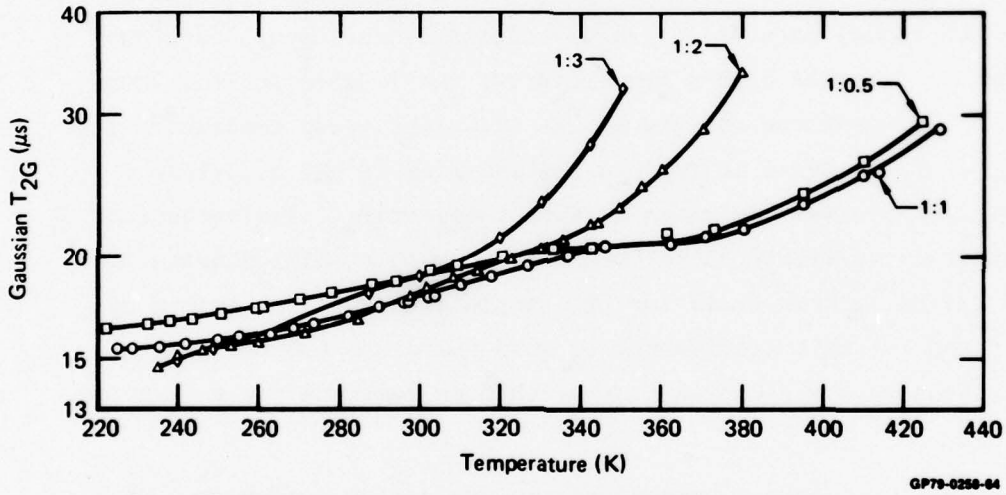

Figure 36 Spin-spin relaxation times for samples of different stoichiometry.

T_2 for the 1:1 and 1:0.5 samples increased only slightly with an increase in temperature. Between 340 K and 375 K, T_2 was almost constant, but at about 380 K, T_2 increased modestly. At 395 K the NMR signal for both the 1:0.5 and 1:1 samples was 96.6% Gaussian and 3.4% Lorentzian. At 425 K the NMR signal was more than 15% Lorentzian, and the remaining 85% had a character midway between that of a Gaussian and a Lorentzian, i.e., the decay followed $\exp(-t^{1.6})$ rather than $\exp(-t^2)$. This behavior indicates extensive molecular motion although it was still restricted motion typical of a highly crosslinked system. While the 1:1 sample is expected to be highly crosslinked, one might expect the 1:0.5 sample to have a low crosslink density because

the number of amine binding sites in the DETA is only half the number required to react with the epoxide groups in the DGEBA. The high crosslink density for the 1:0.5 sample indicated by the T_2 data can be explained by chain-growth polymerization of the epoxy in the presence of a tertiary amine[30]. This reaction was studied with EPR and is explained in Section 2.2.

In general the transition temperatures where T_2 increases abruptly usually indicates the onset of a particular type of molecular motion. In particular, the molecular motion associated with the glass transition produces an increase in T_2. The temperatures at which T_2 suddenly increased is given in Table 5 for samples with different stoichiometries. The temperatures at which a transition occurred in differential scanning calorimeter data is also listed for comparison[19]. The agreement is good except for the 1:0.5 sample; this discrepancy cannot be explained. Figure 36 shows that the rate of increase in T_2 at the transition was least for the samples with the largest crosslink density as expected because the crosslinks inhibit extensive molecular motion.

TABLE 5 COMPARISON OF *SPIN-SPIN RELAXATION TIME* T_2 *AND* DIFFERENTIAL SCANNING CALORIMETER DATA

Stoichiometry	Transition temperature (K)	
	T_2	DSC
1:0.5	~380	311 ± 6
1:1	~380	378 ± 14
1:2	~330	309 ± 27
1:3	~310	298 ± 14

GP79-0258-56

2.8 Effects of Sorbed Water on NMR Signals

The spin-lattice relaxation times for wet ($\sim$ 3 wt% sorbed water) 1:1 samples were obtained as a function of temperature. Figure 37 shows these data for the Gaussian and Lorentzian components compared with the data for a dry sample. At low temperatures, the T_1 data for the dry and wet samples are

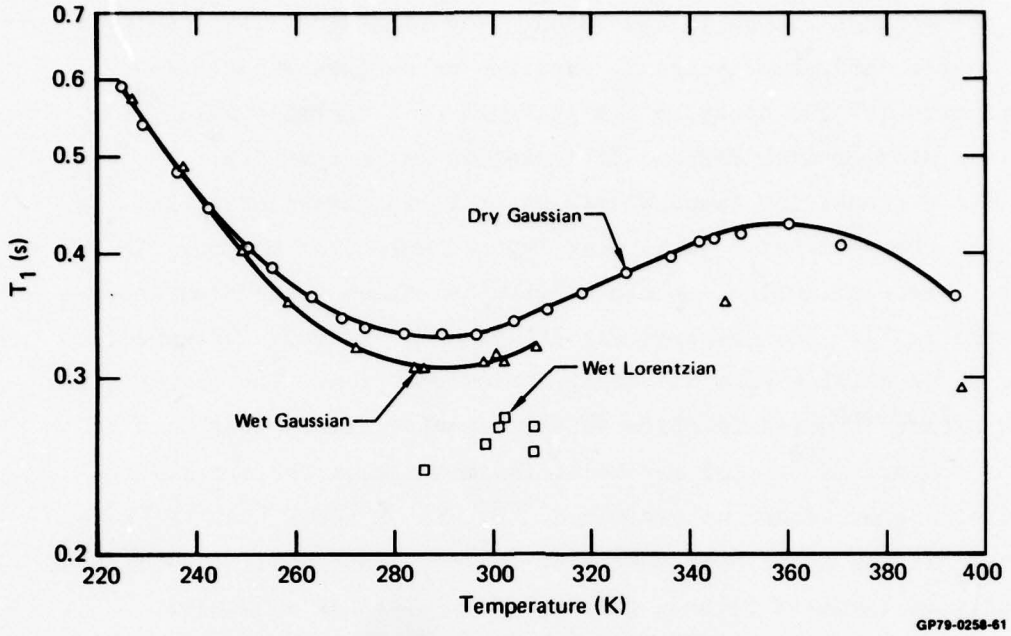

Figure 37 Spin-lattice relaxation times for wet and dry epoxy samples with 1:1 stoichiometry.

identical, indicating that the methyl-group rotation is still the dominant relaxation process. As the temperature increased, the relaxation time for the wet sample steadily decreased relative to the dry sample, indicating an additional relaxation process. T_1 for the Lorentzian component was measured at selected temperatures, and was found to be less than T_1 for the Gaussian component. Thus, the spin-lattice relaxation process associated with the mobile water is more effective than that for the rigid epoxy. However, because the number of hydrogens in the water is small compared to the number of hydrogens in the epoxy, the minimum at 288 K is not significantly changed by the presence of sorbed water.

The data in Figure 38 show that the presence of sorbed water increased T_{2G} of the Gaussian component. Thus, the overall mobility of the rigid epoxy matrix was increased by the presence of sorbed water. In the dry sample at 395 K, the NMR signal had only a 3.4% Lorentzian component, while in the wet sample at 395 K, the Lorentzian component was 15%. Only a 4.4% Lorentzian signal is expected from the hydrogens in the 3% sorbed water. Hence, the remaining 7.2% (15 - 4.4 - 3.4) Lorentzian component was caused by hydrogens in the epoxy network which had been plasticized by the sorbed water.

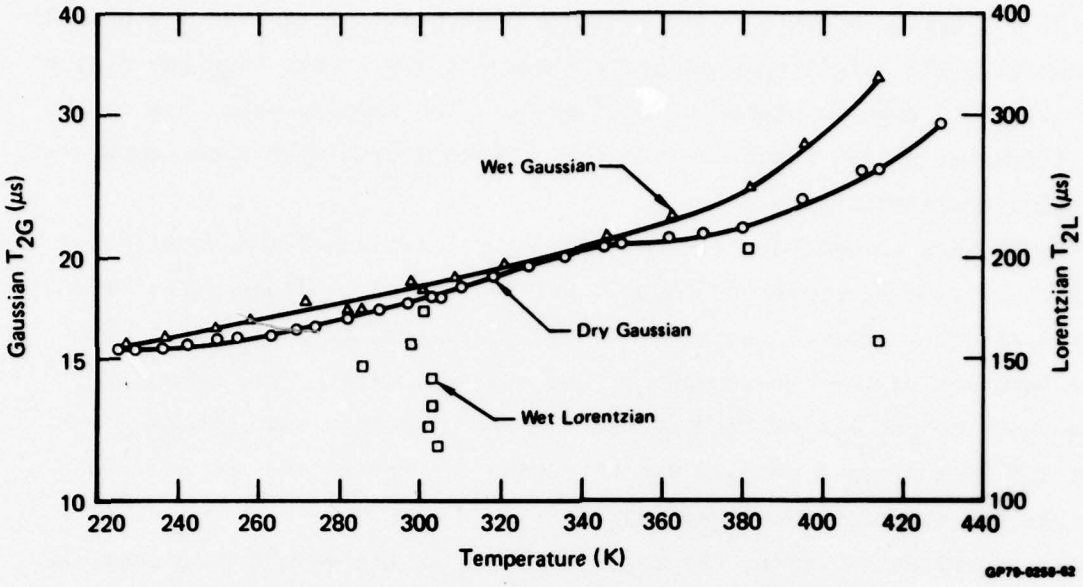

Figure 38 Spin-spin relaxation times for wet and dry epoxy samples with 1:1 stoichiometry.

The effect of sorbed water on the glass transition can be seen in the T_{2G} data of Figure 38. The T_{2G} of both wet and dry samples increases similarly with increasing temperature up to about 350 K, but above 350 K the T_{2G} of the dry sample increases at a lesser rate while the T_2G of the wet sample increases at a slightly greater rate. This difference in behavior is a result of a lower glass transition temperature for the wet sample. While the subtle increase in T_{2G} precludes an accurate determination of the glass transition temperature for the wet sample, it is estimated to be between 350 K and 370 K.

2.9 Effects of Sample History on NMR Signals

The following experiments were performed to determine if the effects of sorbed water were influenced by prior sample history. A group of 1:1 samples from the same lot were room-temperature cured in sealed glass vials for 20 days. The samples were separated into three groups which were subjected to (1) post curing at 370 K for 48 h in a vacuum oven followed by room-temperature storage in a desiccator for 8 months, (2) room-temperature storage in a desiccator for 8 months, and (3) room-temperature storage in a sealed vial containing water vapor. The group 1 samples lost 0.33 $\pm$ 0.05 wt% during post curing and maintained this weight during storage, the group 2 samples lost

0.44 ± 0.01 wt% during storage, and the group 3 samples gained 3.95 ± 0.01 wt% during storage. The weight gain of group 3 samples was larger than the typical gain of < 3.65 wt% upon exposure to 370 K water. The samples were then soaked in distilled water at 370 K, and the progress was monitored with room-temperature NMR and weight measurements.

The Lorentzian to Gaussian ratios A_L/A_G as a function of the square root of the exposure time are shown in Figures 39, 40, and 41. Within experimental error the A_L/A_G ratio for all samples initially changed linearly at the same rate as a function of the square root of the exposure time. This behavior indicates that the process of transferring mobile hydrogens into groups 1 and 2 samples and from group 3 samples was diffusion controlled and the diffusion constant was the same for these samples.

Within experimental error, the ratio of A_L/A_G to the weight gain remained constant during the time the water was diffusing in or out of the samples, as shown in Figures 39, 40, and 41. This ratio was 2.0 ± 0.1 for all samples. If the Lorentzian component were due solely to the hydrogens in the sorbed water, this ratio would be 1.45. Hence, for every sorbed water hydrogen, 1.38 ± 0.07 [(2.0 ± 0.1)/1.45] hydrogens contribute to the Lorentzian component. Stated another way, for every sorbed water hydrogen, 0.38 ± 0.07 epoxy hydrogen is plasticized, and this added mobility is independent of prior sample history.

During these experiments T_{2G} changed insignificantly, while T_{2L} changed as shown in Figure 42. The increase in T_{2L} for samples in groups 1 and 2 occurred over the same time as the diffusion, and therefore it was governed by the diffusion process. The changes in T_{2L} for the samples containing sorbed water were different, not only because T_{2L} decreased, but because the changes occurred more rapidly than the diffusion process permits. During the first 0.25 h of exposure to 370 K water, T_{2L} increased from 184 μs to 220 μs. Then during the next 1 h, a period of time short compared to the time for diffusion, T_{2L} decreased again. Then T_{2L} slowly decreased in a time comparable to the diffusion time.

After these experiments, the samples were dried in a vacuum oven at 373 K for 150 h. The weights of the samples relative to their initial weights immediately after room-temperature curing were: group 1, a loss of 0.33 wt%; group 2, a loss of 0.23 wt%; and group 3, a gain of 0.07 wt%.

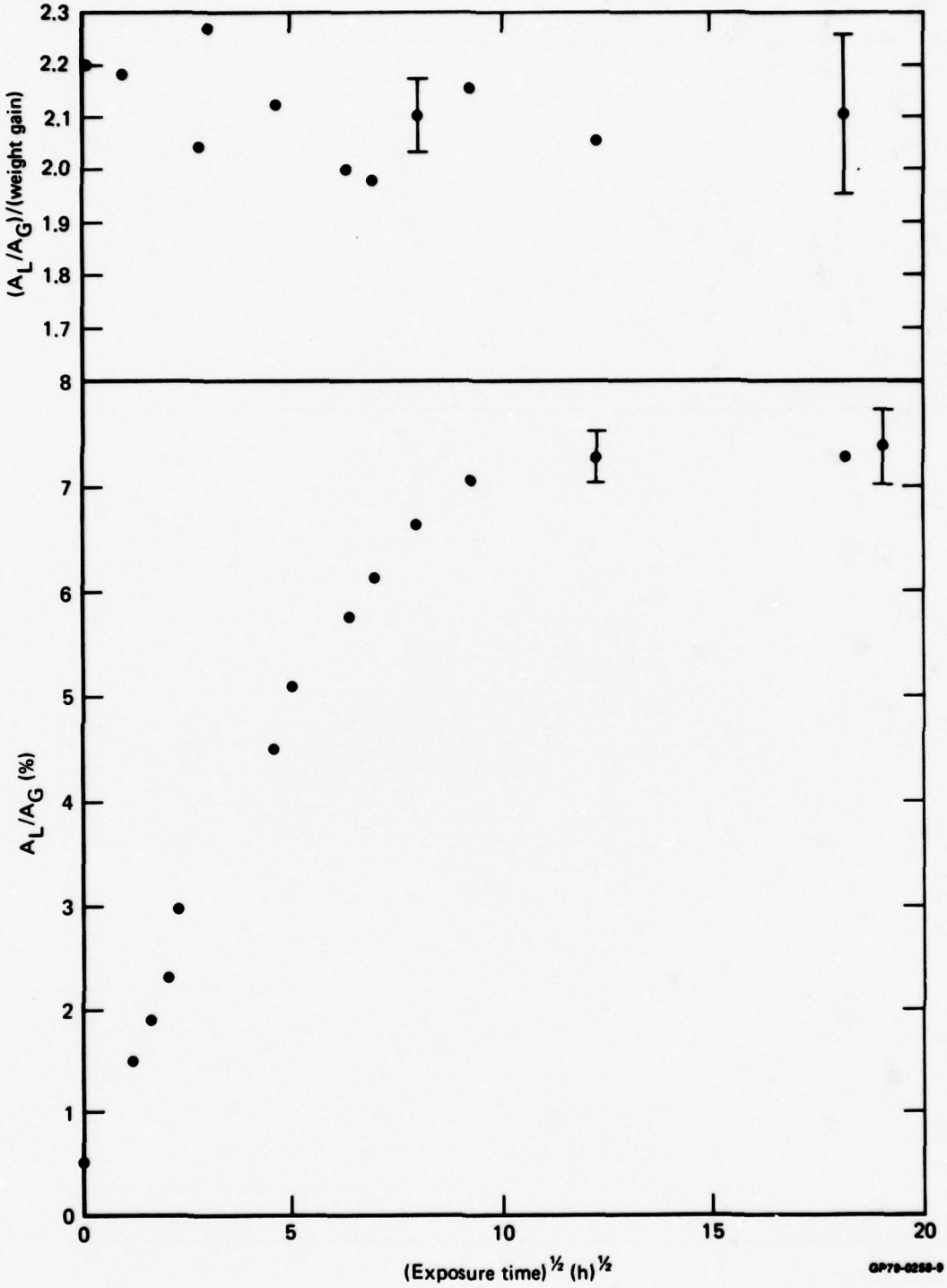

Figure 39 Lorentzian to Gaussian amplitude ratios for dry post-cured epoxy samples (group 1) exposed to 370 K water.

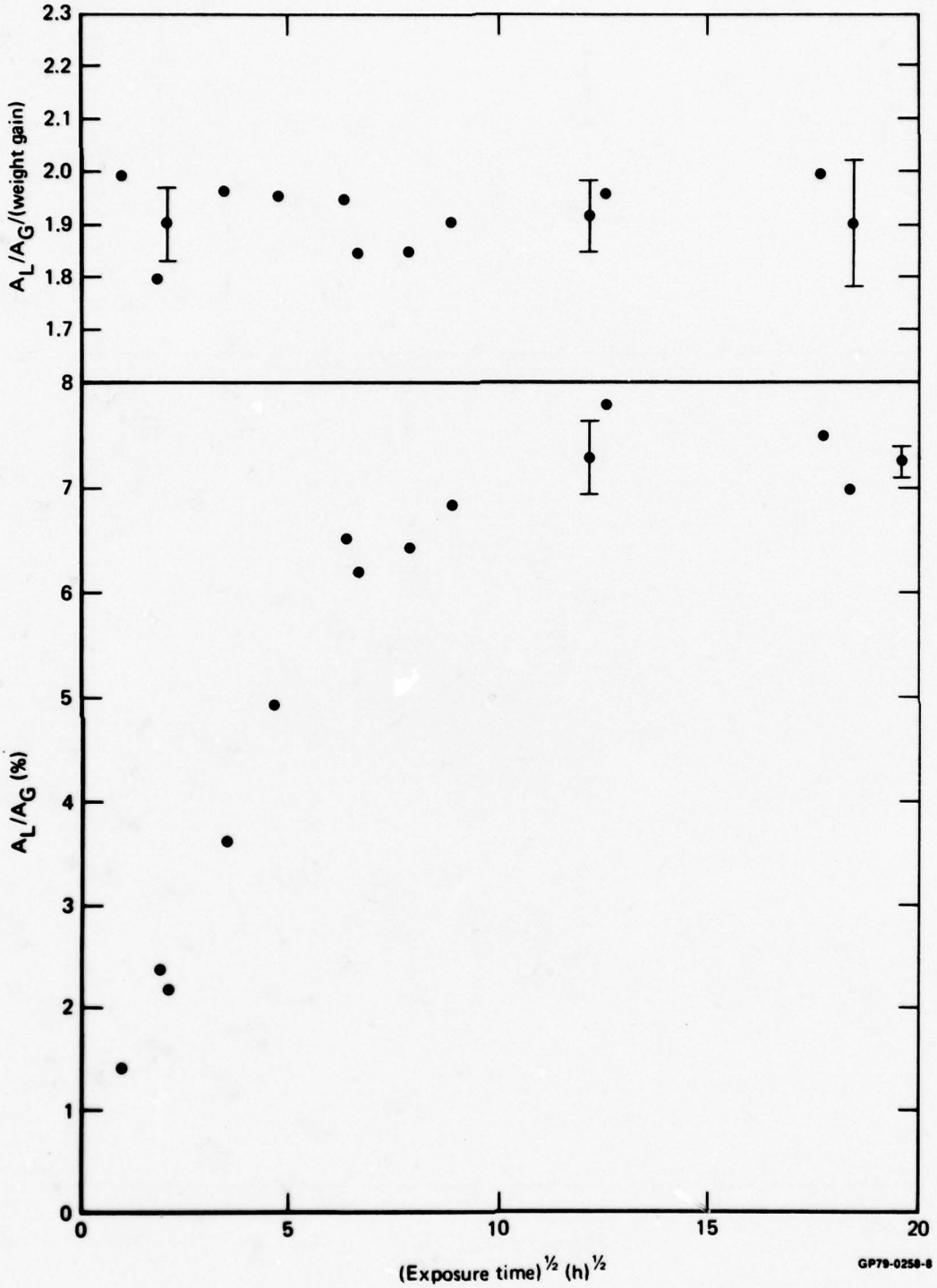

Figure 40 Lorentzian to Gaussian amplitude ratios for dry epoxy samples (group 2) exposed to 370 K water.

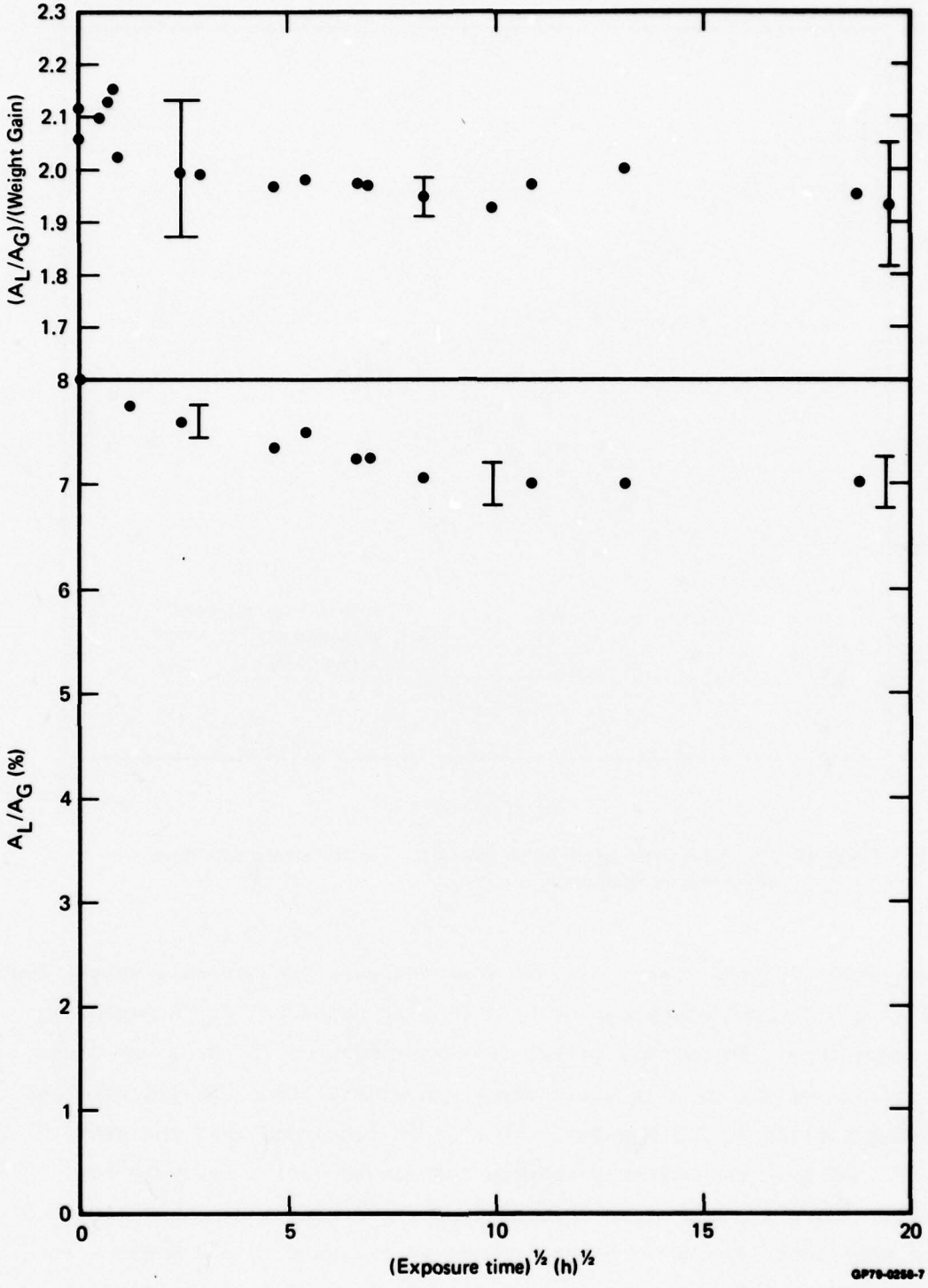

Figure 41 Lorentzian to Gaussian amplitude ratios for wet epoxy samples (group 3) exposed to 370 K water.

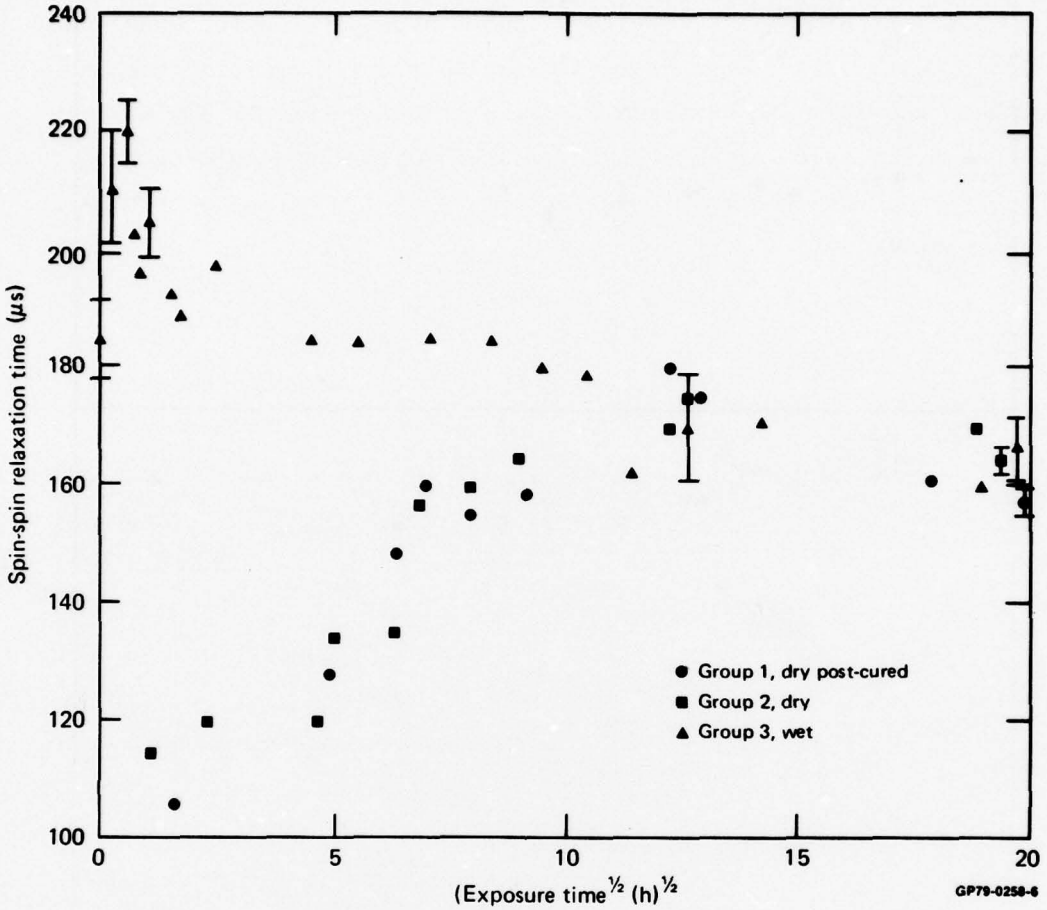

Figure 42 Lorentzian spin-spin relaxation times for 1:1 epoxy samples with three different prior treatments.

These data are tentatively explained as follows. The overall weight loss of groups 1 and 2 samples was caused by a loss of unreacted or incompletely reacted components. No overall weight loss was measured in the group 3 samples, and the initial weight gain in water vapor was greater than usually obtained upon soaking samples in 370 K water. Thus it is concluded that the group 3 samples did not lose incompletely reacted components during exposure to water vapor. However, the group 3 samples contain unreacted components, and these are mobilized (secondary bonds broken) by exposure to 370 K water for less than 0.25 h. This increased mobility caused T_{2L} to increase suddenly. The increased mobility caused by both the heat and the plasticizing effects of sorbed water promoted further curing (primary bond formation). As curing

proceeded, the movement of the mobile components became restricted and T_{2L} decreased within the next ∿ 1 h. Further exposure to 370 K water caused a small amount of water to diffuse from the sample, and T_{2L} again decreased because of the reduced plasticization. During this exposure to 370 K water, unreacted components were not effectively leached from the sample because the enhanced postcuring, which occurred during the first ∿ 1 h, restrained the leachable components.

2.10 Effects of Water on Samples of Different Stoichiometry

Experiments were performed to measure the changes in room-temperature NMR parameters caused by altering the sample stoichiometry. After measuring the NMR parameters in the dry state, the 1:0.5, 1:1, and 1:2 samples were exposed to 370 K water for 144 h, and the 1:3 sample was exposed to 300 K water for 24 h. The 1:3 sample was not placed in 370 K water because DETA would have been leached from it, hence changing the stoichiometry. After exposure to water, the NMR measurements were repeated. The results are summarized in the bar graph shown in Figure 43.

The first bar, which represents the sorbed water content, shows a dramatic increase for an increase in excess DETA. The least water sorption occurs in the 1:1 sample.

The second bar is a composite representing the sum of the percentage of hydrogens in the sorbed water (based on weight gain), and the calculated percentage of hydrogens in the excess DETA or excess DGEBA in the nonstoichiometric samples. The third bar in Figure 43 denotes the percentage ratio of the Lorentzian (mobile) component to the Gaussian (rigid) component in the wet samples measured with the NMR. For the 1:1, 1:2, and 1:3 samples, good correspondence occurs between the heights of the second (composite) and third bars, which strongly implies that the mobile fraction in the wet samples detected by NMR consists of the sorbed water and excess DETA. The fact that this correspondence does not exist for the 1:05 sample is not surprising because DGEBA can undergo chain-growth polymerization in the presence of a tertiary amine. The Lorentzian/Gaussian ratio measured with NMR clearly shows that the excess DGEBA has polymerized into a rigid polymer. This chain-growth polymerization was studied with EPR and is discussed in Section 2.2.

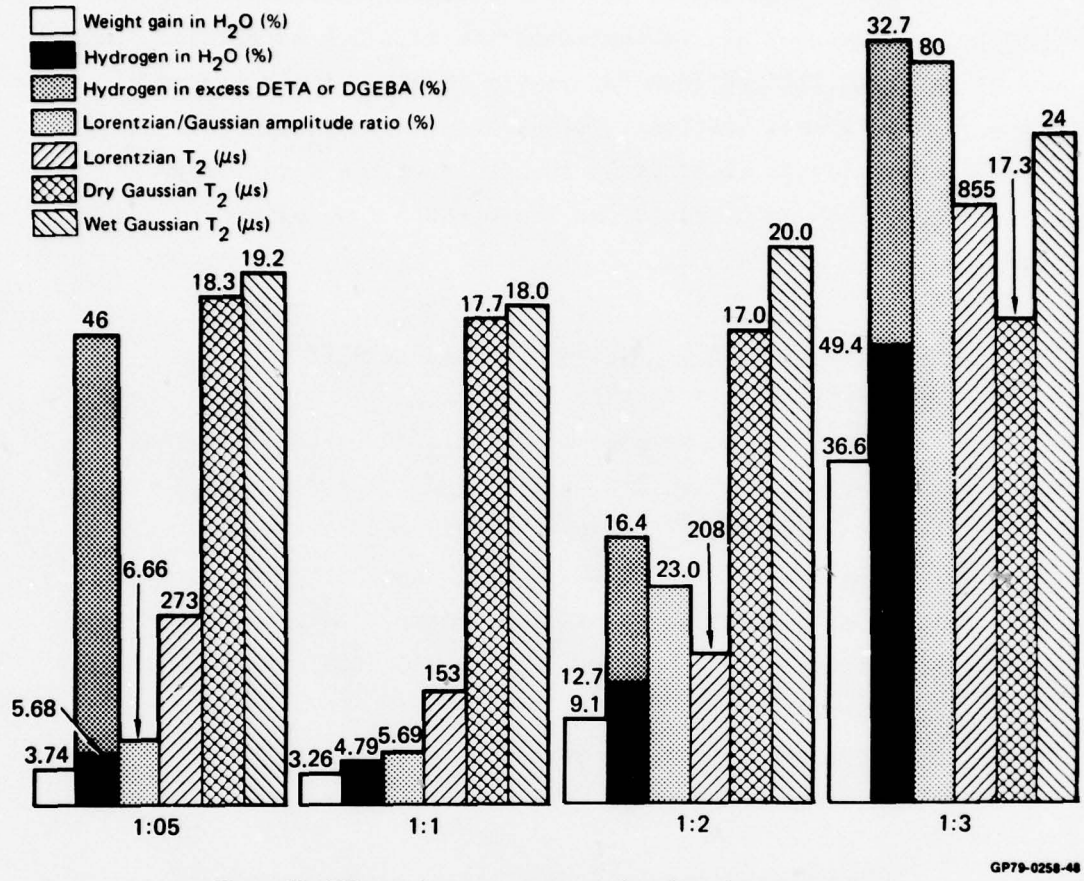

Figure 43 Effects of water on epoxy resins of varying composition.

The fourth bar denotes the spin-spin relaxation time T_{2L} of the Lorentzian component in the wet samples. The low value of T_{2L} for the 1:1 sample indicates that the mobility of the plasticized portion is less than that of the other samples. The large value of T_{2L} in the 1:3 sample indicates extreme plasticization. Great care was taken in determining if the Lorentzian component of the free-induction decay consisted of two or more components; the data indicate only one component. Thus, the T_{2L} of the sorbed water and the T_{2L} of the excess DETA are identical, which, along with the fact that sorbed water content increases with excess DETA, indicates that association of sorbed water and excess DETA exists.

The fifth and sixth bars denote the spin-spin relaxation time of the Gaussian (rigid) component in the dry and wet states, respectively. In the dry state, there is a small but significant decrease in T_{2G} with increasing DETA up to the 1:2 sample and then a small increase for the 1:3 sample. In

the wet state, the T_{2G} data show that the rigid protion of the 1:1 sample is the most rigid of all the samples. The molecular motion in the wet 1:3 sample is so great that the Gaussian component no longer exists; it has become a Lorentzian component with a T_{2L} of 24 μs, which means that liquid-like motion occurs throughout the wet 1:3 sample.

2.11 Effects of Sorbed D_2O on NMR Signals

Because the Lorentzian hydrogen signal from the sorbed water is indistinguishable from the Lorentzian hydrogen signal from the plasticized epoxy resin, it was difficult to determine the details of the plasticizing effect of the sorbed water on the epoxy resin. To eliminate the hydrogen signal from the water, D_2O was used.

Samples of cured DGEBA/DETA epoxy resins with four different stoichiometric compositions, 1:0.5, 1:1, 1:2, and 1:3, were soaked in D_2O solutions at 350 K. The samples had previously been subjected to a post-cure at 373 K in vacuum for 120 h. The weights and NMR signals were obtained at various times during the post-curing and soaking in D_2O solutions. The NMR signal from a dry 1:1 sample was used as a reference so that absolute signal amplitudes could be used as a measure of the number of hydrogen atoms in the samples. The most important results of these experiments are shown in Table 6.

TABLE 6 RESULTS OF SOAKING CURED EPOXY RESIN SAMPLES IN D_2O AT 350 K

Sample stoichiometry DGEBA:DETA	Weight gain (%)	Calculated relative number of labile hydrogens (%)	Relative decrease in hydrogen NMR signal (%)	A_L/A_G before soaking (%)	Maximum value of A_L/A_G during soak (%)	A_L/A_G after 700 h of soaking (%)		A_L/A_G after re-drying (%)
						Expected**	Measured	
1:0.5	3.2	3.7	3.5	1.5	1.5	0	1.4	0.6
1:1	4.5	6.7	6.5	0.5	2.1	0	1.0	0.6
1:2	12.8	11.5	12.8	2.7	2.8	9.2	2.8	0.6
1:3	30.0	14.9 (22.5)*	19 ± 3	3.7	18.5	16.0 (10.7)*	13.6	0.6

* Corrected for weight loss.
** Assumes only excess DETA is plasticized.

GP79-0288-3

The amine and hydroxyl hydrogens were expected to be labile and exchange with D_2O, diffuse from the sample, and thereby reduce the total amplitude of the NMR signal. This mechanism is shown in columns three and four of Table 6, where the calculated number of labile hydrogens (equal to the number of amine hydrogens in the DETA before reacting) is compared with the measured decrease in the amplitude of the total NMR signal after the sample soaked in D_2O for 700 h. The agreement is good for the 1:0.5, 1:1, and 1:2 samples but poor for the 1:3 samples, 14.9% compared with 19 $\pm$ 3%. The 1:3 samples produced problems during the experiments because they swelled and would not fit in the NMR tubes. When this swelling occurred, the samples were cut to smaller sizes, and weight measurements were obtained to estimate the fractions of the samples retained. Finally, to add to the uncertainty, the 1:3 samples were found to weigh 8.7 $\pm$ 0.4 wt% less than their starting weight after the wet-dry cycle. If one assumes that the 8.7 wt% loss was caused by leaching unreacted DETA from the sample, the calculated number of hydrogens lost from the sample increases to 22.5% which agrees better with the measured value of 19 + 3%.

The fifth, sixth, seventh, and eighth columns tabulate the Lorentzian to Gaussian amplitude ratios A_L/A_G for the samples before soaking, at the time when the ratio is the largest, after 700 h of soaking, and after drying, respectively. Also tabulated in the seventh column is the expected A_L/A_G ratio assuming that all excess DETA becomes mobile and nonlabile hydrogens contained in this DETA contribute to the Lorentzian component. Comparing the values in the fifth and eighth columns shows that the A_L/A_G ratios for the dry samples (except the 1:1 sample) decrease after soaking in D_2O at 350 K for 700 h and redrying. This decrease occurs because of hydrogen-deuterium exchange, loss of unreacted components, and possible post-curing during the experiment. The A_L/A_G ratio goes through a maximum early in the soaking before the labile hydrogens can diffuse from the sample; this is shown in the sixth column.

The results in the seventh and eighth columns clearly show the extent D_2O plasticizes the cured resin. A small plasticizing effect is seen in the 1:0.5 and 1:1 samples; no plasticizing effect is expected if the curing is complete. The results for the 1:2 sample are interesting since a 9.2% A_L/A_G ratio was anticipated because of the excess DETA, but only a 2.8% A_L/A_G ratio was observed. This discrepancy, along with the fact that only a 1.1 $\pm$ 0.3 wt% loss was observed for the 1:2 sample after the wet-dry cycle, suggests that most of the excess

DETA was chemically bound to at least one site, and that only 30% (2.8/9.2 x 100%) of the nonlabile hydrogens in the excess DETA were highly mobile. This result was compared with results of experiments obtained by soaking the 1:2 samples in boiling H_2O for 120 h (Section 2.10). In that experiment, less than the expected A_L/A_G ratio was also measured, indicating that only about 60% of the excess DETA was plasticized by sorbed H_2O. In the previous experiment, the samples were not post cured at high temperature which could explain the 60% plasticization measured in that experiment and the 30% plasticization measured in this experiment. The results for the 1:3 sample show much larger plasticization effects. The predicted value is larger than observed, but if corrections are made for the overall weight loss of the sample, the predicted value is less than observed. The larger observed plasticization undoubtedly is caused by the increased free volume which was created when the unreacted DETA was leached from the sample. This conclusion is supported by the character of the NMR signal associated with the rigid phase of the wet 1:3 sample; the signal was no longer Gaussian but was totally Lorentzian. This change of Gaussian to Lorentzian was not observed in any of the other samples.

3. POLYESTER POLYURETHANES

3.1 Hydrolytic Reversion of Polyester Polyurethanes

Polyester polyurethanes contain three types of reactive sites that are susceptible to attack by water.[3] First, the ester group can be hydrolyzed to produce an acid and an alcohol. Since polyester polyurethanes are polyester chains, each containing about 20 ester groups that have been extended by urethane groups, hydrolysis of the ester can lead to reversion to a liquid. Ester group hydrolysis is accompanied by a weight gain since a molecule of water is added across the cleaved ester linkage. Typically a 1% weight gain arising from water addition indicates that an average of one ester group in each polyester prepolymer chain is cleaved. Thus on the average there is one cleavage between each urethane group in the polyurethane chains. Small weight gains can produce significant changes in the mechanical properties, but it may be difficult to detect these changes at an early stage of the reversion. In fact, an attractive feature of the magnetic resonance technique is the potential for detecting the reversion early.

The allophanate group is the second site in polyurethanes susceptible to hydrolysis. At temperatures $\sim$ 373 K, allophanates thermally decompose to yield isocyanate groups which react rapidly with water to yield carbon dioxide and an amine. Although hydrolysis can occur at allophanate sites in polyurethanes, it does not occur exclusively at these sites, since samples containing urethane crosslinks instead of allophanates can also revert when exposed to hot humid environments.

The third site susceptible to hydrolysis is the urethane group. Hydrolysis results in the formation of an alcohol, an amine, and carbon dioxide. The relative hydrolytic stability of this group is greater than that of the ester group, and its thermal stability is greater than that of the allophanate group[31].

3.2 Polyurethane Sample Preparation

In the water-induced reversion studies, polyester polyurethane elastomers with Shore A hardness of 40 to 50 were investigated with EPR and NMR. The diisocyanate employed in the polyurethane synthesis was an 80:20% solution of 2,4-tolylenediisocyanate (2,4-TDI) and 2,6-tolylenediisocyanate (2,6-TDI) obtained from Mobay Chemical Company. It was vacuum distilled as needed prior to use. The diol used was ethylene glycol adipate polyester (EGAP) and was

obtained commercially as Mobay R-14 polyester resin. It was used without further purification, apart from drying at 350 K under vacuum, before mixing with the diisocyanate to form the polyurethane.

Polyurethane samples were prepared from the reactants by three alternative methods[31]:

Method 1: In the first approach, a 10% excess of 80:20 TDI was added dropwise to EGAP while stirring at 325 K under a dry nitrogen atmosphere. The reaction mixture was then stirred at 355 K for 1-2 h, poured into glass flasks, and cured for 2 days at 365 K under a nitrogen atmosphere. Sometimes the sample was subjected to a vacuum before the final 2-day cure to remove trapped bubbles; however, unreacted TDI could be lost during this procedure, so this step was eventually eliminated. The final product was initially a tough rubber having a Shore A hardness of 40 to 50, but it crystallized after a few days to show a Shore A hardness of 90. This product was composed of straight-chain polyurethanes linked by allophanate crosslinks which resulted from a reaction of the 10% excess TDI with the urethane groups (see Figure 44). The crosslinks obtained did not effectively prevent crystallization since they were few in number and did not promote the formation of rigid domains.

Method 2: The following synthesis was used to prepare a product that did not crystallize. Excess (220%) 80:20 TDI was reacted with EGAP to form an isocyanate-capped prepolymer. 1,4-butanediol was added as a final curing agent to 10% excess of the prepolymer, and the mixture was cured at 365 K for 12 h either in a vacuum or a dry nitrogen atmosphere (Figure 45). The final product contained allophanate crosslinks because of the 10% excess TDI and rigid domains composed of associated TDI-butanediol-TDI blocks. This domain structure, which was verified using NMR (see Section 4.4), prevented crystallization in the sample.

Method 3: The third approach to polyurethane synthesis involved the introduction of a triol to produce crosslinking via urethane linkages as opposed to allophanate linkages (Figure 46). This approach has the advantage that only two types of sites vulnerable to hydrolysis are present in the sample, viz., the urethane and ester groups. The allophanate group, also susceptible to attack by water, was eliminated in the sample by using stoichiometric amounts of TDI and hydroxyl groups, as well as keeping the reaction temperature (355 K) below that required for allophanate formation.

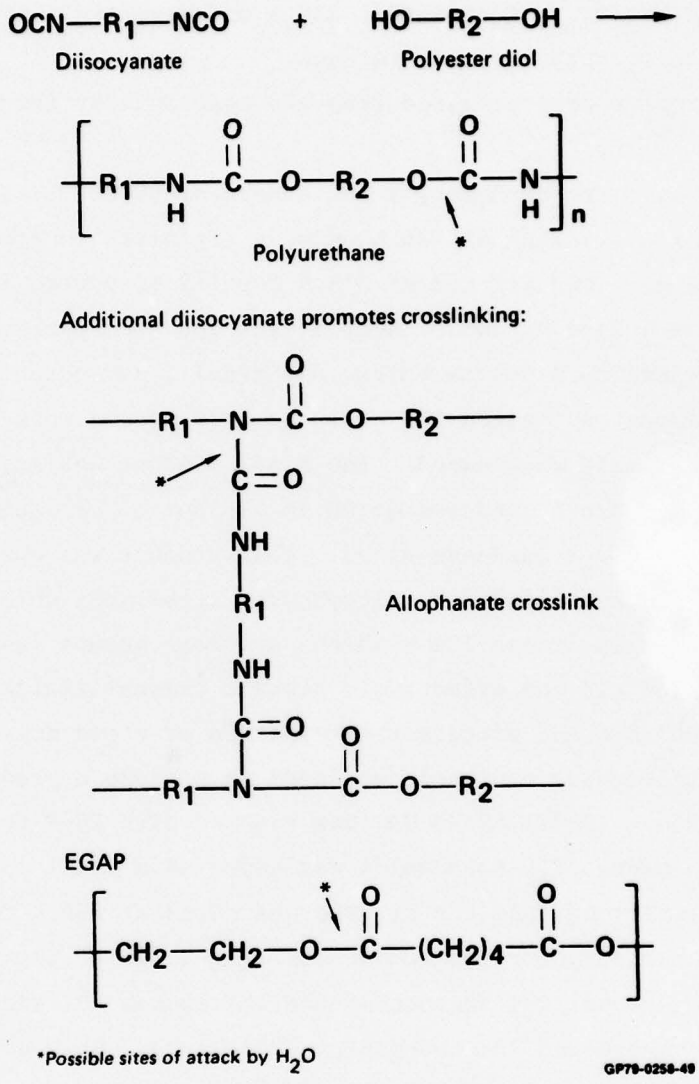

Figure 44 **Formation of an allophanate crosslinked polyester polyurethane by the reaction of a polyester diol with excess diisocyanate. R_1 = 80:20 TDI, R_2 = EGAP.**

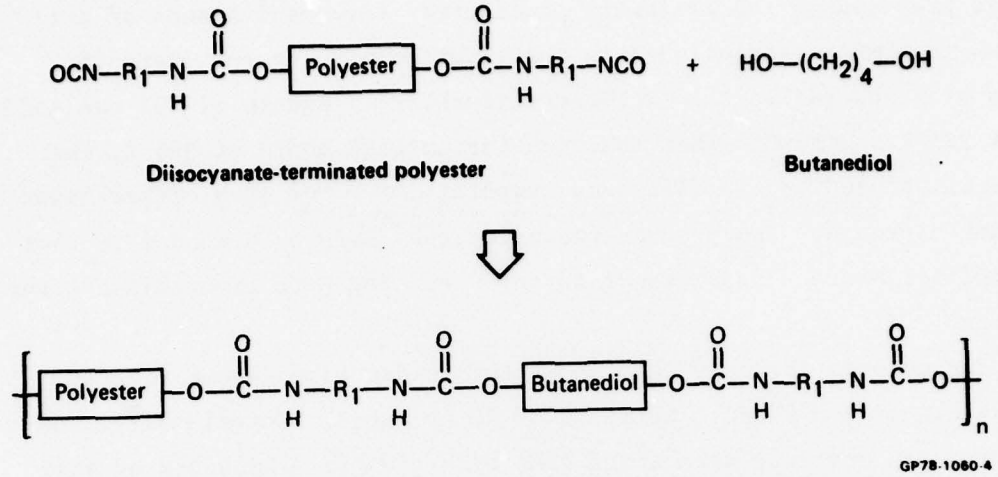

Figure 45 Formation of polyurethane by the reaction of isocyanate-capped EGAP with 1,4-butanediol chain extender (allophanate formation is not shown). R_1 = 80:20 TDI.

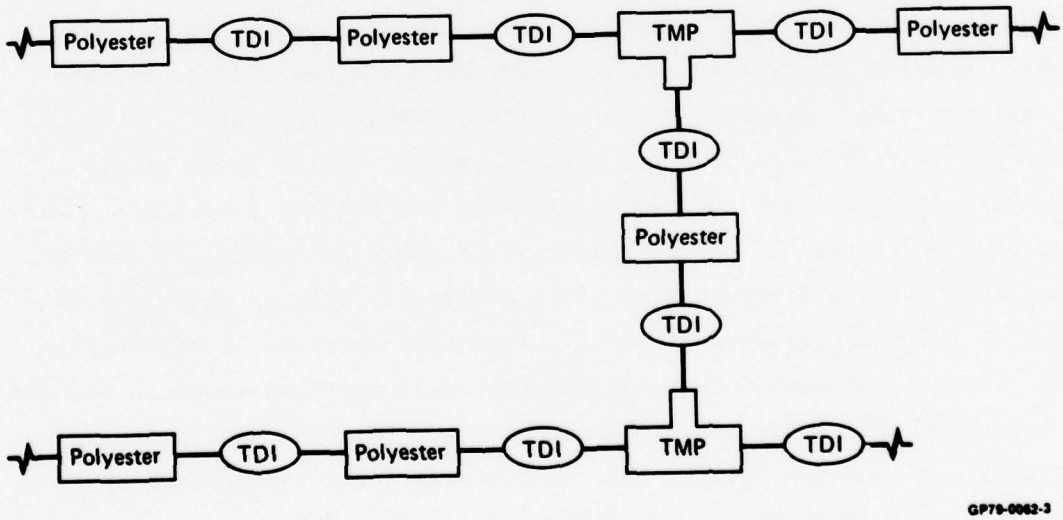

Figure 46 Structure of polyester polyurethane containing TMP sites for urethane crosslinks.

Samples were prepared by the following procedure: five equivalents of trimethylolpropane (TMP) were included in the reaction mixture for every 95 equivalents of EGAP, and to this stirred mixture, a 2% excess of TDI was added dropwise at 325 K. After further reaction for several hours at 355 K, the preparation was poured into a flask and cured at 365 K for 12 h either under vacuum or dry nitrogen. The product resembled that made by Method 1 in that it had an initial Shore A hardness of 40 to 50 and began to crystallize after a few days.

The three methods for polyurethane synthesis described above yielded polymer products with a Shore A hardness of 40 or above. Occasionally, however, the products obtained were stiff gums with a Shore A hardness of only 10 or less. The softer products resulted from two causes: (1) the TDI used was sensitive to moisture or (2) the TDI was volatile. Small amounts of water present in the EGAP or TMP could react with the TDI and upset the stoichiometry of the polyurethane reaction. For example, as little as 0.1 wt% water in a stoichiometric reaction mixture would destroy 10% of the TDI present. This situation was avoided by drying the EGAP and TMP under vacuum at 350 K prior to use, by weighing the reactants inside a nitrogen-filled glove box, and by performing the reaction in a closed vessel. The volatility of TDI was a problem during the final cure at 365 K but was avoided by completing this phase of the synthesis in a tightly sealed container.

NMR experiments were performed on four samples. Two of these samples were synthesized by Method 1 and hence contained allophanate crosslinks. One of the samples was a tough, rubbery solid with a Shore A hardness of over 40, while the other was a softer, more gum-like material. Both of these samples crystallized after several days at 293 K. The first appeared to crystallize uniformly, whereas the second crystallized from what appeared to be nucleation sites. The third NMR sample was prepared using Method 2 and thus contained TDI-butanediol-TDI domain regions. The fourth sample was synthesized by Method 3 and contained urethane crosslinks arising from TMP.

All three EPR samples studied were made using Method 3 so they contained urethane crosslinks at the TMP sites in the polymer. One sample contained the spin probe TEMPO (Figure 2) and had a Shore A hardness of $\sim$ 40. The TEMPO was added just before the final cure at 365 K to prevent the possibility of decomposition of the nitroxide with exposure to hot TDI.

Two polyurethane samples were spin-labeled; one was labeled at the end of the EGAP chain (denoted spin label I) and the other was labeled at an isocyanate site of the TDI molecule (denoted spin label II). These labels were chosen to probe different local environments in the cured samples. In the synthesis of spin label I, the imidazole derivative of 3-carboxy-2,2,5,5-tetramethyl-pyrrolin-1-oxyl (IPNO) was covalently bound to a terminal alcohol group of the EGAP diol as shown in Figure 47. A mixture of 95% (by equivalents) of this diol and 5% TMP was then cured with 80:20 TDI using Method 3. The product obtained was a somewhat incompletely cured polyurethane that resembled a stiff gum whose softness may have been due to evaporation of some of the TDI during the final cure. The sample was judged satisfactory for the reversion studies.

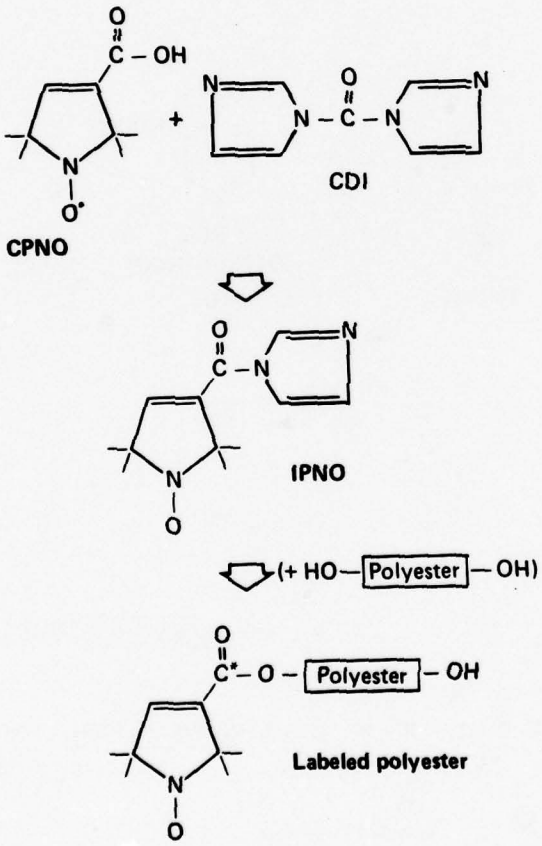

*A possible site for bond scission as a result of attack by H_2O.

GP79-0258-20

Figure 47 **Reaction sequence used to make IPNO-labeled EGAP polyester (spin label I). CPNO = 3-carboxy-2,2,5,5-tetramethylpyrrolin-1-oxyl; CDI = 1,1′-carbonyldiimidazole; IPNO = imidazole derivative of CPNO.**

Spin label II was synthesized by covalently binding the nitroxide TAMIN (Figure 48) to the 80:20-TDI that was subsequently used in the polyurethane synthesis. TAMIN and TDI were mixed in a ratio of 1:99 (by equivalents) and heated to 365 K for 1 h. It is possible that under the reaction conditions, more than one type of spin label might have been formed. When TAMIN was bound to only one TDI molecule, the resulting nitroxide isocyanate (a urea, see Figure 48) acted as an end label when subsequently added to EGAP. If the TAMIN reacted further to bind to two TDI molecules, a nitroxide-diisocyanate label (a biuret) was formed that could act as a bridging group between two EGAP molecules. It is possible that two TAMIN molecules could combine with one TDI molecule to form a biradical which the observed EPR spectrum did not indicate.

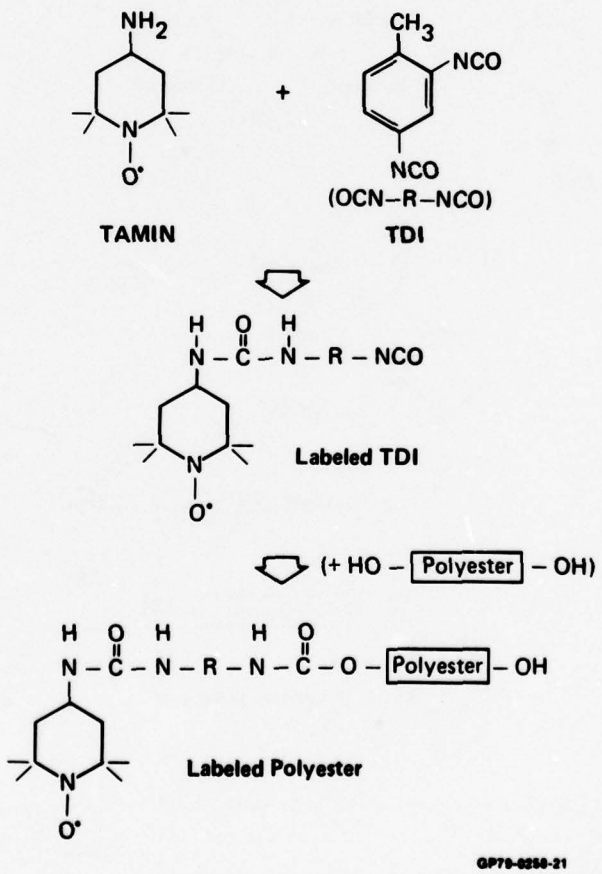

Figure 48 Reaction sequence used to make TAMIN-labeled EGAP polyester (spin label III). TDI = 80:20 TDI.

After TDI had been labeled with TAMIN, a 2% excess of this TDI was reacted with a 95:5 (by equivalents) mixture of EGAP and TMP to form a cured polyurethane. This product was a stiff gum but satisfactory for the EPR reversion studies.

3.3 Spin Probe and Spin Label Results in Polyester Polyurethanes

The EPR spectra of the polyester polyurethane sample containing TEMPO were obtained from 293 K to 400 K. Typical spectra are shown in Figure 49. In this temperature range, the spectra indicate that the motional correlation times are in the fast motion range (i.e., $\tau_c < 10^{-9}$s) so the theory of Kivelson[9] is applicable. The correlation times were evaluated from the relative intensities of the lines assuming isotropic tumbling motion. The equation used[32] was

$$\tau = 4\left[\left(\frac{Y(0)}{Y(1)}\right)^{1/2} + \left(\frac{Y(0)}{Y(-1)}\right)^{1/2} - 2\right] b^{-2}[T_2(0)]^{-1}, \qquad (7)$$

with

$$b = \left(\frac{4\pi}{3}\right)\left[A_{zz} - \frac{1}{2}\left(A_{xx} + A_{yy}\right)\right], \qquad (8)$$

where Y(-1), Y(0), and Y(1) are the intensities of the low, middle, and high field lines respectively. $[T_2(0)]^{-1}$ is the half-width of the center line and A_{xx}, A_{yy}, and A_{zz} are the principal values of the nitrogen hyperfine tensor, A. The values A_{zz} = 3.45 mT, $A_{xx} = A_{yy}$ = 0.6 mT were used.

The temperature dependence of the correlation times T_c, is shown in Figure 50. The results indicate that from 293 K to 345 K, τ_c can be written as

$$\tau_c = \tau_{co} \exp(\Delta E/kT) \qquad (9)$$

with an activation energy $\Delta E = 50.2 \pm 1.5$ kJ/mole and an inverse frequency factor $\tau_{co} = 1.3 \times 10^{-18}$s.

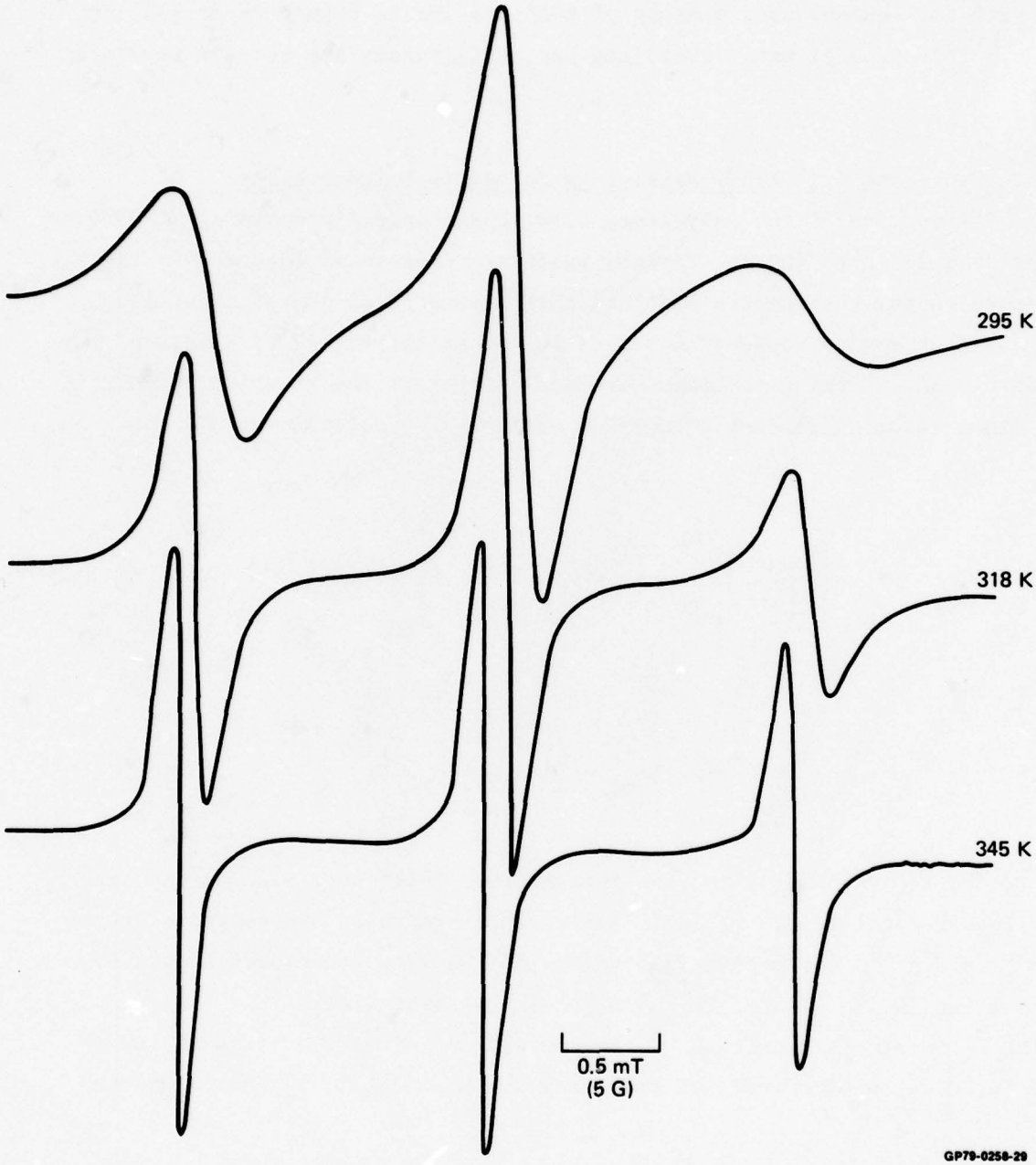

Figure 49 Spectra observed at 295 K, 318 K, and 345 K from the spin probe TEMPO in nonreverted polyurethane.

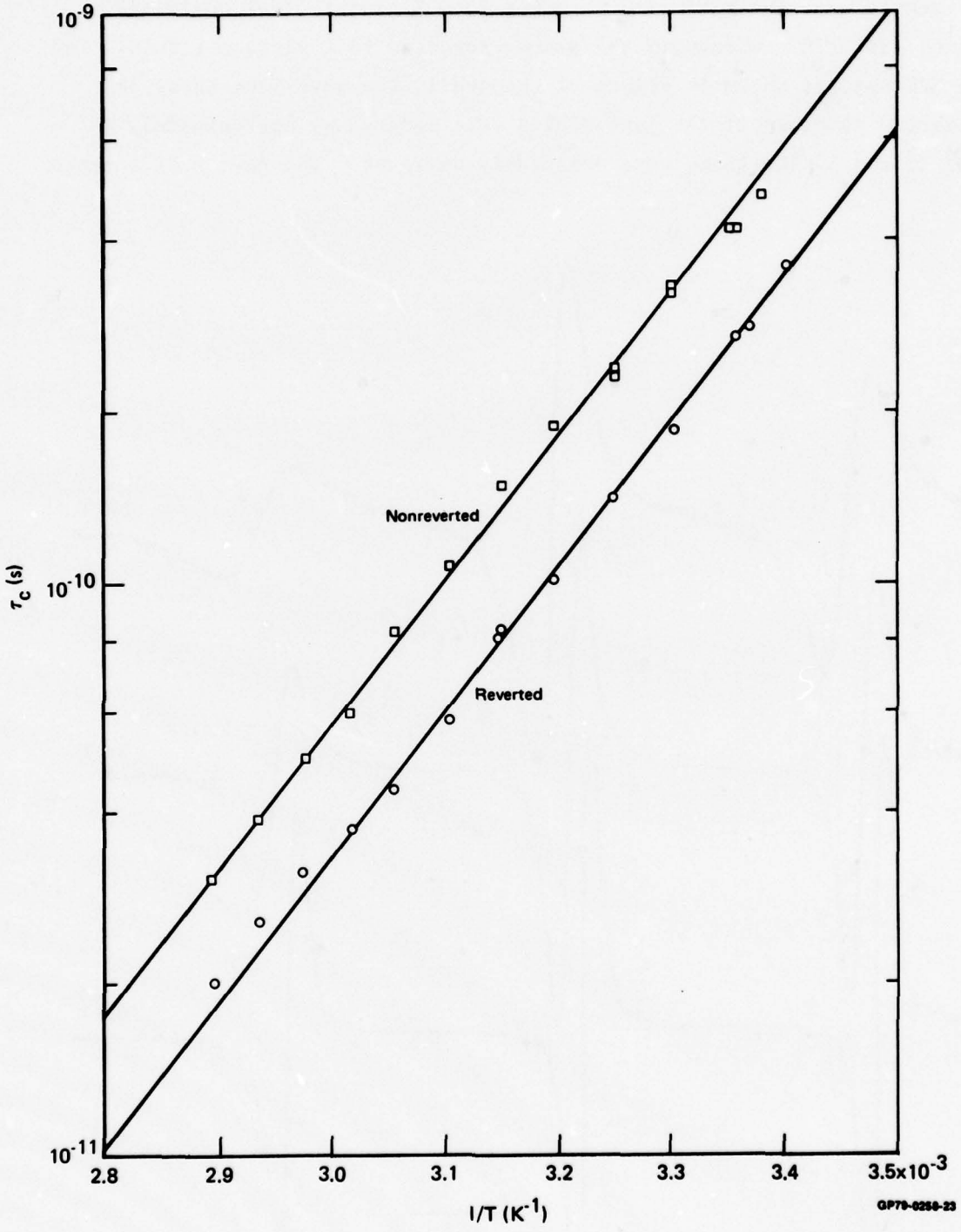

Figure 50 Temperature dependence of correlation times for TEMPO spin probe in nonreverted and reverted polyurethane.

The sample was then subjected to a hot (360 K) moist (100% humidity) environment for ∿ 70 h whereupon the sample reverted to a viscous liquid. The observed EPR spectra shown in Figure 51 changed in two ways from those of the unreverted samples: 1) the intensities were reduced by approximately a factor of 12 and 2) the lines were measurably narrower. The former difference

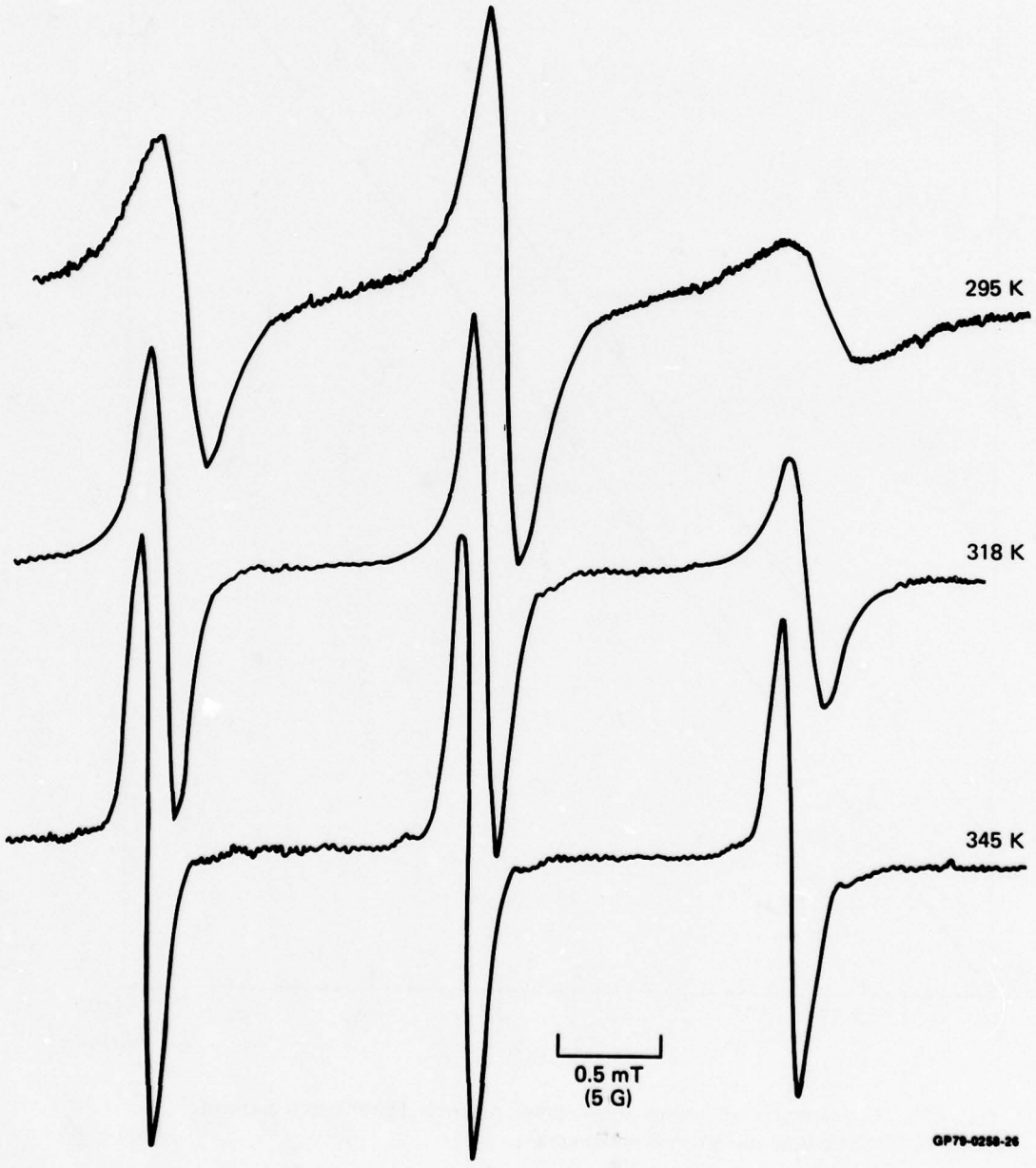

Figure 51 Spectra observed at 295 K, 318 K, and 345 K from the TEMPO spin probe in reverted polyurethane.

was probably a result of acid formation by ester hydrolysis since it is known[33] that nitroxides decompose in an acid medium. Hence, the spin-probe EPR signal intensity might be used as a measure of the extent of the hydrolysis. The latter is a result of the reduction in microviscosity caused by the reversion. The motional correlation times were evaluated from these spectra using Equation (7), and the temperature dependence is plotted in Figure 50. The results indicate that τ_c is also of the form shown in Equation (9) with $\Delta E = 48.8 \pm 1.5$ kJ/mole and $\tau_{co} = 4.5 \times 10^{-19}$ s. Consequently within the experimental error, the activation energy for the correlation time shows no measurable change, whereas the inverse frequency factor changes upon reversion. The correlation time for the spin probe TEMPO is assumed to be of the form

$$\tau_c = \frac{4\pi\eta\, a^3}{3kT(1 + \eta/\delta)} , \tag{10}$$

where η is the viscosity of the polyurethane, a is the radius of the probe, and δ is the microviscosity that determines the values of τ_c when $\eta >> \delta$, i.e., in the rubbery unreverted polyurethane. If $\eta >> \delta$,

$$\tau_c = \frac{4\pi\delta\, a^3}{3kT} , \tag{11}$$

whereas when $\eta << \delta$, as in the reverted polyurethane[8],

$$\tau_c = \frac{4\pi\eta\, a^3}{3kT} . \tag{12}$$

Flory[33] has shown that the viscosity of linear polyester resins can be expressed as

$$\eta = \exp \frac{(A + BZ^{1/2})}{R} \exp[\Delta H/RT], \tag{13}$$

where A, B are constant with the values $A \approx -118$ J/mole/K, $B \approx 2.1$ J/mole/K, Z is a weight average chain length, and ΔH is the activation energy for

viscosity. This activation energy for viscous flow is related to the energy required to form a hole in the liquid. The size of the hole necessary for liquid flow need not be determined by the average chain length but by a constant-length chain segment that is independent of average chain length. This conclusion agrees with the viscosity data where the ΔH values for different polyesters are independent of average chain length.

From 293 K to 370 K, the temperature dependence of η should determine the temperature dependence of τ_c which is given by Equation (12). Therefore, one can expect $\tau_c \propto \eta$; hence from Equations (9)-(13), one obtains

$$R \ln \tau_{co} \propto \frac{1}{R} (A + BZ^{1/2}). \tag{14}$$

Equation (14) implies that the inverse frequency factor depends on the reversion since the average chain length will be reduced following the ester bond scissions occurring in the hydrolytic reversion reaction. Thus, Flory's viscosity data[33] are consistent with the results shown in Figure 50. Moreover, the observation that ΔE is independent of the reversion implies that ΔE is independent of chain length and is in agreement with the ΔH behavior derived from the viscosity data.

Based on these results, we conclude that the EPR spectra are sensitive to the hydrolytic reversion through the inverse frequency factor. Analysis indicates that to increase the sensitivity of the EPR lineshapes to reversion, the values of τ_c in the unreverted polyurethane should be increased. This conclusion implies that δ and a in Equation (11) should be increased, i.e., larger spin probes should be used.

The EPR spectra of the spin label I sample were obtained from 293 K to 370 K. Typical spectra are shown in Figure 52. The motional correlation times of the nitroxide label were evaluated in the fast-motion regime assuming isotropic motion by using Equation (7). The temperature dependence of the correlation time plotted in Figure 53 shows that from 293 K to 370 K, the correlation time to a good approximation is of the form given by Equation (9) with $\Delta E = 42.7 \pm 1.5$ kJ/mole and the inverse frequency factor, $\tau_{co} = 8.3 \times 10^{-17}$s.

This sample was exposed to a hot (360 K), moist (100% humidity) environment for ~ 70 h whereupon the sample reverted to a viscous liquid. The observed EPR spectra of spin label I (Figure 54) showed little change in intensity from those of the unreverted sample but a measurable reduction in linewidth.

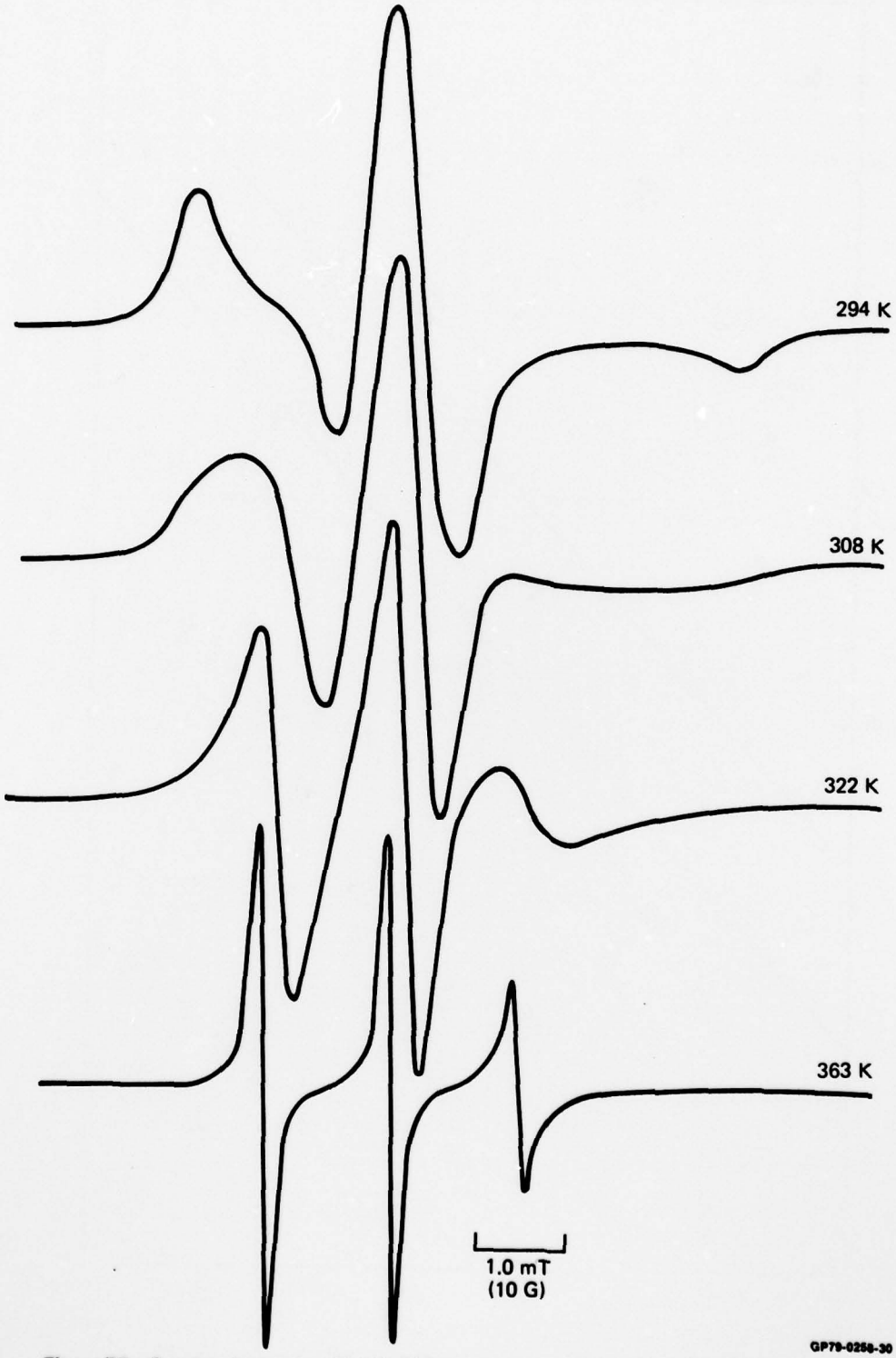

Figure 52 Spectra observed at 294 K, 308 K, 322 K and 363 K from the IPNO spin label (spin label I) in nonreverted polyurethane.

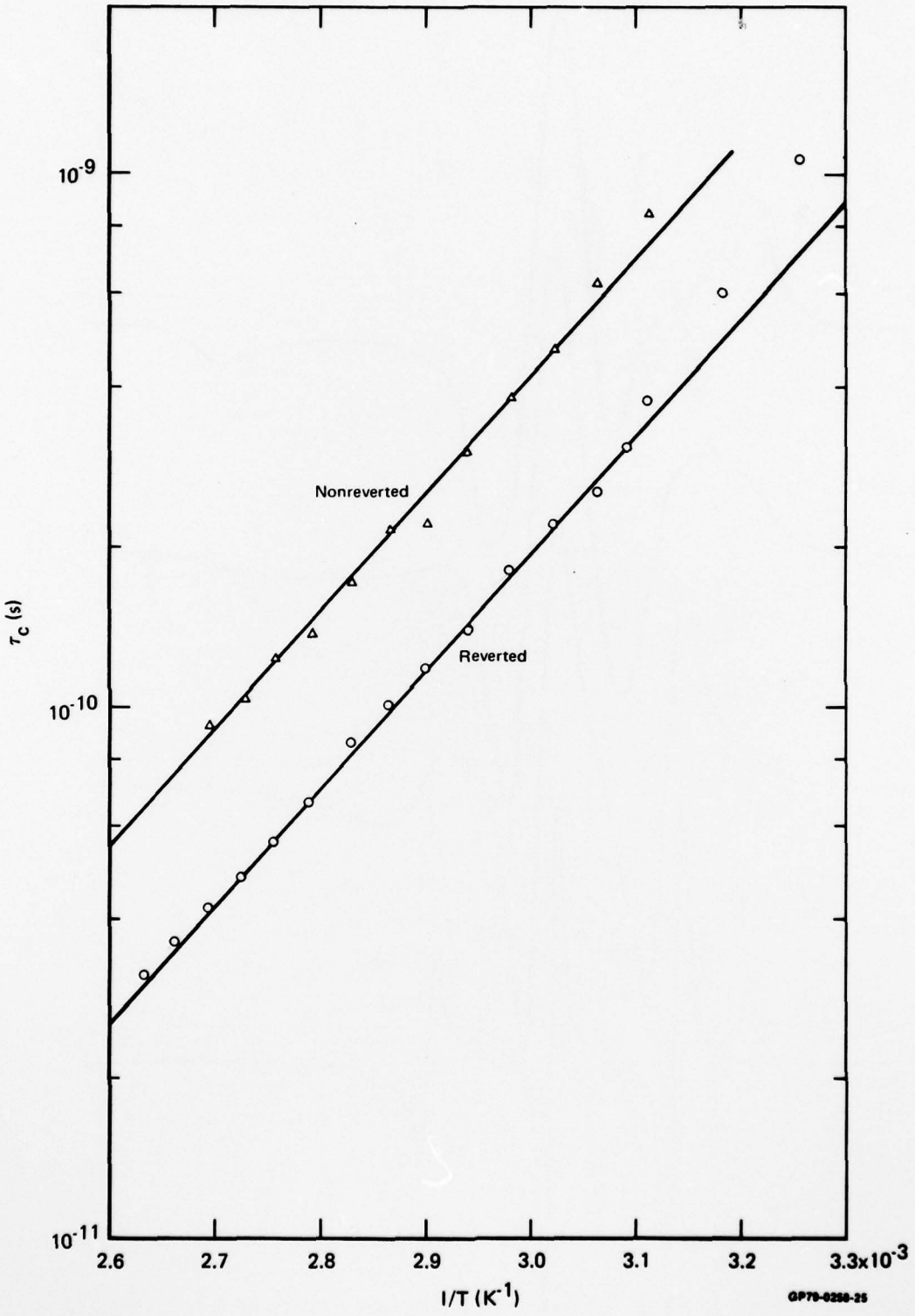

Figure 53 Temperature dependence of the IPNO spin label (spin label I) correlation times in nonreverted and reverted polyurethane containing TMP.

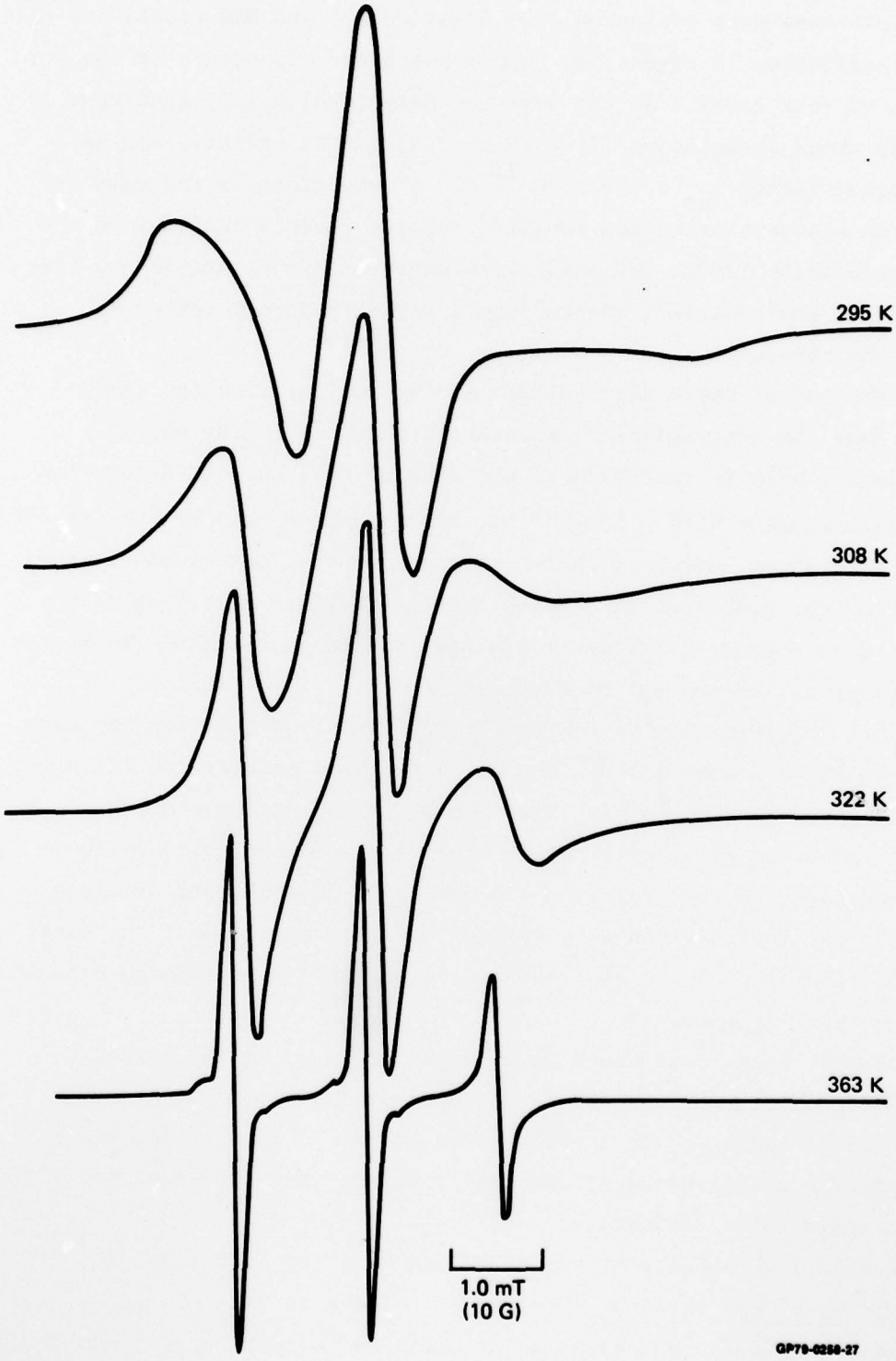

Figure 54 Spectra observed at 295 K, 308 K, 322 K, and 363 K from IPNO spin label (spin label I) in reverted polyurethane.

The correlation times were evaluated from Equation (7) and are plotted as a function of temperature in Figure 53. The temperature dependence of the correlation time of spin label I in the reverted polyurethane indicated that it is of the form shown in Equation (9) with $\Delta E = 42.3 \pm 1.5$ kJ/mole and an inverse frequency factor $\tau_{co} = 4.8 \times 10^{-17}$ s. A comparison of the data for spin label I in the unreverted and reverted samples reveals that, as in the case of the spin probe TEMPO, the activation energy for the correlation time is independent of the reversion whereas the inverse frequency factor is dependent on the reversion.

Interpretations of these results are made by analogy with the TEMPO probe data. Thus the activation energies are determined by the energy required to form a hole in the polymer; the size of this hole is determined by a small chain segment with a length that is independent of the average chain length. The activation energy is therefore still independent of the chain length following the reduction in the average chain length resulting from hydrolytic bond scissions of the ester linkages in the main chain. Hence the activation energy is independent of reversion.

The inverse frequency factor is smaller for the probe than for the corresponding spin label I and implies that the activation entropy for the probe is greater than that for the label. This result is expected since the covalent bonding of the label will impose constraints on the polymer-label spatial arrangements, thereby reducing the number of possible polymer-label conformations. The inverse frequency factors for the spin label I decrease as a result of reversion which implies that the entropy of activation depends on the average chain length.

Since the spin label I is bound as an ester group one might expect to observe the spectrum of a spin probe resulting from hydrolytic scission of the nitroxide-ester linkage. This spectrum could not be identified; hence it implies that the nitroxide-ester linkage is more stable to hydrolytic attack than the main-chain ester linkages.

The temperature dependence of the EPR lineshapes for spin label II, the TAMIN-labeled sample, was obtained from 293 K to 400 K in both the unreverted and the reverted samples. Reversion was accomplished by placing the sample in 100% relative humidity at 365 K for $\sim$ 48 h. The reverted sample was a viscous liquid at 365 K, but it began to crystallize immediately on cooling to

293 K. The spectra in Figures 55 and 56, before and after reversion respectively, indicate that the motions associated with the spin label were highly anisotropic. This conclusion is based on the spectral feature wherein the low field line intensity is larger than that of the center line.[23] This motional anisotropy is a consequence of the TAMIN bonding to the rigid aromatic ring in the polyurethane (see Figure 48) (or possibly to two aromatic rings, if a buiret is formed). Since the label is anchored to the immobile aromatic ring, most motions are restricted with the exception of rotations about the TAMIN-arene bond. The label motions should therefore be characterized by a short correlation time for rotation about the urea linkage, and a longer correlation time for the other slower motions.

Equation (7) could not be used to obtain accurate correlation times since the motion was anistropic. Although it is possible to evaluate both correlation times from computer simulations of the observed spectra[10], as yet good data fits have not been obtained because the relative orientation of the motional axes with respect to the magnetic axes is unknown. However, a qualitative comparison of Figures 55 and 56 reveals that at any given temperature, the label correlation time is shorter in the reverted sample than in the unreverted sample. This conclusion is consistent with the results obtained in the probe and spin label I studies.

The observed lineshapes for spin label II in the reverted and unreverted samples, Figures 55 and 56 respectively, show that there is a superposition of two spectra from different nitroxide species. The overlap is apparent in the 354 K spectrum of Figure 56 where three sharp lines are superimposed on three broader lines and in the 318 K spectrum of the unreverted sample where there is an additional peak between the center and high field lines.

The two nitroxide species present are either unreacted TAMIN and the TAMIN-TDI end-label, or the TAMIN-TDI end-label and a TDI-TAMIN-TDI buiret bridging group. The former seems the more probable since in the 354 K spectrum of Figure 56 the three sharp lines indicate a rapidly tumbling, small molecule such as TAMIN. Thus, the nitroxide causing the more rigid spectrum in Figures 55 and 56 is probably the TAMIN-TDI end-label. Comparison of the spectra of this end-label with the spin-label I spectra in Figures 52 and 54 indicates that the former has a longer correlation time. This increase is a consequence of the greater rigidity of the TDI group compared with the flexible polyester groups.

Figure 55 Spectra observed at 296 K, 318 K, 354 K, and 386 K from spin label II in nonreverted polyurethane.

Figure 56 Spectra observed at 293 K, 318 K, 354 K, and 386 K from reverted TAMIN-labeled polyurethane (spin label II). A superposition of two fast-phase components can be observed in the 318 K, 354 K, and 386 K spectra.

3.4 Characteristics of Polyurethane NMR Signals

The polyurethanes studied had a free-induction decay signal composed of a Lorentzian component $\geq$ 300 μs and a Gaussian component $\sim$ 12 μs. The Lorentzian signal was assigned to hydrogens in the amorphous regions, whereas the Gaussian portion was assigned to hydrogens in the cyrstalline or domain regions. The long spin-spin relaxation time T_{2L} in the amorphous regions permitted both multiple-pulse and conventional Fourier transform NMR experiments to be performed. Since T_{2L} was often greater than 1000 μs, it was not possible to accurately measure T_{2L} from the free-induction decay signal. As a result, when T_{2L} exceeded 800 μs, the Meiboom-Gill[35] modification of the Carr-Purcell pulse sequence[36] was used to measure T_{2L}.

3.5 Crystallization Effects in Polyurethanes

It was noticed that the quantitative details of the NMR signal varied between different samples made at the same time. The reason for this variation was apparent when a sample with a low crosslink density was observed to crystallize into a mottled, milky-white sample with distinctly opaque regions and slightly opaque regions. Samples were selected from both regions and studied with NMR.

The NMR signals from these samples were predominantly Lorentzian in character, which indicates considerable molecular mobility. Table 7 lists the Lorentzian and Gaussian amplitudes and relaxation times for the samples.

The data show a distinct difference between the very opaque and slightly opaque samples. The very opaque samples contain a larger Gaussian component, and the T_{2G}'s are greater. The T_{2L}'s are not significantly different between the two types of samples. Since the samples were of different sizes, no significance should be assigned to any differences in the absolute values of the amplitudes A_G and A_L between the samples.

The ratios A_G/A_L are meaningful, and they differ significantly between the very opaque and slightly opaque samples. (Because A_L dominates in these polyurethane samples, A_G/A_L is calculated rather than A_L/A_G as was done for the epoxy samples where A_G dominated.) The larger values of $A_G/A_L \approx 43\%$ in the very opaque samples indicate that these samples are more crystalline than the slightly opaque samples, which have $A_G/A_L \approx 25\%$. After annealing all of the samples at 353 K for 10 min, the samples became clear and the Gaussian component practically disappeared as shown in Table 7. The value of

TABLE 7 LORENTZIAN AND GAUSSIAN HYDROGEN NMR SIGNALS IN LOW CROSS-LINKED POLYURETHANE SAMPLES.

Sample number and history	Lorentzian component		Gaussian component		A_G/A_L (%)	Appearance
	A_L	T_{2L} (μs)	A_G	T_{2G} (μs)		
1 Twelve-day-old	1100 ± 100	387 ± 26	531 ± 26	15.3 ± 0.6	48 ± 7	Very opaque
2 Twelve-day-old	1441 ± 100	332 ± 19	548 ± 78	16.1 ± 0.5	38 ± 8	Very opaque
3 Twelve-day-old	1325 ± 107	388 ± 16	557 ± 86	15.2 ± 0.8	42 ± 10	Very opaque
4 Twelve-day-old	1247 ± 11	415 ± 15	325 ± 35	12.9 ± 0.8	26 ± 3	Slightly opaque
5 Twelve-day-old	1450 ± 29	416 ± 22	363 ± 45	12.9 ± 1.0	25 ± 4	Slightly opaque
6 Twelve-day-old	1569 ± 47	389 ± 16	368 ± 13	12.4 ± 1.0	23 ± 1	Slightly opaque
1 After anneal	1667	532	< 64	–	< 3.8	Clear
2 After anneal	1958	427	< 64	–	< 3.3	Clear
3 After anneal	1828	572	< 64	–	< 3.5	Clear
4 After anneal	1444	441	< 64	–	< 4.4	Clear
5 After anneal	1731	528	< 64	–	< 4.6	Clear
6 After anneal	1819	452	< 64	–	< 3.5	Clear
1 Two days after anneal	1544	570	272	11.7	18	Opaque
2 Two days after anneal	1683	326	426	12.6	25	Opaque
3 Two days after anneal	1617	526	394	12.0	24	Opaque
4 Two days after anneal	1353	440	302	10.7	22	Opaque
5 Two days after anneal	1630	531	267	12.0	16	Opaque
6 Two days after anneal	1648	497	206	12.5	19	Opaque

GP79-0258-17

A_G/A_L is less than 4.6% for all samples. For each sample, the sum of A_L and A_G before annealing is equal to the sum after annealing to within 3 ± 2% which illustrates the ability of NMR spectroscopy to make quantitative measurements proportional to the total number of hydrogen nuclei present in the sample.

The value of T_2L before annealing ($\approx$ 390 ± 30 μs) was significantly smaller than after annealing ($\approx$ 490 ± 60 μs), indicating that mobility of the rubbery portion of the polyurethane sample was reduced by the crystalline regions. The large scatter in the T_{2L} data is characteristic of the samples and not the NMR measurements.

After two days, the annealed samples became milky again, and the A_G/A_L ratios increased, as shown in Table 7. Prior to annealing, samples 1, 2, and 3 had the largest A_G/A_L ratios. Two days after annealing, samples 2, 3, and 4 had the largest A_G/A_L ratios. Hence, nucleation and growth of crystalline regions do not display a memory effect.

Multiple-pulse proton NMR spectra were successfully obtained in these low crosslinked polyurethane samples. Figure 57 shows the partially relaxed spectra of a partially crystalline sample, before and after annealing. In both sets of spectra, the methylene hydrogens in the adipic acid are resolved from those in the ethylene glycol. The concentration of TDI is too small to permit detection of the aromatic and methyl hydrogens in TDI. Two rates of relaxation are apparent in the spectra of the partially crystalline sample; 0.15 s after the spin inverting pulse, a broad inverted peak is coincident with the pair of narrow upright peaks. The spectra of the annealed sample do not contain the broad peak; hence, it is assigned to the crystalline component present in the unannealed sample. These relaxed spectra also show that the partially crystalline samples relax about 50% slower than the annealed samples.

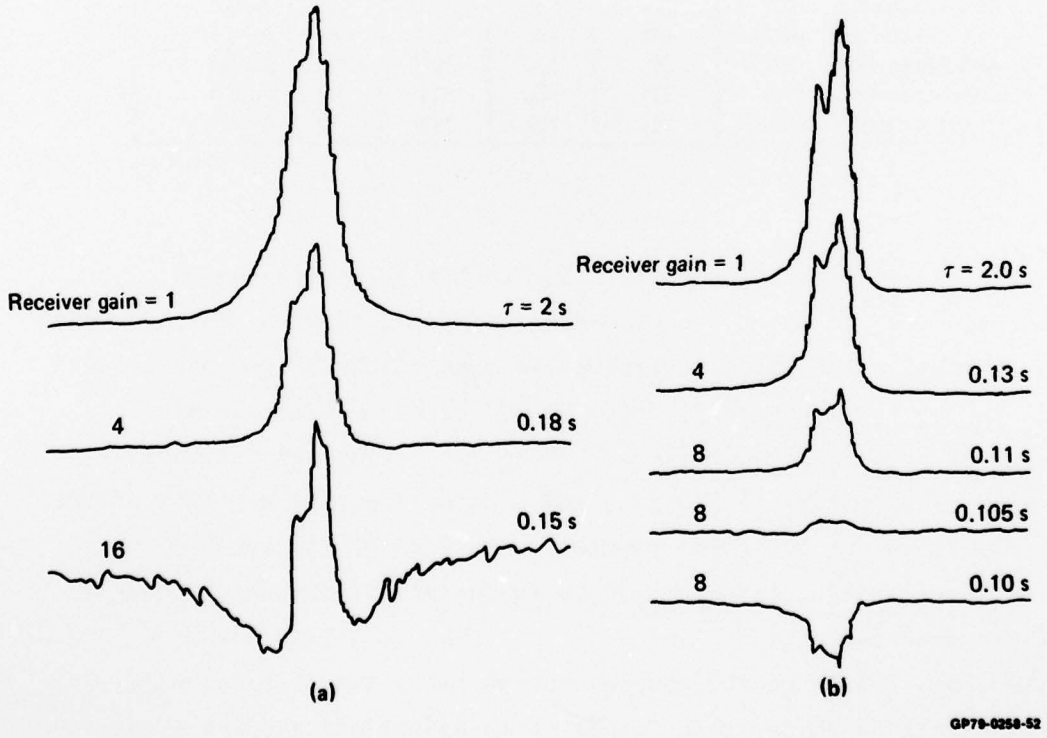

Figure 57 **Multiple-pulse NMR partially spin-lattice relaxed spectra of polyurethane: (a) partially crystalline, (b) after annealing. The time between the spin-inverting pulse and observing the spectra is denoted by τ. In both (a) and (b) the peaks on the left are assigned to the methylene hydrogens of ethylene glycol, and the peaks on the right are assigned to the methylene hydrogens of adipic acid.**

3.6 Effects of Composition on NMR Signals

Three different types of polyurethanes with about the same crosslink density were studied with NMR. They were samples with: (1) 7% allophanate crosslinks, (2) 7% urethane crosslinks, and (3) 11% urethane crosslinks with chain extension to produce hard blocks. The room temperature NMR results for the annealed dry samples are shown in Table 8. The NMR signals from the samples with only allophanate or urethane crosslinks did not contain a Gaussian component, but the NMR signals from the samples containing the allophanate crosslinks and hard blocks did contain a Gaussian component. The amplitudes of the Lorentzian and Gaussian components shown in Table 8 are normalized; their sum is one. Calculations of the amplitudes were made for sample 3 assuming that the hard blocks associated into rigid domains and the hydrogens in the domains contributed to the Gaussian component. The agreement between the measured and calculated values is good and suggests that the hard blocks are in rigid domains.

TABLE 8 NMR RESULTS FOR POLYURETHANE SAMPLES

Sample		A_L	A_G	T_{2L} (μs)	T_{2G} (μs)
(1)	Allophonate links	1	0	680	–
(2)	Urethane cross links	1	0	560	–
(3)	Allophonate links and hard blocks	0.88 (0.87)*	0.12 (0.13)*	370	17

* Values in parentheses were calculated assuming hard blocks were in rigid domains.

GP79-0258-2

The spin-spin relaxation time T_{2L} of the sample with the allophanate links was the greatest (680 μs) and indicates that this sample had the greatest molecular motion. The sample with the urethane crosslinks had a smaller T_{2L} (560 μs), indicating greater restriction to molecular motion, and the sample with the hard blocks and greater crosslink density had still greater restriction to molecular motion because T_{2L} was only 370 μs. The small value of T_{2G} (17 μs) for sample 3 indicates highly restricted molecular motion in the hard domains.

After subjecting the samples to 100% relative humidity at 358 K for various times, a modest weight gain of only about 0.7 wt% was measured. However, definite changes in the NMR signals were measured, even after only 20 h of exposure. For all three samples, the values of T_{2L} increased, indicating increased molecular motion as a result of reversion. A detailed study of the reversion process was conducted on polyurethane samples containing the urethane crosslinks. The results of this study are presented in the following section.

3.7 Effects of Reversion on NMR Signals

Polyurethane samples with 7% urethane crosslinks were exposed to 100% relative humidity at 363 K, and room-temperature NMR measurements were made during the reversion process. As the reversion progressed, there was a tendency for the samples to crystallize at room temperature. In all cases, the NMR measurements were made before crystallization occurred. Thus, the NMR signals contained only a Lorentzian component. The T_{2L} of the Lorentzian component became large during the reversion; therefore the Meiboom-Gill[35] pulse sequence was used to measure T_{2L}.

The results of a reversion study are shown in Figure 58, where T_{2L} for two of the samples is plotted as a function of exposure time. Between 0 and 12 h exposure, T_{2L} increased, and beyond 12 h, T_{2L} tended to level off. However, reversion continued to occur, but the reversion was best monitored with Fourier transform NMR spectra. While the T_{2L} data in Figure 58 are a sensitive indicator of the reversion process, deviations between results for the two samples are large. Despite efforts to treat all polyurethane samples similarly and assure the absence of crystallinity, T_{2L} differences often occurred. The reason for these differences was not determined.

The partially spin-lattice relaxed Fourier transform NMR spectra of a 7% urethane crosslinked sample after 30 h of exposure to 100% relative humidity at 363 K are shown in Figure 59. The fully relaxed spectrum resolves the three different nonequivalent hydrogens. From low field to high field they are: (1) the ethylene glycol methylene hydrogen, strongly deshielded by the adjacent ester groups, (2) the adipic acid methylene hydrogen adjacent to the carbonyl groups, and (3) the centrally located adipic acid methylene hydrogen barely resolved from the methylene hydrogen adjacent to the carbonyl groups. At low field, below the ethylene glycol hydrogen resonance, a slight

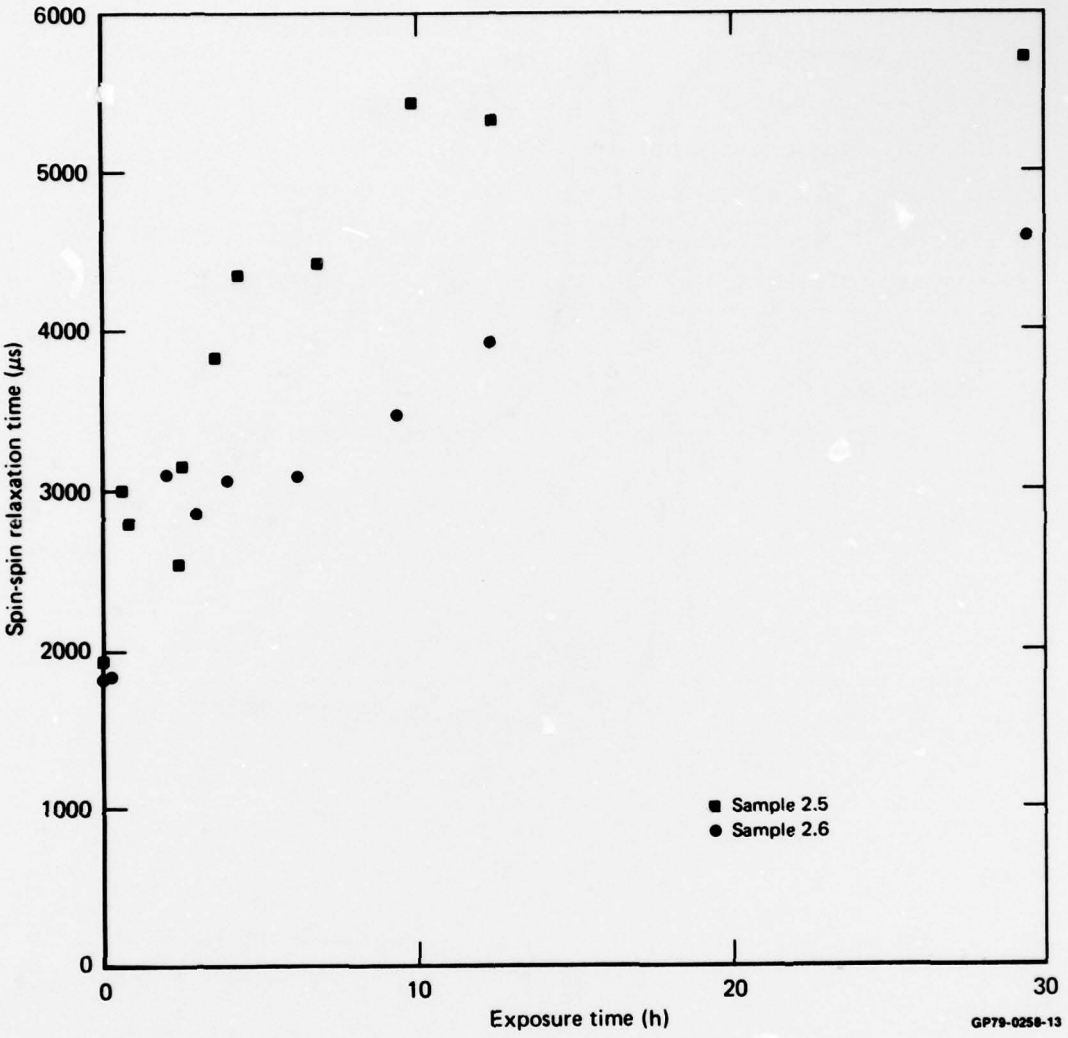

Figure 58 Increase in spin-spin relaxation time caused by reversion.

shoulder is seen which may be the aromatic hydrogens in the TDI. This is better seen in the spectrum for τ = 0.092 s (i.e., after 0.092 s relaxation) where it appears as an inverted broad line. The TDI aromatic hydrogens are expected in this region of the spectrum, but the acid hydrogens from the reverted polyester could be superposed, so positive identification is not possible. The hydrogen relaxing most rapidly is the ethylene glycol CH_2 hydrogen. These groups are followed by the centrally located adipic acid CH_2 hydrogen, the adipic acid hydrogen adjacent to the carbonyl groups, and finally the unidentified low-field hydrogens.

AD-A073 590 MCDONNELL DOUGLAS RESEARCH LABS ST LOUIS MO F/G 11/9
MAGNETIC RESONANCE STUDIES OF EPOXY RESINS AND POLYURETHANES.(U)
MAY 79 I M BROWN, A C LIND, T C SANDRECZKI N00019-78-C-0031
UNCLASSIFIED MDC-Q0673 NL

2 OF 2
AD A073590

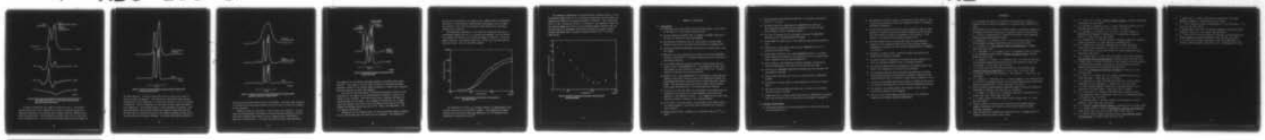

END
DATE FILMED
10-79
DDC

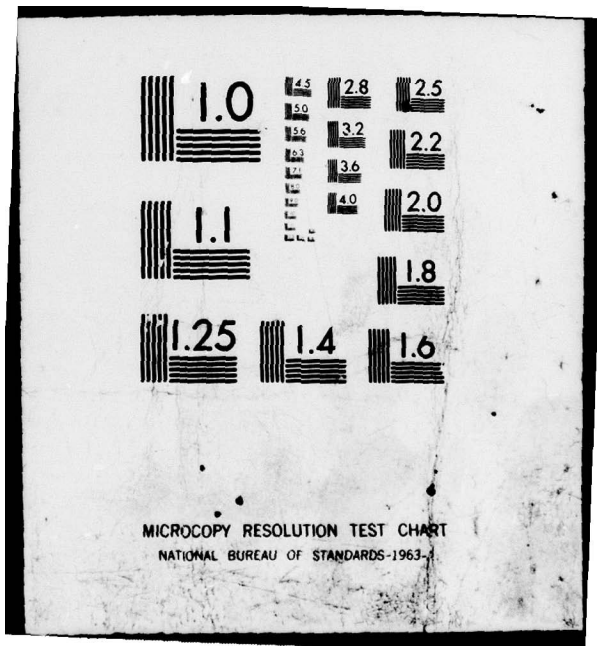
1.0
1.1
1.25
1.4
1.6
1.8
2.0
2.2
2.5
2.8
3.2
3.6
4.0
4.5
5.0
5.6
6.3
MICROCOPY RESOLUTION TEST CHART
NATIONAL BUREAU OF STANDARDS-1963-A

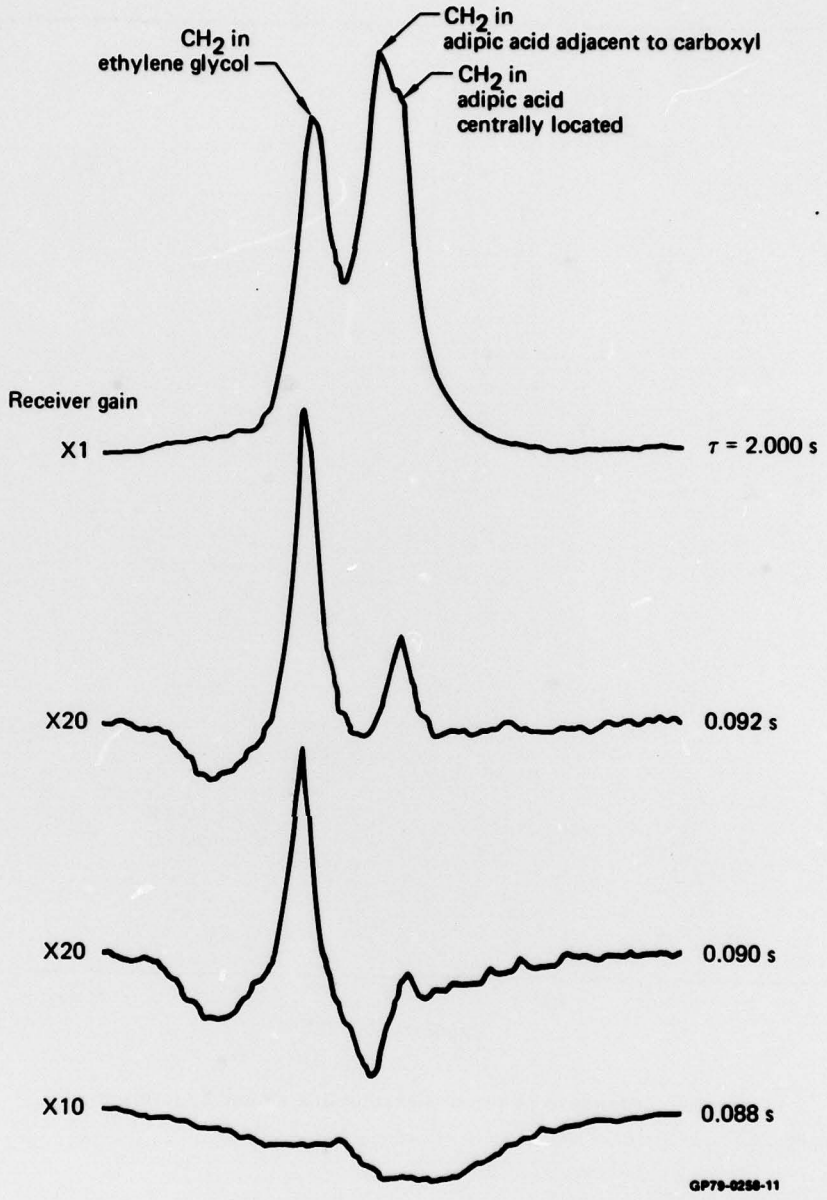

Figure 59 Partially spin-lattice relaxed spectra of polyurethane after 30 h exposure to 363 K 100% relative humidity. τ is the time between the spin-inverting pulse and the sampling of the spectra.

To improve resolution, the sample was heated to 316 K. The Fourier transform spectrum at this temperature is shown in Figure 60 along with a comparison spectrum of the ethylene glycol adipate polyester (EGAP) used to make the polyurethane. Three resonances correlate well, but two small low-field resonances seen in the reverted polyurethane spectrum do not appear in

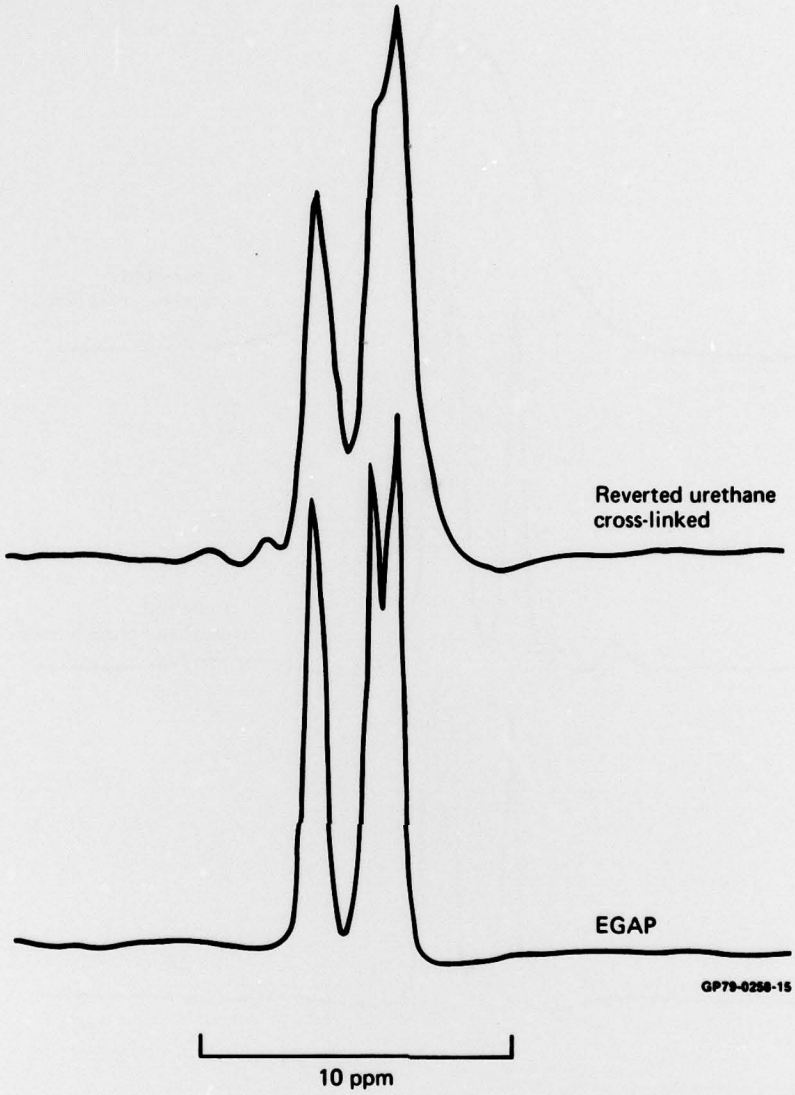

Figure 60 Comparison of reverted polyurethane spectrum and EGAP spectrum. Both spectra were obtained at 316 K.

the EGAP spectrum. To improve resolution further, spectra were taken at 350 K, as shown in Figure 61. The spectrum for unreverted sample narrows sufficiently at this temperature to reveal some structure, so it is included in Figure 61. The two resonances at low field are more clearly resolved at this temperature. The chemical shifts of these resonances (relative to the known resonances) and the areas beneath the resonance peaks show that the low-field peak is caused by the sum of the aromatic hydrogens in TDI and the reverted adipic acid carboxyl hydrogen. The small peak slightly upfield is

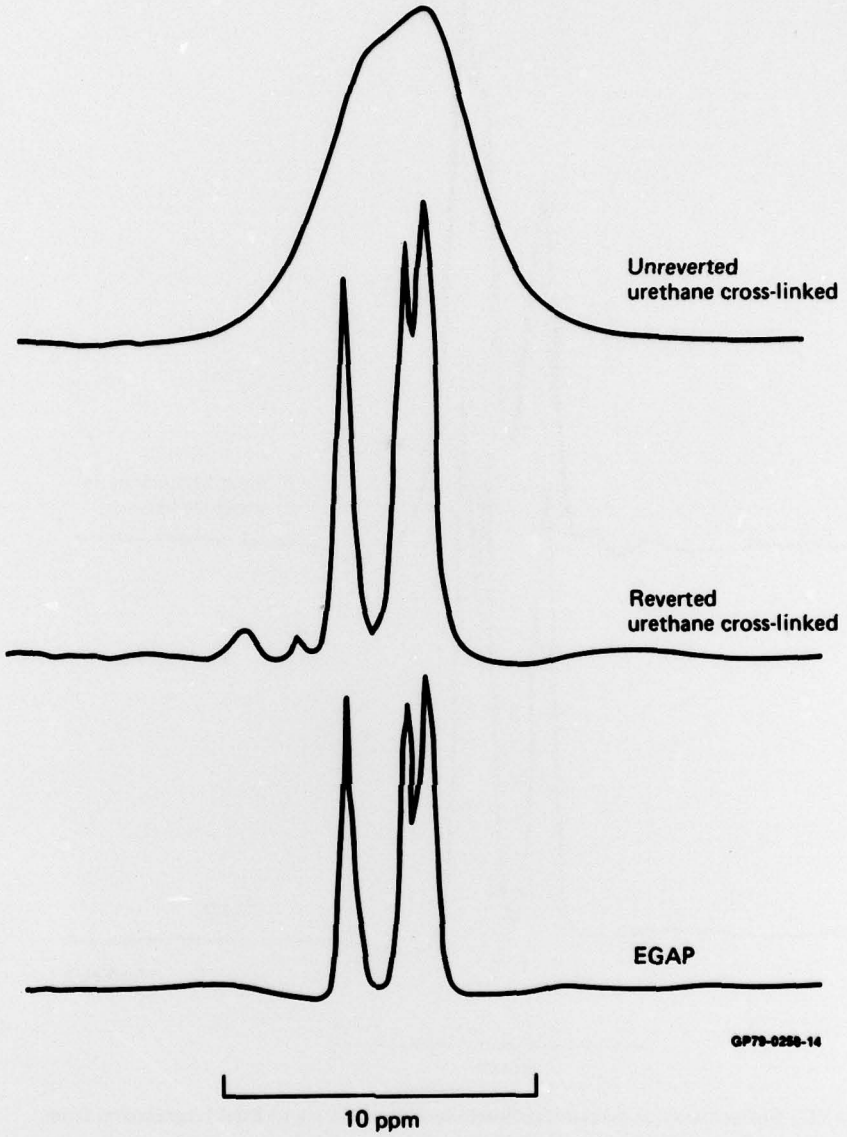

Figure 61. Comparison of spectra for unreverted polyurethane, reverted polyurethane, and EGAP. All spectra were obtained at 350 K.

caused by the reverted ethylene glycol OH hydrogen. This small peak increases in intensity with increasing reversion and can be used to follow the progress of the reversion.

Figure 62 shows the spectrum at a later time in the reversion. At this stage the COOH hydrogen, OH hydrogen, and water hydrogen exchange so rapidly that their resonance peaks merge into one resonance peak, identified in Figure 62 as the OH peak. It is known that when the ester bond hydrolyzes,

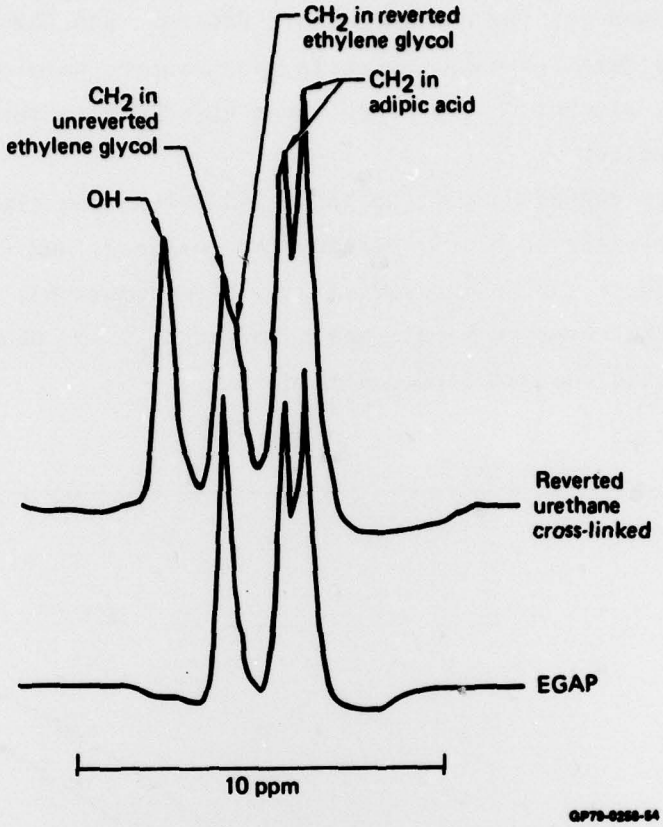

Figure 62 Room-temperature spectrum of extensively reverted polyester polyurethane.

the resonance of the adjacent methylene hydrogen in ethylene glycol moves upfield[37]. This shift is seen in Figure 62 where the methylene hydrogen resonance consists of two closely spaced resonances of nearly equal intensity. Thus the reversion is nearly 50% complete.

The ratio of the total number of COOH and OH hydrogens produced by the hydrolysis to the number of CH_2 ethylene glycol hydrogens is equal to the extent of the reversion. This ratio can be used to measure the amount of unreacted water in the sample. As an example, in Figure 62, for a sample about 50% reverted, the ratio of the area beneath the OH peak to the area beneath the ethylene glycol CH_2 peak is 73%. Hence, the additional $\sim$ 23% is unreacted sorbed water.

Examination of the chemical shifts of the OH resonances shown in Figures 60, 61, and 62 shows that the shifts are all different. This behavior is

typical for OH resonances; the chemical shift depends upon the temperature and acidity. While detailed chemical-shift measurements were not taken, the position of the alcohol OH resonance moved upfield with increasing temperature as expected.

The temperature dependence of the spin-spin relaxation time T_{2L} of a polyurethane sample after 30 h of reversion was measured, and the results are compared with those for an unreverted sample in Figure 63. Above the glass transition, the reverted sample has a larger T_{2L}, and hence greater molecular motion than the unreverted sample.

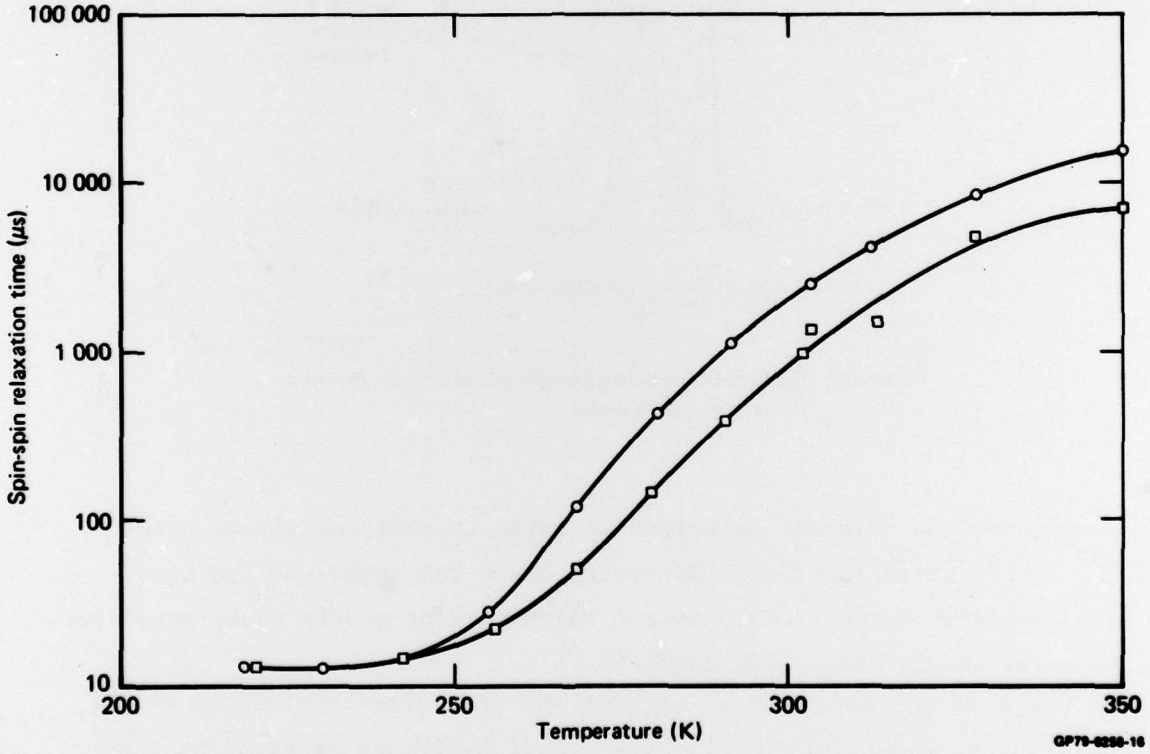

Figure 63 Spin-spin relaxation times of reverted (○) and unreverted (□) polyurethane samples.

The temperature at which T_{2L} increases abruptly is approximately 250 K for both the reverted and unreverted samples. This temperature compares favorably with the glass transition temperature of 237 K measured with differential scanning calorimetry[19].

The temperature dependence of the spin-lattice relaxation time T_1 of the polyurethane sample after 30 h of reversion was measured, and the results are compared with those for an unreverted sample in Figure 64. The results show that T_1 is not a sensitive indicator of reversion. The minimum at ~308 K for the reverted sample and ~314 K for the unreverted sample indicates that the ethylene glycol CH_2 hydrogens (previously determined as the most rapidly relaxing hydrogens) have a motional correlation time of 10^{-9} s at these temperatures.

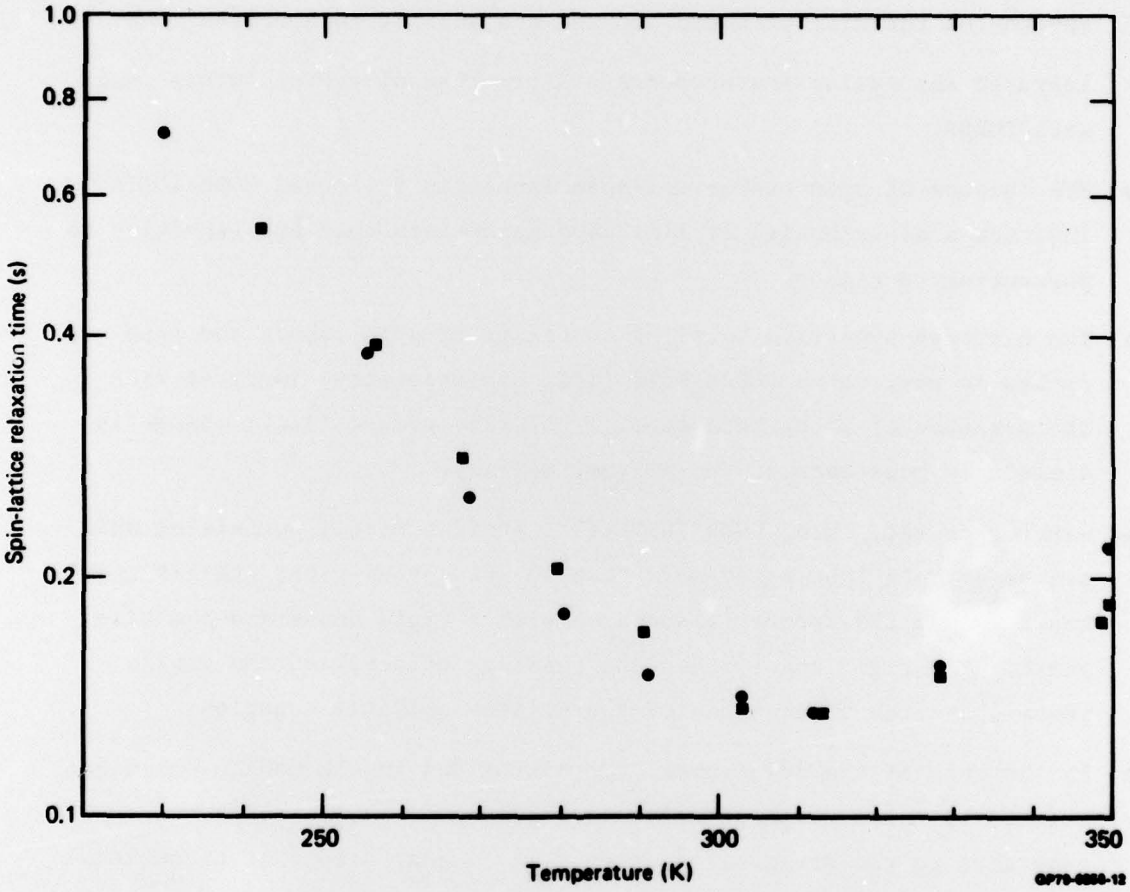

Figure 64 Spin-lattice relaxation times of reverted (●) and unreverted (■) polyurethane samples.

4. SUMMARY OF CONCLUSIONS

4.1 Epoxy Resins

- DGEBA epoxy can be spin-labeled with nitroxide amines to form either an end-label or a spin-labeled quaternary salt.
- The spin-labeled quaternary salt can undergo a Hofmann elimination reaction to release the spin probe TEMPENE.
- The motional correlation time for a spin probe in uncured DGEBA depends on the size of the probe and its ability to hydrogen bond.
- Infrared absorption measurements confirm that nitroxide amines react with DGEBA.
- EPR spectra of spin probes and spin labels in dry, cured DGEBA/DETA indicate a distribution of lineshape parameters that are sensitive to postcuring reactions.
- The nitrogen hyperfine coupling constants of spin labels and spin probes in wet, cured DGEBA/DETA (1:1 stoichiometry) increase with the presence of water because of a polarity effect (i.e., change in dielectric constants of the polymer matrix).
- Samples of wet, cured DGEBA/DETA (1:3 stoichiometry) containing spin probes or spin labels and more than 10 wt% sorbed water exhibit two superimposed EPR spectra associated with a rigid phase and a mobile phase. The rigid phase shows the polarity effect, and the mobile phase obeys the predictions of the Fujita-Doolittle equation.
- In the case of the spin label, the nitroxides in the mobile phase are relaxed by local modes of main-chain segmental motion which are sensitive to the presence of water. It is suggested that these local modes are located in regions of low crosslink density.
- In the case of the spin probes, the nitroxides in the mobile phase are either relaxed by local modes and/or the probes are located in water clusters.
- Methyl group rotation in DGEBA has a correlation time of 10^{-9} s at 288 K.

- Molecular motion associated with DETA has a correlation time greater than 10^{-9} s at 420 K.
- The glass transition temperatures of DGEBA/DETA with different stoichiometries correlated with the temperature at which the spin-spin relaxation time T_2 increased abruptly.
- The rate of increase in T_2 at the glass transition of DGEBA/DETA decreased as the crosslink density increased.
- Excess DGEBA is rigid; hence it has undergone chain-growth polymerization.
- Sorbed water is more mobile than the rigid DGEBA/DETA but not as mobile as bulk liquid water.
- Sorbed water plasticizes the rigid DGEBA/DETA network of a stoichiometric sample only slightly at room temperature, but the plasticizing effect increases with increasing temperature.
- Water sorbed at room temperature enhances subsequent postcuring at elevated temperatures; this reaction was monitored with NMR.
- Sorbed D_2O in DGEBA/DETA experienced hydrogen-deuterium exchange that was monitored with NMR.
- Sorbed water associates with excess or unreacted DETA in DGEBA/DETA polymer.
- The mobility of excess DETA is indistinguishable from that of sorbed water.
- The sum of the excess DETA and sorbed water accounts for the mobile fraction observed with NMR.
- Sorbed water has a greater plasticizing effect on DGEBA/DETA with excess DETA, and the least effect on resins with stoichiometric composition.

4.2 Polyester Polyurethanes

- Polyurethane samples have been spin-labeled at an ester site and also at an isocyanate site.

- The motional correlation times of spin probes and spin labels in polyurethanes above the glass transition temperature exhibit an Arrhenius temperature dependence.
- The activation energies of the spin probe correlation times are independent of reversion, whereas the inverse frequency factor and therefore the activation entropy are dependent on the reversion. This behavior is consistent with published viscosity data.
- The spin-labeled ester in polyurethane shows the same Arrhenius behavior of the correlation times in that the activation energy is independent of reversion and the inverse frequency factor is dependent on reversion.
- Existence of domains and/or crystalline regions was detected and quantitatively measured with NMR.
- The glass transition temperature correlated with the temperature at which the spin-spin relaxation time T_2 increased abruptly.
- Multiple-pulse NMR resolved the hydrogen in the ethylene glycol and adipic acid components of the polyester polyurethane.
- The increased molecular motion resulting from hydrolytic reversion caused large increases in the spin-spin relaxation times which were detectable after only 1 h exposure to 100% relative humidity at 363 K.
- A shift of the ethylene glycol CH_2 resonance to higher fields during the reversion confirmed that the ester bond was undergoing hydrolysis.
- The change in the ethylene glycol OH resonance could be used to determine the extent of the reversion.
- The T_2 of the reverted sample exceeded the T_2 of the unreverted sample above the glass transition temperature.

REFERENCES

1. C. E. Browning, The Effects of Moisture on the Properties of High Performance Structural Resins and Composites, Technical Report AFML-TR-72-94 (1972).
2. AFOSR Workshop on the Effects of Relative Humidity and Elevated Temperature on Composite Structures, University of Delaware, Newark, DE (March 1976).
3. W. R. Griffin, Reconstitution of Reverted Polyurethane Potting Compounds, Technical Report AFML-TR-68-398 (1968).
4. N. Bloembergen, E. M. Purcell, and R. V. Pound, Relaxation Effects in Nuclear Magnetic Resonance Absorption, Phys. Rev. 73, 679 (1948).
5. L. J. Berliner, ed., Spin Labeling: Theory and Applications, (Academic Press, New York, 1976).
6. A. L. Buchachenko, A. L. Kovarskii, and A. M. Wassermann, Study of Polymers by the Paramagnetic Probe Method, Advances in Polymer Science, (Halsted Press, New York, 1976).
7. S. A. Goldman, G. V. Bruno, C. F. Polnaszek, and J. H. Freed, An ESR Study of Anisotropic Rotational Reorientation and Slow Tumbling in Liquid and Frozen Media, J. Chem. Phys. 56, 716 (1972).
8. J. H. Freed, Theory of Slow Tumbling ESR Spectra for Nitroxides, Spin Labeling: Theory and Applications, (Academic Press, New York, 1976).
9. D. Kivelson, Theory of ESR Linewidths of Free Radicals, J. Chem. Phys. 33, 1094 (1960).
10. R. P. Mason, C. F. Polnaszek, and J. H. Freed, Comments on the Interpretation of Electron Spin Resonance Spectra of Spin Labels Undergoing Very Anisotropic Rotational Reorientation, J. Phys. Chem. 78, 1324 (1974).
11. David W. McCall, Nuclear Magnetic Resonance Studies of Molecular Relaxation Mechanisms in Polymers, Acc. Chem. Res. 4, 223 (1971).
12. J. S. Waugh, L. M. Huber, and U. Haeberlen, Approach to High Resolution in Solids, Phys. Rev. Letters 20, 180 (1968).
13. D. L. Fanter, Method for Casting Epoxy Tensile Coupons, Rev. Sci. Instr. 49, 1005 (1978).
14. These nitroxide free radicals were obtained from the Eastman Chemical Company, Rochester, New York,and also the Aldrich Chemical Company, Milwaukee, Wisconsin.
15. These nitroxide free radicals were obtained from R. P. Haugland and R. P. Haugland, Molecular Probes, Plano, Texas.

16. L. F. Fieser and M. Fieser, Advanced Organic Chemistry, (Reinhold Publishing Corporation, New York, 1961).
17. J. C. Williams, R. Mehlhorn, and A. D. Keith, Synthesis and Novel Uses of Nitroxide Motion Probes, Chem. Phys. Lipids 7, 207 (1971).
18. M. P. Eastman, R. G. Kooser, M. R. Das, and J. H. Freed, Studies of Heisenberg Spin Exchange in ESR Spectra, I. Linewidth and Saturation Effects, J. Chem. Phys. 51, 2690 (1969).
19. W. R. Matthew and T. T. Bartels, Analytical Chemistry Laboratory, McDonnell Douglas Corporation, St. Louis, Missouri, unpublished data.
20. E. F. Cuddihy and J. Moacanin, Superposition of Dynamic Mechanical Properties in the Glassy State, J. Polym. Sci., A2, 8, 1627 (1970).
21. P. L. Kumler and R. F. Boyer, ESR Studies of Polymer Transitions, Macromolecules 9, 903 (1976).
22. O. H. Griffith and P. C. Jost, Lipid Spin Labels in Biological Membranes, Spin Labeling: Theory and Applications, (Academic Press, New York, 1976).
23. Z. Veksli and W. G. Miller, The Effect of Good Solvents on Molecular Motion of Nitroxide Free Radicals in Covalently Labeled Polystyrene and Poly (Methyl Methacrylate), Macromolecules 10, 686 (1977).
24. J. D. Ferry, Viscoelastic Properties of Polymers, (John Wiley & Sons, New York, 1970).
25. W. K. Rhim, D. D. Elleman, and R. W. Vaughan, Enhanced Resolution for Solid State NMR, J. Chem. Phys. 58, 1772 (1973).
26. A. C. Lind and D. P. Ames, Multiple-Pulse Reduction of Proton Dipolar Broadening in Solid Copolymers, J. Polymer Sci. B 12, 339 (1974).
27. G. E. Pake, Nuclear Resonance Absorption in Hydrated Crystals: Fine Structure of the Proton Line, J. Chem. Phys. 16, 327 (1948).
28. D. W. Larsen and J. H. Strange, Pulsed NMR Study of Molecular Motion in the Diglycidyl Ether of Bisphenol-A Cured with 4,4'-Methylenedianiline, J. Polymer Sci. 11, 449 (1973).
29. J. E. Anderson and W. P. Slichter, Nuclear Spin Relaxation in Solid n-Alkanes, J. Phys. Chem. 69, 3099 (1965).
30. K. J. Saunders, Organic Polymer Chemistry, (Chapman and Hall, London, 1976).
31. J. H. Saunders and K. C. Frisch, Polyurethanes: Chemistry and Technology, (John Wiley & Sons, New York, 1962 and 1964). Vols. I and II.
32. P. L. Nordio, General Magnetic Resonance Theory, Spin Labeling: Theory and Applications, (Academic Press, New York, 1976).

33. Z. Veksli and W. G. Miller, Penetration of Nonsolvents into Glassy Amorphous Polymers, J. Polymer Sci. 54, 299 (1976).

34. P. J. Flory, Absolute Viscosity Measurements in Linear Polyesters, J. Am. Chem. Soc. 62, 1057 (1940).

35. S. Meiboom and D. Gill, Modified Spin-Echo Method for Measuring Nuclear Relaxation Times, Rev. Sci. Instrum. 29, 688 (1958).

36. H. Y. Carr and E. M. Purcell, Effects of Diffusion on Free Precession in Nuclear Magnetic Resonance Experiments, Phys. Rev. 94, 630 (1954).

37. W. W. Simons and M. Zanger, The Sadtler Guide to the NMR Spectra of Polymers, Sadtler Research Laboratories, Inc., Philadelphia, PA (1973).

DISTRIBUTION

	Copies
Commander, Naval Air Systems Command Department of the Navy Washington, DC 20361 Attn: AIR-5163D5	20
Commander, Naval Air Systems Command Department of the Navy Washington, DC 20361 Attn: AIR-954-320A	1
Commander, Naval Air Systems Command Department of the Navy Washington, DC 20361 Attn: AIR-954 (DDC)	12
Commander, Naval Surface Weapons Center White Oak, Silver Spring, MD 20910 Attn: WR-31	2
Commanding Officer Naval Ship R&D center Annapolis Laboratory Annapolis, MD 21402	1
Plastics Technical Evaluation Center Picatinny Arsenal Dover, NJ 07801 Attn: Code SMUPA-VP3	2
Army Materials & Mechanics Research Center Watertown, MA 02172 Attn: Dr. George Thomas	2
Director, Air Force Materials Laboratory Wright-Patterson AFB, OH 45433 Attn: AFML/MBE AFML/MXE AFML/MBC AFML/MBP	1 1 1 1
Commanding Officer Naval Air Development Center Warminster, PA 18974 Attn: Code 606	2
Commander Naval Weapons Center China Lake, CA 93555 Attn: Code 385	1
Director, Naval Research Laboratory Washington, DC 20375 Attn: Code 6110 Code 6120 Code 6170	1 1 1
Office of Naval Research 800 N. Quincy St. Arlington, VA 22217 Attn: Code 472	1
Stanford Research Institute 333 Ravenswood Avenue Menlo Park, CA 94025	1
National Bureau of Standards Institute for Materials Research Washington, DC 20234 Attn: Dr. Leslie Smith	1
Goodyear Aerospace Corporation Akron, OH 44315 Attn: Hugh Boyd	1
W. E. Woolam Southwest Research Institute 1150 Connecticut Ave., Suite 613 Washington, DC 20036	1
W. J. Versino Aerospace Corporation P.O. Box 92957 Los Angeles, CA 90009	1
Battelle Columbus Laboratories 505 King Avenue Columbus, OH 43201	1

	Copies
Fred A. Keimel, President Adhesive & Sealants Newsletter P. O. Box 72 Berkeley Heights, NJ 07922	1
D. R. Ulrich Air Force Office of Scientific Research Bolling AFB Washington, DC 20332	1
Lockheed Missile & Space Company, Inc. P.O. Box 504 Sunnyvale, CA 94088 Attn: Clayton A. May	1
R. W. Lauver NASA Lewis Research Center Cleveland, OH 44135	1
Boeing Aerospace Company Seattle, WA 98008 Attn: John Hoggatt	1
Columbus Aircraft Division Roxkwell International 4300 E. Fifth Avenue Columbus, OH 43216 Attn: J. Fasold	1
General Electric R&D Center P.O. Box 8 Schenectady, NY 12301	1
Office of Naval Research Boston Branch Office 495 Summer St. Boston, MA 02210 Attn: L. H. Peebles	1
Vought Corporation Aeronautics Division P. O. Box 5907 Dallas, TX 75222 Attn: A. Hohman	1
Dr. J. O. Brittain Dept. of Materials Science & Engineering Northwestern University Evanston, IL 60201	1
ITT Research Institute 10 W. 35th Street Chicago, IL 60616	1
University of California Lawrence Livermore Laboratory P. O. Box 808 Livermore, CA 94550 Attn: T. T. Chiao	1
Dr. N. Johnston Head, Polymer Group NASA Langley Research Center Hampton, VA 23665	1
Northrop Corporation 3901 W. Broadway Hawthorne, CA 90250 Attn: D. Crabtree (Nonmetallic Research Dept.)	1
Westinghouse Corp. R&D Center 1310 Beulah Rd Pittsburgh, PA 15235 Attn: Z. N. Sanjana	1
U. S. Army Research Office Box CM, Duke Station Durham, NC 27706 Attn: Dr. John Hurt	1
Polymer Research Institute University of Massachusetts Amherst, MA 01002	1
McDonnell-Douglas Corporation P.O. Box 516 St. Louis, MO 63166 Attn: Dr. James Carpenter	1
Prof. John F. Fellers Polymer Science & Engineering Program 419 Dougherty Engineering Bldg. University of Tennessee Knoxville, TN 37916	1
The Boeing Company Aerospace Division P. O. Box 3707 Seattle, WA 98124	1

	Copies
Lockheed California Co. Dept. 74-54, Bldg. 63 Box 551 Burbank, CA 91503 Attn: Mr. J. H. Wooley	1
University of Maryland College Park, MD 20742 Attn: Dr. W. J. Bailey	1
TRW One Space Park Rodundo Beach, CA 90278 Attn: R. W. Vaughn	1
Vought Corporation Advanced Technology Center P. O. Box 6144 Dallas, TX 75222	1